ISSN: 2164-5388 Volume 12, Number 2, April 2022

Scientific Research Publishing

Open Journal of Biophysics

ISSN: 2164-5388

https://www.scirp.org/journal/ojbiphy

Journal Editorial Board

ISSN Print: 2164-5388 ISSN Online: 2164-5396
https://www.scirp.org/journal/ojbiphy

Editor-in-Chief

Associate Editors

Editorial Board

Scientific Research Publishing

Open Journal of Biophysics, 2022, 12, 89-163
https://www.scirp.org/journal/ojbiphy
ISSN Online: 2164-5396
ISSN Print: 2164-5388

Table of Contents

Volume 12 Number 2 April 2022

Stimulation and Control of Homeostasis

A. Szasz.....89

Evaluation of Peppermint Leaf Flavonoids as SARS-CoV-2 Spike Receptor-Binding Domain Attachment Inhibitors to the Human ACE2 Receptor: A Molecular Docking Study

M. L. P. Júnior, R. T. de Sousa Junior, G. D. A. Nze, W. F. Giozza, L. A. R. Júnior.....132

A Bio-Physical Analysis of Extracellular Ion Mobility and Electric Field Stress

X. D. Zhang, H. Zhang.....153

Open Journal of Biophysics (OJBIPHY)
Journal Information

SUBSCRIPTIONS

The *Open Journal of Biophysics* (Online at Scientific Research Publishing, https://www.scirp.org/) is published quarterly by Scientific Research Publishing, Inc., USA.

Subscription rates:
Print: $79 per issue.
To subscribe, please contact Journals Subscriptions Department, E-mail: sub@scirp.org

SERVICES

Advertisements
Advertisement Sales Department, E-mail: service@scirp.org

Reprints (minimum quantity 100 copies)
Reprints Co-ordinator, Scientific Research Publishing, Inc., USA.
E-mail: sub@scirp.org

COPYRIGHT

PRODUCTION INFORMATION

For manuscripts that have been accepted for publication, please contact:
E-mail: ojbiphy@scirp.org

Scientific Research Publishing

Open Journal of Biophysics, 2022, 12, 89-131
https://www.scirp.org/journal/ojbiphy
ISSN Online: 2164-5396
ISSN Print: 2164-5388

Stimulation and Control of Homeostasis

Andras Szasz

Department of Biotechnics, Szent Istvan University, Budaors, Hungary
Email: biotech@gek.szie.hu

How to cite this paper: Szasz, A. (2022) Stimulation and Control of Homeostasis. *Open Journal of Biophysics*, **12**, 89-131.
https://doi.org/10.4236/ojbiphy.2022.122004

Received: January 19, 2022
Accepted: March 19, 2022
Published: March 22, 2022

Abstract

Healthy homeostasis is a principal driving force of the dynamic equilibrium of living organisms. The dynamical basis of homeostasis is the complex and interconnected feedback mechanisms, which are fundamentally governed by the nervous system, mainly the balance of the sympathetic and parasympathetic controlling actions. The balancing regulation is well presented in the heart's sinus node and can be measured by the time-domain heart-rate variation (HRV) of its frequency domain to analyze the constitutional frequencies of the variation. This last is a fluctuation that shows $1/f$ time fractal arrangement (f is the composing frequency). The time-fractal arrangement could depend on the structural fractal of the His-Purkinje system of the heart and personally modify the HRV. The cancers gradually destroy the homeostatic harmony, starting locally and finishing systemically. The controlling activity of vagus-nerve changes the HRV or the power density spectrum of the signal fluctuations in malignant development, presenting an appropriate control of the cancerous processes. The modified spectrum by a non-invasive radiofrequency treatment could arrest the tumor growth. An appropriate modulation could support the homeostatic control and force reconstructing of the broken complexity.

Keywords

Homeostasis, Vagus Stimulation, Heart-Rate Variability, Immune-Stimuli, Cancer, Time-Fractal Modulation, Bifurcations, $1/f$ Noise, mEHT, Personalized Therapy

1. Introduction

Homeostasis is the vital basis of the dynamic stability of living organisms. The network of negative and positive feedback reactions creates the backbone of complex regulatory processes. The synergy of chemical and physical actors generates homeostasis in a stochastic harmony. The water is a mandatory consti-

tuent. The aqueous electrolytes provide the active fundament of various changes in the living systems. The water molecules participate in the harmonization of the complex processes in the separated solutions. The cellular lipid structures (membranes) and some specialized tissues divide the electrolytes, but at the same time, these surfaces regulate most of the chemical reactions for living equilibrium by intensive dynamic processes of various ionic exchanges and electromagnetic forces.

The control of the stochastic regulatory processes has highly self-organized accuracy creating the appropriate products, but some perturbances could disorient the standard mechanisms. The homeostatic system has a variety of tools to correct errors. A significant challenge arose when the collaborative networks were disrupted, and the natural processes could not correct this fault. Such complication happens in the development of malignancy, driven by the unicellular individualism of the involved cells. The malignant structure breaks the multicellular organization (healthy networking). The autonomous cells adapt to the challenges and avoid homeostatic control. These cells hide their erroneous structure, imitate a wound, and force the homeostatic control to heal, support them [1]. This activity changes the micro and macro environment of the malignant cells, disorganizing the network and the harmonic interactions of the multicellular structure. Due to the high individual energy demand, these cells use a primitive transcriptional program [2]. The tumor organizes a unicellular autonomy to safeguard the survival of the "colony" of malignant cells [3]. The healthy host provides active support to cancer, trying to "heal" the abnormality. Neo-angiogenesis, induced injury current, and numerous other boosts appear, guided by misled general homeostatic regulation of the body.

Cancer starts locally but becomes systemic when the structurally and dynamically disordered tissue appears in the body. The dynamic control is not able to repair the local malignant development due to various reasons: genetic aberration [4], mitochondrial dysfunction [5], and other intra [6] and extracellular [7] hallmarks of cancer. Furthermore, the permanent uncontrolled stress [8], the recognition of the lesion as an unhealed wound [9], the permanent inflammation [10], and the missing apoptotic activity [11] worsen the situation.

Cancer is the disease of the multicellular system disrupting the organized network, exchanging the cooperative advantages to the selfish individual demands [12]. One therapeutic help could support multicellular harmonic control, boosting the standard natural homeostatic regulation for effective action. The task is as complex as life itself, so the external actions are limited. We do not expect any changes from the therapy alone. The intention is only backing the natural control to do the job. Our approach is an electromagnetic action [13]. The fundamental tool for this task is the amplitude-modulated radiofrequency (RF) carrier with $1/f$ spectrum, which supports the homeostatic multicellular harmony, helps to correct the malignant lesion's cellular disorder, and induces apoptosis of the malignant cells. The forcing cooperative harmony may influence the precancerous cells to return to the healthy network. Our objective is to study this possibil-

ity considering the personalization of the modulation.

2. Method—The 1/*f* Spectrum

2.1. Embedded Bifurcation Dynamism

The control of life reaction has stochastic feedbacks [14], which drive all the processes in complex, embedded structures. Positive feedback is a process to generate a specific new product or state, with a point of no return. The positive feedback mechanisms are usually complex and have some intermediate potential wells keeping the process controlled and avoiding the expansive quick unregulated outcome. A characteristic example is the catabolism of humans, where the positive feedback is driven with the never-resting electrons: "Life is nothing but an electron looking for a place to rest" [15]. In the metabolism of the eukaryotic cells, the glucose has a degradation, and finally, the process ends in $CO_2 + H_2O$ products, while the liberated energy kept the cells living **Figure 1**.

The positive feedback has no direct general balancing, but the subsequent steps in this have metastable positions, requiring some extra energy to overcome the barriers. The simplest and most common negative feedback regulation processes in a living system have two opposite regulation effects: the promoter and suppressor balance each other. This balancing process compensates for the opposite factors, fluctuating between two possible states **Figure 2**. When the negative feedback is out from the pre-set limits, the process becomes unbalanced, the negative feedback weakens, and a sign of irregularity appears.

The bifurcation potential wells usually have a longer chain of embedded bifurcations as part of the complex process. In this way, the complexity develops a

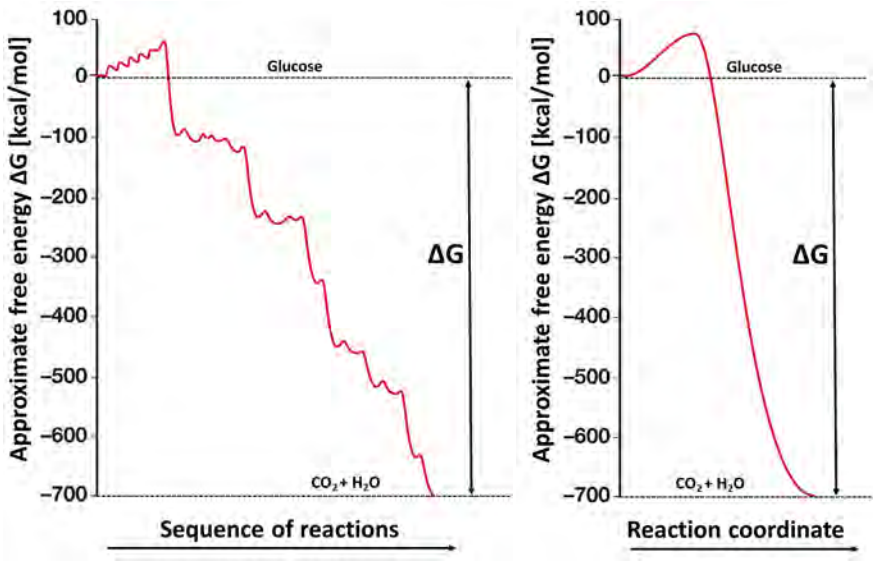

(a) (b)

Figure 1. The approximate "degradation" of glucose to the final molecules $CO_2 + H_2O$ of catabolism. All peaks are transition states assisted by devoted enzymes, and the wells are metastable intermediate states.

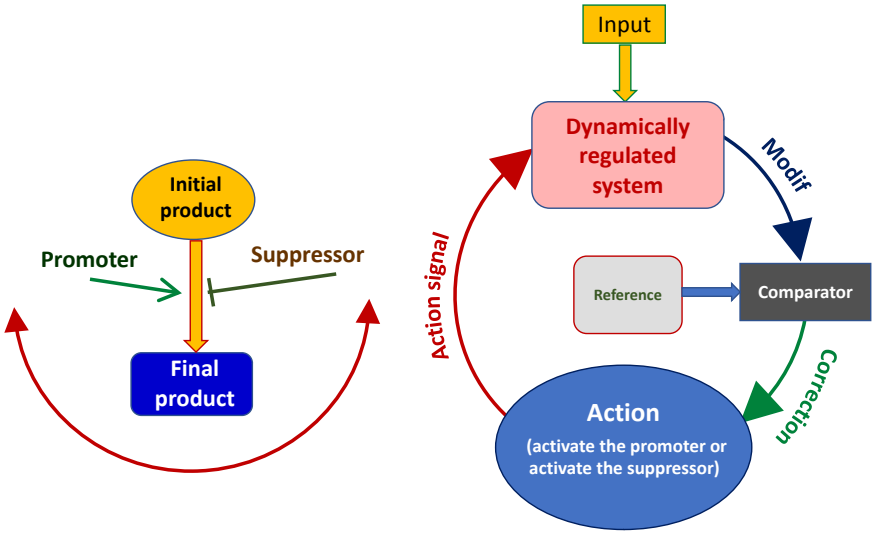

Figure 2. The dynamic balance of the homeostatic negative feedback control. (a) balance of the promoter-suppressor pair (b) the complete circle of the regulation.

multifurcation system at the level of the entire living organism. The primary step of the embedded multifurcation starts with the water structure. The hydrogen bridges allow a chain transport of H^+ ions, creating a fundamental mechanism in living systems [16]. The proton tunneling (jumping) between the water molecules forms low dissipation ionic transport (the proton migrates) [17] [18]. The involved ion multifurcates in the potential wells of the chain connected by the bifurcative hydrogen bridges, connecting the water molecules dynamically. Such construction from bifurcative to multifurcative connection appears in the whole organism following the hydrogen-bridge mechanisms [19] [20] [21]. The bifurcative steps appear in structural connections of the DNA helix connecting the nucleotides, which may cause protein's bending and be involved massively in the stochastic processes of life. Self-organized processes connect the bifurcation steps, which are arranged in fractal structure **Figure 3**.

The amplitudes of the harmonically oscillated particles of the bifurcative potential wells in the self-organized setting form a Cantor set, which is in mathematical expression:

$$x \to f(x) = \frac{\left[\frac{1}{2} - \left|x - \frac{1}{2}\right|\right]}{r} \tag{1}$$

where r is the section removed from the middle of the Cantor's template. The vibration produced by the *k*-th bifurcation-set (multifurcation) has the following shape

$$x_k(t) = A_k \sin\left(2\pi f_k t + \varphi_k\right) \tag{2}$$

The power spectrum of the vibration superimposed on these in the case where f_k is a multiple of f_1 fundamental frequency. The average of x^2 is:

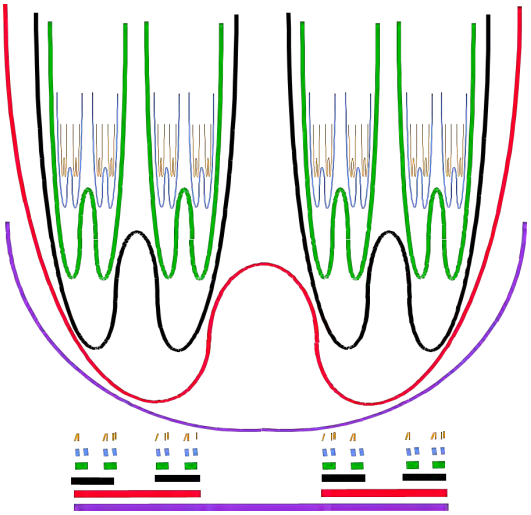

Figure 3. The self-similarity produces the embedded multifunction system. Stochastic resonances promote the bifurcation steps. The probability distribution follows a Cantor-dust fractal.

$$\left\langle x^2 \right\rangle = \sum_k \frac{A_k^2}{2} \tag{3}$$

We suppose the expected $1/f$ spectral behavior, so it is a condition of the spectral density $S(f_k) \propto A_k^2$

$$S(f_k) \propto A_k^2 \propto \frac{1}{f_k} \tag{4}$$

Due to the Cantor-set character, using the assumption of (4) when $r = 3$

$$\frac{A_{k+1}}{A_k} = \sqrt{\frac{f_{k+1}}{f_k}} = 3 \tag{5}$$

So the frequencies form a geometric series

$$\frac{f_{k+1}}{f_k} = 3^2 \tag{6}$$

So the k-th frequency

$$f_k = 3^{2k} f_1 \tag{7}$$

This is a discrete power spectrum, but their amplitudes follow the assumed $1/f$ pink noise (4). In the above described discrete subsequent embedding, the particles oscillate in one dimension and are independent from each other. However, the reality differs. The oscillation is three-dimensional. All the directions of the space could be active, and these oscillating dimensions could be dependent. Weak interactions connect the wells, forming networks and dynamical harmony. The net of the weak interactions ensures a stable system with low vulnerability [22]. The natural overlaps create a continuous $1/f$ spectrum, even in this simple model. Self-similarity and self-organization are the general features of the living system, generalizing pink noise in stationary random stochastic processes [23].

The living systems are far from thermodynamical equilibrium, seeking to realize the lowest available energy with the highest efficacy in dynamic stability (homeostasis), balancing the energy incorporation and the energy combustion. The natural processes seek to minimize their energy consumption, using the least-action principle, which drives the biological processes and the biological evolution.

2.2. The Frequency-Order

The living systems show $1/f$ noise in homeostasis, a distribution of the stochastic processes keeping the system in dynamic equilibrium. However, this character does not identify the system because the $1/f$ is a spectrum, a distribution of the frequencies by their power density, without the time series of signals in the organism. The time-dependence vanishes with the Fourier transformation, and the obtained power density gives general information like the status of self-organizing, the scaling, and the dynamic equilibrium of the body; the time-function disappears. Some general info about the interaction chains could be derived from the autocorrelation function, but the actual time-dependent signal remains hidden.

The $1/f$ frequency spectrum is a distribution, which defines various frequencies, taking no attention to their sequences in the actual signal. For example, most musical pieces have near $1/f$ distribution, but they are, of course, very different in their musical sounds. The frequency distribution does not inform us about the temporal sequences of the frequencies. However, the temporal signal is used for modulation, so derive this information from the spectral density function to increase the theranostics approach's efficacy and accuracy. Facing this problem, study first the power spectrum of pink noise, assuming a trivial, energetic criterion for self-similarity. When $f(t)$ is a self-similar function on the whole real axis, we know:

$$f(\tau t) = \tau^k f(t) \tag{8}$$

when the function in (8) is chosen as integrally quadratic:

$$0 < \int_{-\infty}^{\infty} \left| f(t) \right|^2 \mathrm{d}t < \infty \tag{9}$$

The used $\left| f(t) \right|$ is the absolute value of the signal allows complex functions. This is physically a possibility to examine self-similar function pairs. The above criterion for physical signals usually means that the energy of the signal is finite. This is true of all physically meaningful signs [24]. Note the integral of the quadratic function with E:

$$E = \int_{-\infty}^{\infty} \left| f(t) \right|^2 \mathrm{d}t \tag{10}$$

So using (8):

$$\begin{aligned} E &= \tau \int_{-\infty}^{\infty} \left| f(\tau z) \right|^2 \mathrm{d}z \\ &= \tau \left(\tau^k \right)^2 \int_{-\infty}^{\infty} \left| f(z) \right|^2 \mathrm{d}z \\ &= \tau^{1+2k} \int_{-\infty}^{\infty} \left| f(z) \right|^2 \mathrm{d}z \\ &= \tau^{1+2k} E \end{aligned} \tag{11}$$

with substitution of E from (10) to (11):

$$\tau^{1+2k} = 1 \to k = -\frac{1}{2} \tag{12}$$

Below we prove that Equation (12) leads to the $1/f$ power spectrum. The quadratic integrity (finite energy signals) has a Fourier transform, which is also self-similar in a frequency domain, so:

$$F\left[f(t)\right] = X(j\omega) = \frac{B}{(j\omega)^{1+k}} = \frac{B}{(j\omega)^{\frac{1}{2}}} \tag{13}$$

Taking advantage of this, the Wiener-Khinchin theorem [25] states that

$$\int_{-\infty}^{\infty} \left|f(t)\right|^2 \mathrm{d}x = \int_{-\infty}^{\infty} X(j\omega) X^*(j\omega) \mathrm{d}\omega = \int_{-\infty}^{\infty} \frac{BB^*}{\omega} \mathrm{d}\omega \tag{14}$$

Hence the power spectrum of the self-similar finite energy signal is $1/f$. Note that the signal can also be deterministic, and even as we show below, the theorem does not apply to stationary noises in the above form. In the case of the principle of infinitely long stationary self-similar signals, finite energy cannot be guaranteed. In this case, the physically meaningful claim is the finiteness of the average:

$$0 < \lim_{T\to\infty} \frac{1}{T} \int_{-T/2}^{T/2} \left|f(t)\right|^2 \mathrm{d}t < \infty \tag{15}$$

The repeated above calculation resulting (12), the average power of (15) delivers the same result, namely that the power spectrum of the self-similar signals with finite average power is $1/f$. We have to make some theoretical remarks and move on to ergodic signals and correlation functions to discuss the stochastic processes in the above way. In the case of stationary ergodic signals, the correlation functions can be formed from each representation by forming the following limit value:

$$R(\tau) := \lim_{T\to\infty} \frac{1}{T} \int_{-T/2}^{T/2} f(t) f(t-\tau) \mathrm{d}t \tag{16}$$

Because we assumed finite mean performance, this correlation function exists. Introduce the notation for the T-length representation of the signal. This is defined as:

$$f_T(t) = \begin{cases} f(t) & -\frac{T}{2} \le t \le \frac{T}{2} \\ 0 & \text{otherwise} \end{cases} \tag{17}$$

The Fourier transform of the T-length representation:

$$X(j\omega, T) = \frac{1}{2\pi} \int_{-T/2}^{T/2} f(t) \mathrm{e}^{j\omega t} \mathrm{d}t \tag{18}$$

The average power density of T-length representations approaches the Fourier transformation. Based on this, it might be supposed that every single being's autonomic nervous system produces an individually coded $1/f$ homeostatic noise.

In this sense, we can talk about personalized $1/f$ noise. Transform of the autocorrelation function [26], so

$$\Phi(\omega)=\lim_{T\to\infty}\pi\frac{X(j\omega,T)X^{*}(j\omega,T)}{T}=\frac{1}{2\pi}\int_{-\infty}^{\infty}R(\tau)\mathrm{e}^{-j\omega t}\mathrm{d}t \tag{19}$$

Conversely, the inverse Fourier transform of the average power density is the autocorrelation function, so

$$R(\tau)=\frac{1}{2\pi}\int_{-\infty}^{\infty}\Phi(\omega)\mathrm{e}^{j\omega\tau}\mathrm{d}\omega \tag{20}$$

From this, we obtain the average performance of

$$R(0)=\lim_{T\to\infty}\frac{1}{T}\int_{-T/2}^{T/2}\left(f(t)\right)^{2}\mathrm{d}t=\frac{1}{2\pi}\int_{-\infty}^{\infty}\Phi(\omega)\mathrm{d}\omega \tag{21}$$

expression, which is the Wiener-Khinchin theorem for stochastic signs. As shown above, the Fourier transform of the self-similar signal is a self-similar signal in the frequency domain. With the substitution in (21):

$$\begin{aligned}R(0)&=\frac{1}{2\pi}\int_{-\infty}^{\infty}\Phi(\omega)\mathrm{d}\omega\\&=\tau\frac{1}{2\pi}\int_{-\infty}^{\infty}\Phi(\tau\varpi)\mathrm{d}\varpi\\&=\tau\tau^{\alpha}\frac{1}{2\pi}\int_{-\infty}^{\infty}\Phi(\varpi)\mathrm{d}\varpi\\&=\tau^{\alpha+1}R(0)\end{aligned} \tag{22}$$

According to (11), $R(0)$ is self-similar. The power spectrum $S(\omega)$ equal with $\Phi(\omega)$, as it is shown in (19), which is its definition, so

$$S(\omega)=\Phi(\omega)=\frac{A^{2}}{\omega}=\frac{A}{\sqrt{\omega}}\frac{A^{*}}{\sqrt{\omega}}=\frac{|A|\mathrm{e}^{i\varphi(\omega)}}{\sqrt{\omega}}\frac{|A|\mathrm{e}^{-i\varphi(\omega)}}{\sqrt{\omega}} \tag{23}$$

The power density spectrum is the product of the signal and its conjugate spectrum. Then the temporal representation of the stochastic signal is:

$$f(t)=inverseFourier\left(\frac{|A|\mathrm{e}^{i\varphi(\omega)}}{\sqrt{\omega}}\right) \tag{24}$$

where the phase $\varphi(\omega)$ is an arbitrary function that can be deterministic but can also be random, characterized by its distribution functions. When an ergodic function represents the stochastic process, it facilitates the characterization.

Like it is shown in (24) that each $1/f$ signal differs in the distribution (power spectrum) of a random variable in phase. Since the phase is the carrier of the information, its distribution determines the signal's temporal form, which allows a better understanding of the step-by-step changes of the signal in the biological processes, while the power spectrum gives systemic information.

The scaling of the power density by frequency is a piece of general information about the system. The cancerous lesion is a local disorder that hurts the standard healthy conditions. Consequently, cancer cannot accept harmonic

modulation. The signal attacks the cells by absorbing energy, while in the healthy harmonic tissues, these absorptions are much weaker, keeping the harmony in proper rhythm.

It is essential to identify when the system does not work correctly, so have tissues out from the overall self-organized control. The general request of the homeostatic harmony can be forced by a compulsory force by the $1/f$ signal. The following ways could personalize the general harmonization attempt:

1) Apply a $1/f$ random spectrum. This spectrum generates the frequency components randomly, but their distribution is strict. This method well shows the general harmony of the homeostasis, but no information about the actual processes in the molecular reactions of the cells. However, with the relatively high frequency (in the audio range up to 20 kHz, which changes 20.000 times in a second) and the vast number of enzymatic reactions, this method satisfactorily approaches reality stochastic meaning. The reactions occur in a randomized fashion in a large target. There are stochastically several proper excitations from the few billion excited molecular reactions. This is presently the best harmonizing approach.

2) Measure one of the personal electric signals (like heart rate, nerve-activity), and apply it as a compulsory modulator. This approach is very personal, but the signal depends on the patient's actual state, stress, mood, or the development of the disease, so it may be that its power density function deviates from the ideal $1/f$ scaling. In such a case, the modulation is suboptimal.

3) The local physiological signals could detect the target-oriented control signal. This method could compare the harmonic healthy host tissue with the anharmonic malignant tumor. This simple principle, however, has complications:

a) The non-invasive impedance measurement is inaccurate, depends on many internal and external modifying factors, so it is unsatisfactory. If the impedance measurement is not accurate, then why accurate enough treatment with a non-invasive impedance basis? The treatment uses a high-frequency carrier of the modulation, and the radiofrequency delivers the information to the target, and the electrical nonlinearity of the cellular membrane applies the info directly to the targeted cells.

b) Choosing the control target is not easy in such a complex disease as malignancy, where we have no precise information about the systemic effect of the tumor. (The present imaging and measuring technique or not cellular accurate.)

c) An electric signal is requested directly from the control target to measure its physiological harmony. This is usually the local arterial blood-flow fluctuation. In most cases, it needs invasive measurements, and even with this, the accuracy to form an appropriate signal is low.

4) The modulation signal may be applied not only for the treated target but also for the central energy supply manifested in the heart rate. The heard delivers the oxygen, nutrients, and electrolyte components (including special cells and compounds) which energize the dynamics all over the body. The heart-rate

variation is the result of the parasympathetic and sympathetic controller signal summary in the sinus nodes [27]. The $1/f$ signal of the vagus nerve could harmonize the overall metabolism by nerves' action and control the oxygen supply by the heart rate, which determines the homeostatic stochastic process.

3. Result—The Personalization

The template will number citations consecutively within brackets [1]. The sentence punctuation follows.

The study of biomarkers evaluates the actual status of the organism with possible indications of the presence of locally systemically derail of homeostasis, forming pathological condition [28]. A particular group of biomarkers is the tumor markers, which refers to an elevated amount of body-identical substance in a tumorous patient, while it has only a low amount or not at all in a non-tumor patient. The tumor markers do not have enough diagnostic value in prevention, so the biomarkers have emerging importance indicating deviation from the healthy homeostatic balance. The deviation of the biomarkers from the healthy standard has three values [29], which are especially important for cancer [30].

1) Diagnostic biomarkers help the accurate analysis [31], and the design of clinical trials [32];

2) The prognostic biomarkers can indicate the possible prognosis of the disease [33];

3) The predictive markers can inform about the efficacy of the applied therapy [34].

The medicine practice needs reliable biomarkers indicating a disease/tumor early, showing its growth, spreading, being effective, or ineffective in therapy. It is extremely important to assess and monitor the general condition of patients during treatment to assess how well they are receiving the therapy they are receiving, but we can also obtain the information needed to maintain an adequate quality of life. The Karnofsky scale (in the range of 0 to 100, the patient's state of health), the ECOG system (scale of 0 to 5) may be helpful. In addition, questionnaires assessing physical, social, emotional, and functional well-being, such as EORTC QLQ-C30 or FACT-G [35].

According to the present practice, sampling is necessary to determine the prognosis of the cancerous patient. The pathologist provides staging and grading based on the standardized categories. The basic guidelines and protocols describe a generalized proposal for treating patients considering the pathological results. However, the prognostic factors used at present lack stable reliability [36]. Although it would be desired to provide personalized prognosis and decision-making, taking into account the patient's individual clinicopathological and psychological status. Any new reliable prognostic factor and connected therapies (theranostic methods) are expected to step towards personalized treatment. According to the principal considerations [13] [14], and the emerging practices [37], the modulation of a carrier signal could be a reliable option of personalized

therapy. The application of modulated carrier presently applied mostly on oncology, but its non-oncological applications are also possible [38] [39] [40] [41].

3.1. Systemic Regulation

The homeostatic regulation shows some measurable electric signals for non-invasive detection of its proper functioning. The non-invasive detection of biomarkers has an extra advantage: less burdensome for the patient and more straightforward for the physician. This practical request emerges the various electromagnetic signal detection, like the Electroencephalogram, (EEG); Electrocardiogram, (ECG); Electromyogram, (EMG); Electrooculogram, (EOG); Electroretinogram, (ERG); Electrogastrogram, (EGG); Galvanic skin response, (GSR); electrodermal activity, (EDA), electrical impedance tomography (EIT), etc. These signals have not only prognostic and diagnostic value, but could be active therapeutic option to correct the deviations [42] [43] [44] [45]. In the following, we study two undoubtfully systemic regulatory signals: the heart rate and the nervous activity.

3.1.1. Vagus Nerve Signal

There are several methods for studying the autonomic nervous system. There are studies based on cardiovascular reflexes elicited by provocative maneuvers. Neurotransmitter levels can also be examined. The cholinergic part of the autonomic nervous system can be performed, for example, by examining sudomotor function (the reaction of sweat glands to various stimuli) [46].

The vagus nerve has an important homeostatic role. Its efferent position gives regulation signals for many muscles and various organs. It participates in the cardiovascular, respiratory, gastrointestinal, metabolic, control, and glucose homeostasis (pancreas, liver, kidney) regulation and controls inflammation by the spleen [47]. The afferent activity includes a significant part (>80%) of the nervous structure transmitting information to the central nervous system about the functioning of the organs of the body [48].

Several studies proved the therapeutic effect of vagus nerve stimulation (VNS) [49]. The emerging application of VNS is transcutaneous, primarily focusing on the auricular branch of the vagus nerve [50]. This non-invasive method targets several disorders, like migraine, tinnitus, headache, pain, applied in both cervical and ear sides. Importantly intensive studies started to clear the possible application of the VNS autoimmune and autoinflammatory diseases [51] and immunity [47].

The importance of studying the autonomic nervous system, among other sciences, is already outlined in oncology. Autonomic neuronal dysfunction has been shown to affect 80% of patients with advanced cancer [52]. The vagus nerve controls glucose homeostasis [53], which is particularly important for cancerous processes. Vagus nerve activity affects tumor growth by inhibiting tumor-promoting mechanisms. The significance of its study in a wide variety of tumors is known. The results of several articles show that vagus activity may play a prog-

nostic role in cancer.

Tumor cells can take advantage of the benefits provided by factors secreted by nerve fibers to produce a stimulating microenvironment for the survival and proliferation of their cells. A reciprocal interaction exists between tumor cells and nerves in humans [54]. Tumor cells induce nerve growth in the tumor microenvironment by secreting neurotrophic factors. The nerves show up as essential regulators of tumor progression. Sympathetic nerves drive tumor angiogenesis with noradrenaline release, increases the migration capacity of tumor cells, and determines the direction and development of metastases, while the cholinergic fibers of the parasympathetic nervous system, in turn, infiltrate tumor tissue and affect tumor cell invasion, migration, and distant metastases [55]. The sensory and parasympathetic nerves stimulate tumor stem cells, while at the same time, the parasympathetic nerves tend to inhibit tumor progression. This balance forms the dynamic complexity of the nervous interactions [56].

The vagus has been an essential pathway in the early preclinical stage of tumorigenesis through the information to the brain about preclinical tumors with an immune-nerve information transformation. It partially regulates tumor formation and progression [57].

The tumor microenvironment has a fundamental influence on its features [58]. It contains innate and adaptive immune cells [59], which have Janus-face behavior, could inhibit [60] or support tumorous processes [61]. A clinical trial shows the feasibility of vagal neuroimmunomodulation as the prognostic factor for pancreatic cancer, and so, the method offers a new prognostic biomarker of advanced cancers [62]. Furthermore, active adjuvant therapy of neuromodulation of cancers improves the quality of life in advanced cases [63]. It is clinically shown that the VNS increases the complexity of heart-rate variability, allowing more stable homeostatic control [64], having a higher probability of a better quality of life and more prolonged survival.

The experimental and clinical observations indicate that one of the most promising and far more objective methods for studying the autonomic nervous system is to analyze heart rate variability (HRV).

3.1.2. Heart Rate Signal

It was a long time ago realized that the chaos in physiology has special meaning [65]. The "constrained randomness" [66] is usual in physiology, and its study is a valuable tool to understand its mechanisms as well as recognize the deviation from "normal". The analysis of the noise-like profile of hear-beat in the healthy subject shows $1/f$ power-law distribution was recognized early [67], and this "chaos" was associated with time-fractal processes in the living organisms. The heart frequency components' expected flat or normal distribution became long-tail, self-similar distribution with scaling possibility.

The heart rate variability (HRV) describes the variability in the intervals between heartbeats. The temporal fluctuation of heart rate is due to autonomic nervous system regulation; it is created by interacting the sympathetic and para-

sympathetic nervous systems contributing to the measured variation of the signals [68]. HRV strongly correlates with vagus activity [69]. The most common area of HRV analysis is the study of cardiological problems [70]. However, it is often used for other diseases, like diabetes [71], renal failure [72], neurological [73], and psychiatric changes [74], but it is also used for sleep disorders [75] and some psychological phenomena [76]. The viability of using HRV measurement is based on non-invasiveness, ease of construction, and reproducibility [77]. Nowadays, the HRV offers a possible prediction of disease onset and prognosis [78], and so, its application has a significant increase in oncology [79].

The change in heart rate from beat to beat (RR [ms] intervals, the most observable peak in QRS complex in ECG signals) results from the balancing interaction of parasympathetic and sympathetic effects on the sinus node [80]. The RR is frequently estimated by heart rate (HR [beat/min]), which is easy to measure in daily practices. The variability is most frequently measured by time-domain analysis. The basic parameters to evaluate its uses the n^{th} RR interval ($(\text{RR})_n$), and the average value ($\langle \text{RR} \rangle = \frac{1}{N}\sum_{n=1}^{N}(\text{RR})_n$). The calculated time-domain evaluation parameters are:

- the standard deviation of RR ($\text{SDNN}[\text{ms}] = \sqrt{\frac{1}{N-1}\sum_{n=1}^{N}\left[(\text{RR})_n - \langle \text{RR} \rangle\right]^2}$)
- the square-root differences between the successive RR intervals:
  ($\text{RMSSD}[\text{ms}] = \sqrt{\frac{1}{N-1}\sum_{n=1}^{N-1}\left[(\text{RR})_{n+1} - (\text{RR})_n\right]^2}$).

Some other characterization of the time domain of HRV is used for particular purposes, like

- NNxx [beats], is the number of successive RR interval pairs that differ more than xx [ms];
- pNNxx [%] is the NNxx divided by the total number of RR intervals.

The time-domain of HRV changes is analyzed for its short-range (SD1), which is connected to the RMSSD [81] and long-range (SD2) features [82]. The Poincare plot is an excellent visualization of the short and long-range changes by studying the subsequent RR-intervals; plots each RR_{n+1} as a function of the previous RR_n interval [83]. Poincare plot analysis gives info about long-range by the $\text{RR}_{n+1} = \text{RR}_n$ line visualizing how continuous the development in step-by-step points, while its perpendicular line in the midpoint (zero points) shows how the short-range deviates from the long trends, compared the beat-to-beat info to the expectation of the longer performance of the heart [84]. The nonlinear homeostatic regulation could be followed by Poincare sections [85], with "stroboscopic flashes" synchronized to the neuron activity. Due to its simplicity and clearness, an emerging quantitative-visual technique categorizes the degree of heart failure by functional classes in patients [86]. The SD1 and SD2 can be calculated with standard time-domain parameters [87]. The calculation needs to introduce the standard deviation of the successive differences of the RR intervals,

denoted by $\mathrm{SDSD}=\sqrt{\left\langle\left(\Delta \mathrm{RR}_n\right)^2\right\rangle-\left\langle\Delta \mathrm{RR}_n\right\rangle^2}$, where the $\langle\,\rangle$ a sign denotes the mean (average) value, and so $\left\langle\Delta \mathrm{RR}_n\right\rangle=\left\langle\mathrm{RR}_n\right\rangle-\left\langle\mathrm{RR}_{n+1}\right\rangle$. The short and long-range characteristic values are: $(\mathrm{SD1})^2=\frac{1}{2}(\mathrm{SDSD})^2$ and $(\mathrm{SD2})^2=2(\mathrm{SDNN})^2-\frac{1}{2}(\mathrm{SDSD})^2$. In stationary conditions: $\left\langle\Delta \mathrm{RR}_n\right\rangle=\left\langle\mathrm{RR}_n\right\rangle-\left\langle\mathrm{RR}_{n+1}\right\rangle=0$. In this case, we get statistically: RMSSD = SDSD. In consequence, RMSSD has a role in both the short- and long-range interactions in stationary conditions. Naturally, the HRV results and parameters depend on the time length of the registration [88].

The detrended fluctuation analysis (DFA) method is devoted to the scaling of correlation inside the time-domain of the signal [89]. This particular method scales the slopes (trends) of the linear regression fit to the *n*-length grouped segments of measured points in various scales. The sum of actual deviation of the points in the group from their average value is: $y(k)=\sum_{j=1}^{k}\left(\mathrm{RR}_j-\langle\mathrm{RR}\rangle\right)$. Fit a linear regression (least-squares method) to these points. The obtained regression line is $y_n(k)$, and so the detrended series $F(n)$ is scaled by *n*: $F(n)=\sqrt{\frac{1}{N}\sum_{k=1}^{N}\left[y(k)-y_n(k)\right]^2}$, calculating it with different segments and shown in double logarithmic scale vs. *n*, [90] **Figure 4**. The categorization of the noises is similar to the power density, but the DFA slopes differ from the power density slopes.

The relation of the SDNN and the DFA shows a connection to predicting the survival of patients studying in 7 years intervals [91]. When both parameters (SDNN and DFA) are high, all patients survived 7.5 years. When both were low, 50% of the patients involved in the study died within 2 years. In the groups with high DFA and low SDNN 60% died under 2.5 years, while the SDNN was high and, DFA low, 70% died within 3.5 years. Results support the idea that the health status needs high self-organizing in the system. When the self-organized chaos starts to disappear, and a series of subharmonic bifurcations appear, the ventricular fibrillation becomes more likely [92] [93], the bifurcation phenomena are pathological [94]. Note, the bifurcation in this meaning decreases the self-similar time-fractality, which appears again when the bifurcative processes are sequentially inserted into each other (fractal process) and form Cantor-like fractal in the dynamics, shown in **Figure 3**.

The variation evaluation with time-domain has some problems because the form of the signal could substantially differ while the RR average and the RR standard deviation could be identical [95]. The frequency domain, determining the *S*(*f*) power density, gives information about the distribution of the frequency components, so it clears the form of the signal [96]. The spectral analysis is a valuable tool in the analysis of the autonomic function of HRV [97]. The study of the frequency spectra reveals the healthy dynamics of the heart and is related to the overall homeostatic condition.

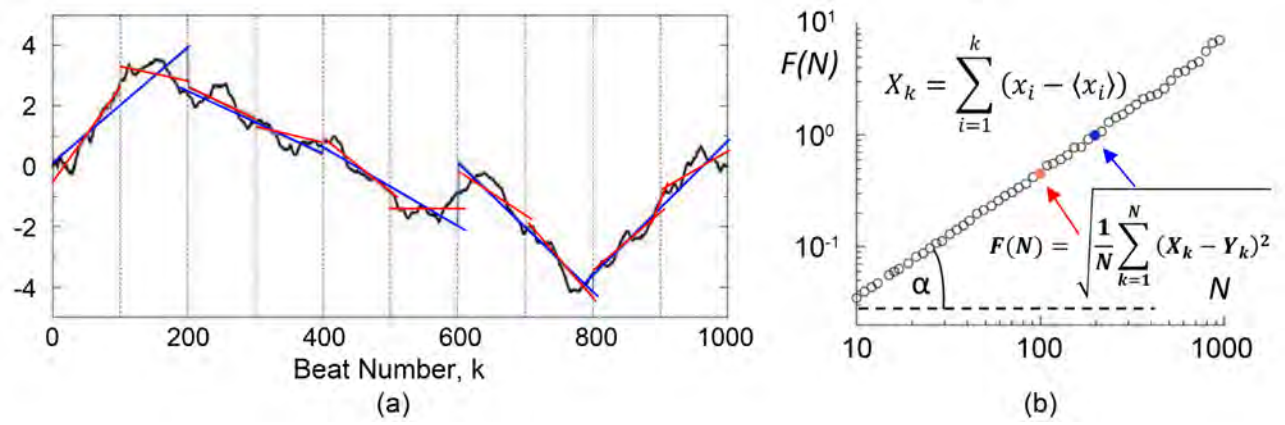

Figure 4. The detrended fluctuation analysis (DFA) method [90]. (a) The process of evaluation of scaled groups of noise parts by the linear regression model. Red lines are the best fit for the subsequent intervals counting 100 beats. The blue fits 200 beats and so on with all possible groups of the beats. (b) The measured slopes from (a). The points for red and blue fits are indicated on the line. The scaling clearly shows linear dependence of grouped slopes.

The frequency domains divided by the physiological ranges [98] like:

- Power ($S_{ULF}(f)$[ms^2]) ultra-low frequency range (≤0.003 Hz) power density ($S_{ULF}(f)$[ms^2]), follows the change s of the body's core temperature, the circadian rhythm, the renin-angiotensin controlling system, and the metabolic processes;
- Power ($S_{VLF}(f)$[ms^2]) of the very-low-frequency range (0.0033 - 0.004 Hz) observes the long-range controlling mechanisms, hormonal processes, heat-control;
- Peak frequency ($P_{LF}(f)$[Hz]) in the low-frequency range (0.004 - 0.15 Hz) is connected to the baroreflex activity and the balancing of sympathetic and parasympathetic nerve actions;
- Power ($S_{LF}(f)$[ms^2]) in the low-frequency range (0.004 - 0.15 Hz) is connected to the baroreflex activity and breathing;
- Peak frequency ($P_{HF}(f)$[Hz]) in the high-frequency range related to vagus nerve tone;
  - for adults (0.15 - 0.40 Hz);
  - for babies (and sometimes after sports activity) (0.24 - 1.04 Hz);
- Power ($S_{LF}(f)$[ms^2]) in the high-frequency range related to vagus nerve tone (0.15 - 0.40 Hz);
- Sometimes the ratio of the power of low (0.004 - 0.15 Hz) and high (0.15 - 0.40 Hz) frequency bands ($\frac{S_{LF}(f)}{S_{HF}(f)}[\%]$) is used to study the balance of the vagal and sympathetic activity.

Through the connections of the autonomic nervous system, vegetative, somatic, and psychic effects are integrated into the instantaneous heart rate and variability [99]. Due to the neuro-controlled (sympathovagal) balancing, the HRV is a feasible parameter to quantify homeostasis [100]. In consequence of the homeostatic character, its measurement could be a valuable tool in clinical practic-

es [101].

The vagus-mediated HRV may be associated with higher-level (brain) executive functions. One region, the anterior cingulate cortex, was interestingly found to be associated with both vagus activity and cellular (NK-cell) antitumor immunity [102].

Inflammatory markers and HRV parameters show correlation. The LF-HRV was inversely proportional to CRP, IL-6, fibrinogen, and HF-HRV was inversely proportional to CRP and fibrinogen. These also supported the existence of the vagal anti-inflammatory pathway [102] [103].

Vagus tone (measured by HRV) influences the nervous-immune response to acute stress. This was demonstrated in a study in which people with low and high baseline HRV participated and were presented with a learning task (acute stress factor). With this acute stress, NK-cell and noradrenaline levels in peripheral blood changed only in the high HRV group. Both prefrontal cortex and striatum activity correlated only with values indicative of the immune system only in the high HRV group. It is hypothesized that high vagus tone may mean a more flexible top-down (brain) -down (immune system) regulation [104].

The frequency domain is a helpful tool for analyzing the signal components, but the obtained frequency distribution does not inform us about the signal trends and how the segments correlate. For the personalization, the amplitude-phase has to be considered, as shown in (24).

The HRV can be a valuable biomarker to assess disease progression and outcome, and even it could be the future remote, wearable biomarker technology [99], which controls not only the diseases, b but also nutrition and wellness [104].

The HRV contains the homeostatic stage of the patient, so it mirrors the various, not disease-connected parameters (like the age, gender, medications, physical and mental status, and even such simple parameters as the body-position, respiratory rhythm, stress) [105]. This sensitivity of general conditions could influence the medical decisions, which develops a distrust in the method. High practical routine and well-controlled conditions are necessary to obtain the medical value of the results. Furthermore, HRV does not directly measure parasympathetic or sympathetic activity. Its features are indirect, only qualitative information on the autonomic activity, the quantitative measures need independent methods. In addition to methodological errors, there may also be technical pitfalls in data collection, signal processing, and interpretation, leading to inaccurate HRV measurement, l and wrong medical decisions [106] [107]. The mixed information causes that the HRV application as a diagnostic tool does not widely apply in medical practice.

3.2. Local Effects

The modulation is well applied locally in the tumor treatment [108] by forcing the local arrangement order in space-time to fit homeostasis. The local applica-

tion has similar goals that the systemic VNS, forcing the healthy balance. However, the local application is only in the small part act on the nervous system (mainly on parasympathetic, while the selection is connected to the function of the vagus). The dominant effect forces the healthy local arrangement in space (intercellular bonds) and in time (intracellular signal-transmissions). The practice of local application is the modulated electrohyperthermia (mEHT, trade name: oncothermia®), which is widely applied in clinical practice [109].

3.2.1. Pattern and Molecular Recognition

The differences between the tumor and healthy host tissue are significant. The tumor cells have a higher metabolic rate than the host because of proliferative energy demand, have no networking connection with the neighboring cells, separate individually, have different membrane structures with more transmembrane lipid rafts, and differ in their overall structure too. This last is used by the pathologist when studying the pattern of the specimens and recognizing the pattern deviation from the expected healthy order. This pattern recognition is one of the factors of the diagnosis, staging, and prognosis too. So, the tumor structure differs, which can be recognized by the homeostatic signal, due to the missing dynamic harmony. In this way, the disordered tumor selectively absorbs energy from the harmonic fluctuation (modulation with $1/f$ noise), and the various consequences kill the cells. The free genetic information allows recognizing the deviation by the adaptive immune system, which may act against [110] [111].

A part of the modulation effect is the broken cadherin complexes' re-bonding and allowing the intercellular connections again [112] [113]. This reconstruction turns the individual precancerous cells to the network and blocks their movement, decreasing the risk of metastases. The rebuild network allows the intercellular connections, gives the cell a chance to return to normal conditions, or has a signal, and turns to apoptosis.

The physical analysis of temperature-dependent effects of mEHT [114] calculated that the most likely effect is electromagnetic excitation, which develops non-thermal effects of radiofrequency electromagnetic fields [115]. The physical assumptions successfully indicated the possibility that the physical methods may recognize and use the heterogeneity of the target [116]. The vagus nerve assists the body's thermal sensitivity and thermoregulation [117].

3.2.2. Molecular Excitation

Other important local effects of mEHT are the molecular excitations of the cellular receptors and, in general, the transmembrane proteins. The nonthermal membrane's temperature-independent effects of electromagnetic fields had serious debates and controversial opinions. The present research provides some preclinical and clinical data for the nonthermal antiproliferative effects of exposure to mEHT. The excitation promotes membrane vibrations at specific resonance frequencies, which explains some nonthermal membrane effects, and/or

resonances causing membrane depolarization, promoting the Ca^{2+} influx [118], or even form a hole on the membrane. mEHT may be tumor-specific owing to cancer-specific ion channels and because, with increasing malignancy, membrane elasticity parameters may differ from that in normal tissues. The Arrhenius plot fits the thermal properties in mEHT experiments [119], so the treatment is a complex mixture of the thermal and nonthermal processes [120]. The protecting chaperones induced by the heat shock are exhausted [121], so the safeguarding does not suppress the electromagnetic reaction. This mechanism resolves the radiotherapy resistance of pancreas adenocarcinoma cells [122].

The molecular excitation is proven in vitro, showing how different the mEHT complex electromagnetic therapy is from conventional heat-therapies [112]. The recent review of the tumor-damage mechanisms collects the preclinical results [113].

4. Discussion

The modulation of the external bioelectromagnetic signals has well-explained principles [13]. The carrier frequency helps in the selection mechanisms, while its modulation acts. The modulation supports homeostasis by its time fractal ($1/f$) frequency distribution [108]. The modulation could have multiple effects locally and systematically. The local force for the homeostatic control acts as a further selection factor regarding the lost control of the tumorous cells. Furthermore, the modulation forces the healthy dynamical order providing a compulsory process for apoptosis of the out-of-control cells. HRV may characterize the homeostasis [124], presenting the complexity of the system.

The well applied time-fractal current flow may activate the structural fractals in the living systems, and the personal fractal structure could modify the time-fractal pattern, too [125]. The fundamentally non-linear physiological system dynamics work on the edge of chaos, a border of order and disorder showing a constant dynamic interplay between these states [126]. The challenge of the homeostatic equilibrium is the apparent chaos. The chaos looks complete randomness which is only ostensible. The chaos in biosystems results from the stochastic self-organizing and the energetically open system, which directly and permanently interacts with the environment. Its structural and temporal structure is fractal, which appears in the fundamental arrangements of the self-similar building and dynamism of the energy exchanges internally and externally. The living processes are complex. They are in self-organized criticality (SOC) [127], which is formulated, as the "life at the edge of chaos" [128]. This chaos is the realization of a well-organized stochastic (probabilistic) system [129]. The disordered chaos is apparent [130].

A simple bifurcation could help to understand this "edge of the chaos" phenomenon. The processes must keep their dynamic energized form. When their energy at the energy breaking point is too low, the process stops and "freeze" in one of the potential wells. However, when the provided energy is too high, the

system loses its control, the promoter-suppressor balance can't regulate the processes Figure 5. (Like Einstein formulated: "Life is riding a bicycle. To keep your balance, you must keep moving." [131]) The common idea that bio-systems evolve toward equilibrium is a misperception of reality.

Self-organized chaos was studied in all the living processes like, for example, in immune activities [132], in nerve system [133], in genetic phenomena [134]. The realization of the "edge of chaos" is very personal due to the determining parameters, and their intensity differs from person to person [135]. This character of the living complexity requests personalized treatments.

DFA evaluation of the signal measures the self-similarity scaling of the fluctuations by scaling parameter. This evaluation is similar to the box methods in structural evaluation of the fractals when the scaling is the size of the box like in DFA, the size of the scaling interval. The other time-domain studies focus on the standard deviations of the fluctuations (like the HRV methods the SDNN), which also depends on the length of the investigated interval so also has similarities with boxing evaluations. The standard deviation changes by the s box-sizes in the N_s step-number, and has a scaling behavior:

$$S(s)=\sqrt{\frac{1}{N_s}\sum_{i=1}^{N_s}\left(x_i-\langle x_i\rangle\right)^2}\propto s^H \tag{25}$$

The exponent is named in honor of HE. Hurst, who first observed this scaling at the water level fluctuations at the Aswan dam in Egypt. The Hurst exponent, H characterizes the scaling exponent of the $S(f)=f^{-\beta}$ power density function (PDF, frequency domain) fitted to the scaling function (calculated for $q=2$) in the time domain:

$$\begin{aligned}\beta&=\begin{cases}2H-1 \text{ if } -1<\beta<1 \text{ (PDF)}\\ 2H+1 \text{ if } +1<\beta<3 \text{ (PDF)}\end{cases}\\ \alpha&=H+1 \text{ (DFA)}\end{aligned} \tag{26}$$

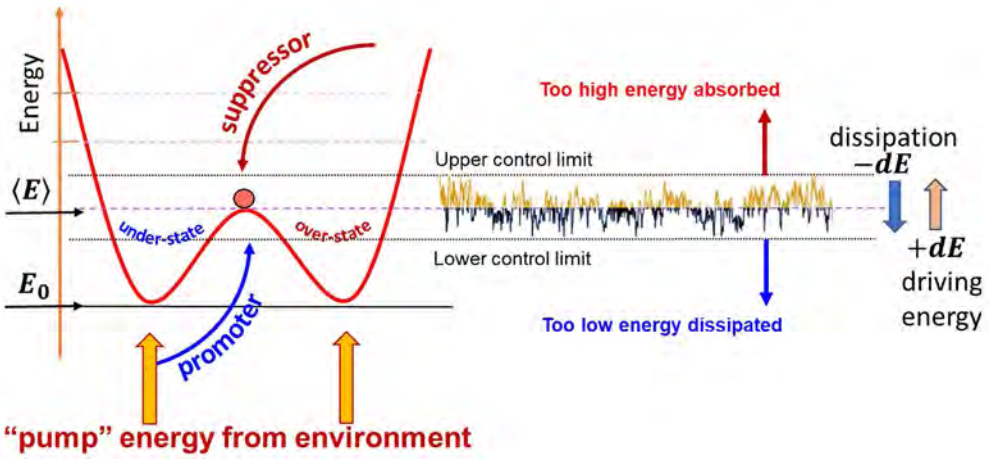

Figure 5. Permanent dynamic changes of the energetically open system cause a never rest situation. The dissipation consumes the energy, while the open, energetic situation drives the process. Promoters and suppressor balance never stop, the dynamism makes life on the "edge of chaos".

In time series: $0 < H < 1$. The $0 < H < 0.5$ describes anticorrelation, while $0.5 < H < 1$ characterizes the correlation, long-memory process. There are two border values: $H = 0.5$ is the while noise (no correlation), $H = 1$ is the pink noise [136].

However, most complex systems have no single scaling. The living body contains variants of fractal templates in space-time, and so the exponents of self-similarity could change by parts. The multifractal analysis considers the scaling as not a global behavior but local (multifractality). The multifractality appears in the dynamics of the biological processes. The scaling varies in time. The nonlinearity of the processes strongly influences the multifractality.

In the case of multifractality since the scaling property is heterogeneous, H will be different for smaller and larger fluctuations in the process and thus the generalized Hurst exponent, $H(q)$ is obtained as a function of q [137]. It is the scaling of the q^{th} momentum of the fluctuation and called generalized Hurst exponent. The generalized scaling function is:

$$S(q,s) = \left(\frac{1}{N_s} \sum_{i=1}^{N_s} \left(x_i - \langle x_i \rangle \right)_s^q \right)^{1/q} \propto s^{H(q)} \tag{27}$$

The generalized multi-scaling gives back the mono-scaling Hurst exponent when $q = 2$ so $S(2,s) \propto s^H$. In the case of monofractality, the scaling property is homogeneous and thus independent of q. With the growth of the "box-size" by growth of s the different variances (scaling functions by q) approaches each other, and at the largest size (the L size of the entire sample) point on a common focus [138] $S(q,L) = SD(L)\ \forall q$, where $SD(L)$ is the standard deviation character of the entire signal.

The fingerprint of the personalized "chaos" is the self-similar noise of interconnected HRV and VNS in both the time (variation-based evaluations) and frequency ($S(f)$ based evaluation) domains. The characteristic behavior of the frequency-based approach is the $1/f$ noise. Consequently, forcing the homeostatic control needs $1/f$ spectrum in the frequency domain. In an ideal case, the frequency domain has a single exponential character. However, it is not the general case; it only approaches a part of the anyway curved double logarithmic plot of the spectral density $S(f)$, which characterizes a multifractal behavior of the system's dynamics.

The multifractal structure changes the frequency by time, so the Fourier transformation, which produces $S(f)$ power density function (PDF) in the monofractal approach, is not constant in all the observed time. The problem of the multifractal analysis has similarity to the Heisenberg principle: one cannot get the infinite time and frequency resolution beyond Heisenberg's limit: $\Delta t \Delta E \geq \frac{h}{4}$ so $\Delta t \Delta f \geq \frac{1}{4}$. Consequently, one can calculate high-frequency resolution accompanied by an insufficient time resolution or has high resolution in time with a poor frequency resolution. The method of wavelet transformation was developed

for space-time multifractal description [139].

For proper multifractal analysis, a local power-law had been developed. This method approaches the function with its Taylor series and observes the scaling in the difference of the real and approached function:

$$\left| f(x) - \sum_{k=0}^{N} b_k (x - x_0)^k \right| \le C \left| x - x_0 \right|^{h(x_0)} \tag{28}$$

The $h(x_0)$ value is the Hölder exponent. This is a local power-law, showing local self-similarity in a given discrete t time-point. In the case of any (multi or mono-fractal) approach $h(t)$ is the power of the scale. In monofractals the exponent is constant: $h(t) = \text{const}$. The Hölder exponent forms trajectories when calculated in real-time. The fractal dimension of disjunct sets of the same Hölder exponents in the histogram approach is the multifractal or singularity spectrum, with generalized dimension $D(h)$, which is mostly used for multifractal characterization. The "size" of the singularity components is $\propto s^{D(h)}$. The monofractal Hurst exponent $H(2)$ tightly connected (but not equivalent) to the maximum (middle) Hölder exponent of the singularity spectra, while the $\Delta H(n)$, the multifractal character described by $\Delta H(n) = H(-n) - H(n)$ is the width of the multifractal spectra. The maximum of $D(h)$ is connected to the autocorrelation and the width of the non-linear character of the processes, introducing the multifractal scale exponent $\tau(q)$ from wavelet transformation [140]. This exponent connects all the multifractal characters:

$$\tau(q) = qH(q) - 1, \quad h(q) = \frac{\mathrm{d}\tau(q)}{\mathrm{d}q}, \quad D(h) = \inf_q qh(q) - \tau(q) \tag{29}$$

The behavior of $\tau(q)$ describes the locally changing dynamic fractals, specifying the details that distinguish these from the global single-exponent character [141], **Figure 6**.

The well-established, widely applied and approved methods of evidence-based medicine (EBM) work with averages in many respects, as the inclusion criteria, like the sub-grouping of the eligible patients by various aspects. The monofractal application fits this approach, representing an overall average of the homeostatic

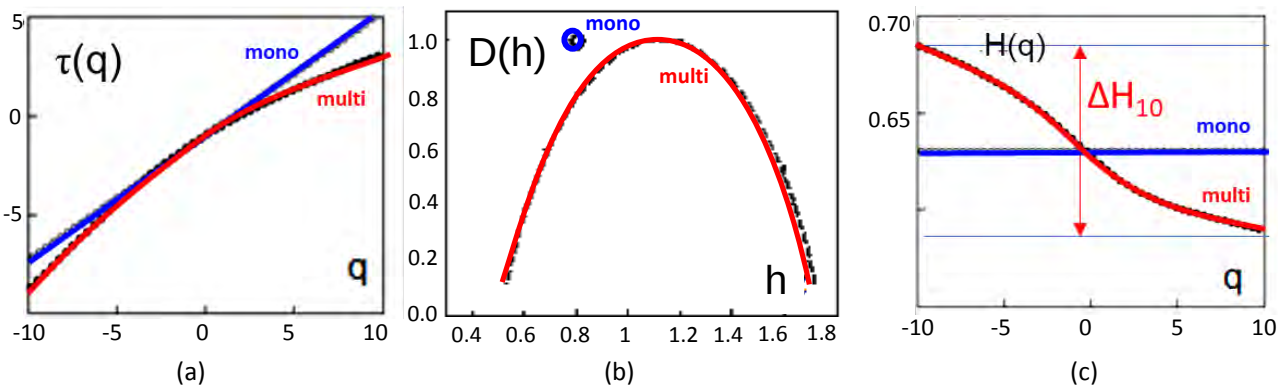

Figure 6. The changes of characteristic scaling exponents in mono-fractal and multifractal stochastic approaches. (a) scaling exponent by q^{th} momentum; (b) multifractal spectrum; (c) the generalized Hurst exponent does not change by $q = H(2)$.

control of the patients. However, the averaging has multiple pitfalls [135] [142]. The primary challenge is the averaging, despite that no such "average patient" who is supposed in the study exists. More personalization is necessary to avoid the averaging errors.

The fine-tuning of the information has to consider the time-domain signal analysis. The personalization principle is the inverse transformation of the time-series from the personally $S(f)$ by the distribution of the amplitude phases ($\varphi(\omega)$) shown in (24). The precise time domain is reconstructed, but it has also averaged in the distribution function of the phase $\varphi(\omega)$. The HRV time-domain has also high averaging due to the form of the signal is not present, only the mean and its standard deviation. However, the HRV and the inverse transformation of the amplitude of $S(f)$ by (24) represent different information about the person, so the combination of the two methods looks the most accurate in our present knowledge. The complex number of the amplitude $A=|A|e^{i\varphi(\omega)}=|A|\left[\cos(\varphi(\omega))+i\cdot\sin(\varphi(\omega))\right]$ of $S(f)$ in (24) contains the personal frequency order. The geometric representation of the single term of $S(f)$ in the complex sheet is a circle with the radius $R=|A|$, and a vector with angle of $\varphi(\omega)$. The personal order by geometric description of $\frac{|A|e^{i\varphi(\omega)}}{\sqrt{\omega}}$ from (24) connects these vectors where their size is proportional with $\frac{|A|}{\sqrt{\omega}}=\frac{|A|}{\sqrt{2\pi f}}$ **Figure 7**.

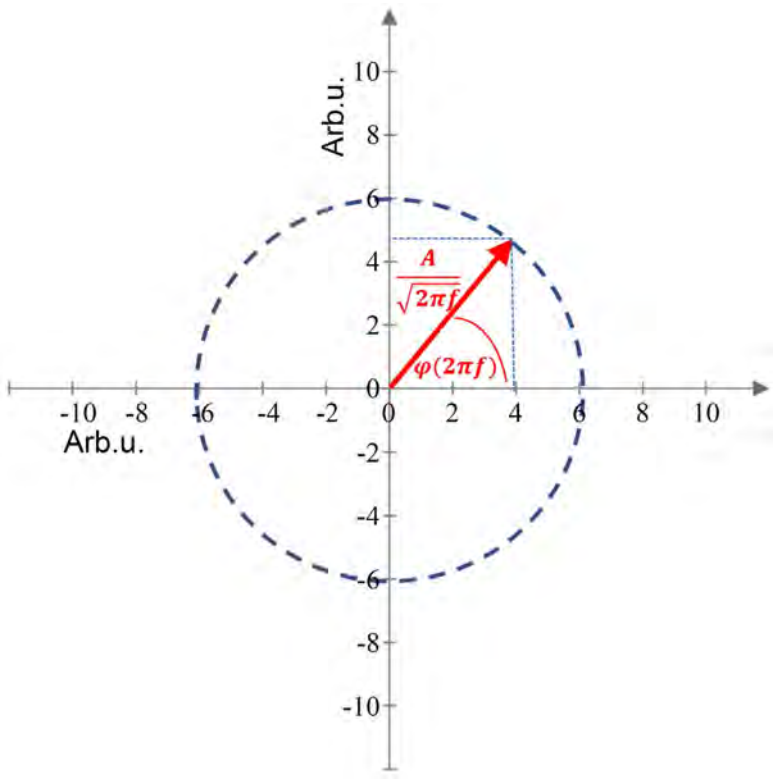

(a)

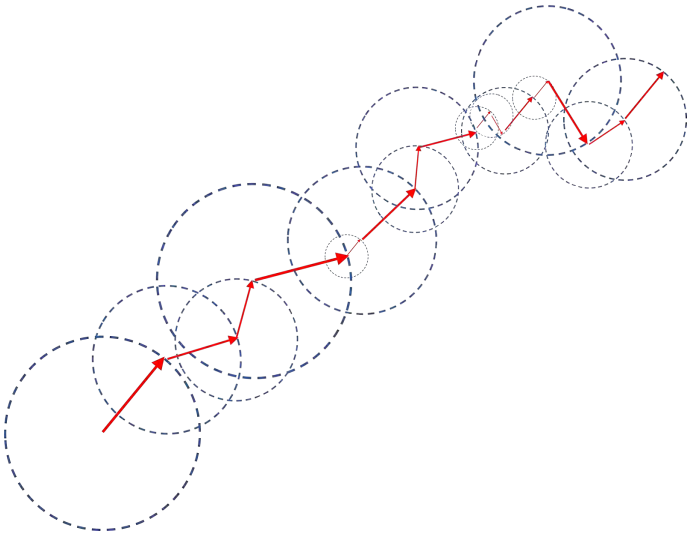

(b)

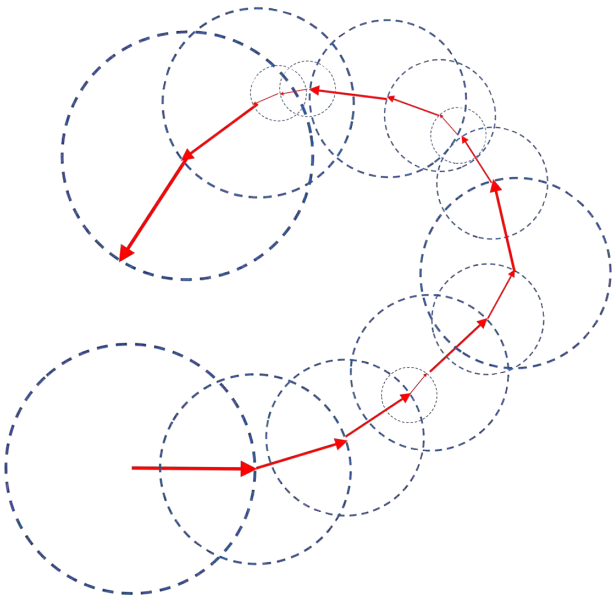

(c)

Figure 7. The series of the $\sqrt{S(f)}$ in personalization. (a) the vector representation of a single component. The vector rotates as the $\varphi(\omega)$ phase angle changes by the changing $S(f)$. (b) an example of the series of $S(f)$s, when the vectors jointly follow each other. The $S(f)$ changes hectically (noisy). (c) another example of the $S(f)$ series with monotonously growing phase angle $\varphi(\omega)$ in a series.

In reality $\varphi(f)$ has a personal distribution, which arranges the frequency order. In a random distribution, we may check the system how we construct the $Si(t)$ time-series of the signal from frequency series with inverse Fourier transformation **Figures 8-10**. Noteworthy that the $S(f)$ function is identical in all reconstruction processes from the $\varphi(f)$ series, because the phase angle does

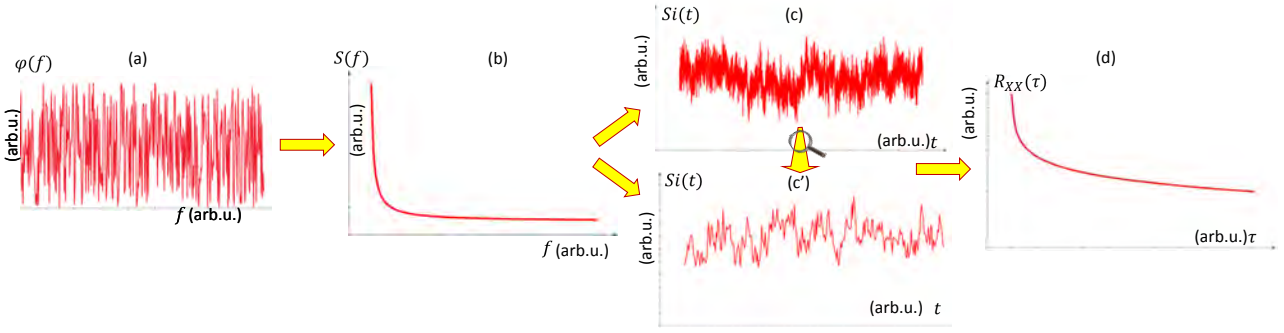

Figure 8. Reconstruction of the time-series from the power density function (PDF) (a) when the $\varphi(\omega)$ phase has a random distribution. (b) The distribution of phase by frequency from the $S(f)$ phase function on the (a). (c) The signal function in time (the time series); (c') the enlargement of the signal function in a small time interval; (d) the correlation function of the $Si(t)$ signal function.

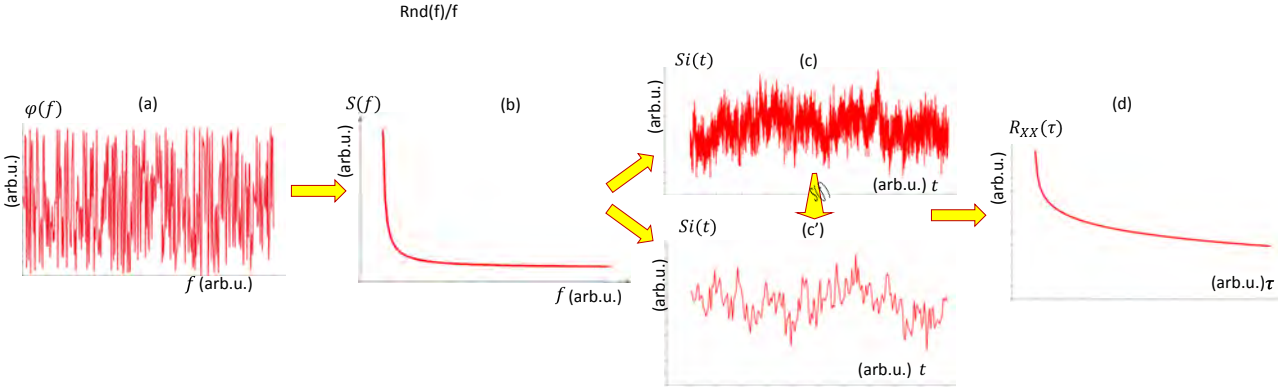

Figure 9. Reconstruction of the time-series from the power density function (PDF) when the $\varphi(\omega)$ phase has $1/f$ distribution. [this figure well follows **Figure 8**; the difference is most obviously seen on the incoming excitation and the $Si(t)$ spectrum] (a) distribution of phase by $1/f$ frequency; (b) the $S(f)$ function from the phase shown in (a) [it is identical with that, repeated only for the control of the calculation]; (c) the signal function in time (the time series); (c') the enlargement of the signal function in a small time-range; (d) the correlation function.

not change the value of the amplitude, only its direction changes on the complex coordination system.

The strong, definite Weibull distribution causes only minimal and mostly regular time series. Probably this is irrealistic in living systems. The periodicity-like form in correlation length is also the consequence of the well-defined original distribution shown in **Figure 10(a)**.

4.1. Forcing Homeostasis by Modulation

The next step of the personalized idea needs to force healthy homeostasis in the patient, who lost it due to the disease. First, the deviation from the healthy state must be measured, which could be checked with the time-(HRV) or frequency-($S(f)$) domain as well. This global information could be the reference for the development of the disease and the chosen treatment's success. Increased risk of progressive disease is connected with the gradual loss of complexity in the decrease

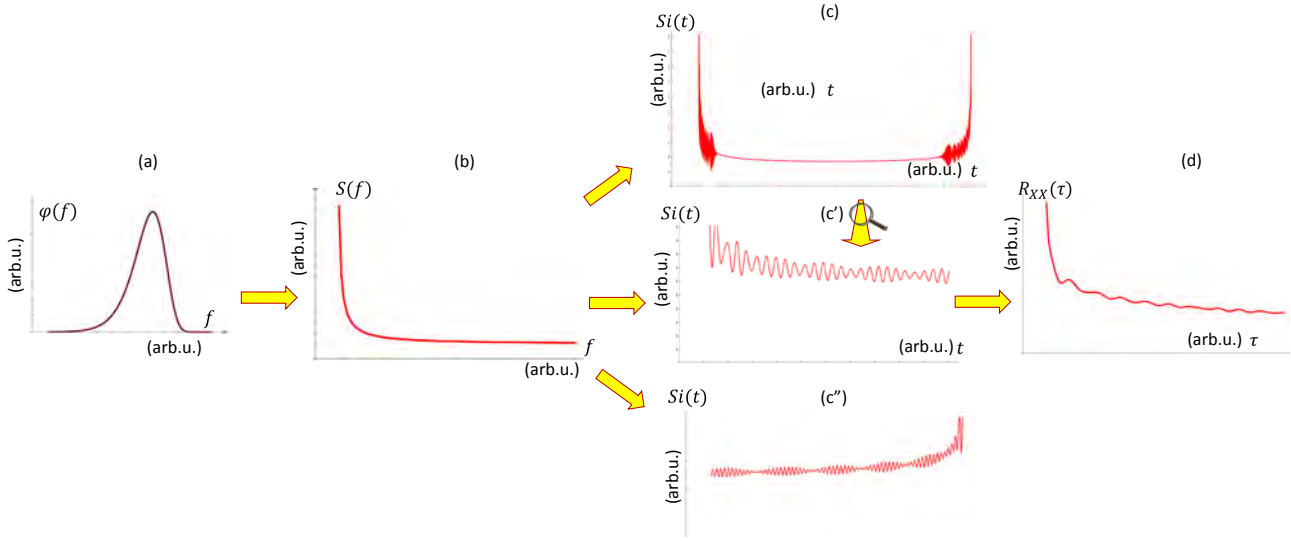

Figure 10. Reconstruction of the time-series from the power density function (PDF) when the $\varphi(\omega)$ phase has Weibull distribution. (a) distribution of phase by frequency; (b) the $S(f)$ function from the phase shown in (a) [it is identical with that, repeated only for the control of the calculation]; (c) the signal function in time (the time series); (c') the enlargement of the signal function in a small time-range; (d) the correlation function.

of the HRV in patients with cardiovascular diseases [64]. It is observed that the VNS associated to the parasympathetic tone, decreases the heart rate accompanied with increased complexity (increased HRV) especially in sleep [64]. The higher HRV values in various bands were positively correlated with disease regression in the actual band category. Higher HRV meant more advanced coping ability and thus better prognosis.

Together with the dynamic equilibrium's general character, it might be supposed that every person has an individual part of homeostatic control. The overall neuronal surveillance by the autonomic nervous system, the immune system, the transport systems, etc., has a particular path specific for a person and produces an individually coded $1/f$ homeostatic noise. In this sense, we can talk about personalized $1/f$ noise. As the (24) shows, the $1/f$ noise spectrum carries many kinds of information which are hidden in the $\varphi(\omega)$ phases of the amplitudes. The phase distribution carries the sequential information of the frequency series.

In the case of one individual subject, the information in the homeostatic noise has the same phase code since these are all results of the work of the same regulatory system. Important perspectives open with the personal homeostatic noise:

- In diagnostics, the measured noise spectrum's irregularities could signal that specific organs do not work correctly.
- In control of the therapy control, the measured changes of the noise spectrum could show the direction of the treatment triggered changes.
- In prognosis, the stored spectrum in individual "noise bank" taken when the patient is healthy could be compared with the actually measured noise prognoses the possible start of the irregularities in the body.

- In therapy, when the healthy fluctuation forces the homeostasis to correct the irregularities and blocks the iatrogenic processes, the healing is actively forced.

The last point is an active function of the noise. We concentrate on this application by personalization forming uniform general $1/f$ signal it is power spectrum. Like all the homeostatic control, the nervous system also follows $1/f$ power spectrum. The general regulator of physiological responses to internal and external stimuli is the nervous system. It is based on two large nervous sets like promoter/suppressor pairs: the sympathetic, which mediates catabolic responses, and the parasympathetic, which regulates anabolic responses. The main component of the parasympathetic nervous system is the vagus nerve. The vagus innervates most tissues dealing with nutrient metabolism, which is crucial for many body functions and cancer development [102] and therapy [58]. The balance of vagus activity with sympathetic regulation needs proper homeostasis [53]. The vagal nerve signals contribute to the care of homeostasis [143] [144].

The homeostatic time-fractal frequency domain (in general, the $1/f^{\alpha}$ noise) is optimal forcing information when no more personal parameters are available This average contains the optimal time-domain fluctuations also when the sole in log-log scale is near to $\alpha \cong 1$. The deviations of $\alpha \gg 1$ mean more step-by-step regulated dynamics (like the brown-movements) while $0 \le \alpha \ll 1$ goes to the white noise direction, to uncorrelated noise.

A possible constraint of proper homeostasis could be an external electromagnetic compulsory signal. The electromagnetic force is an overall effective influence because electromagnetism represents the biologically active force. Choosing the $1/f$ signal is a natural selection to induce a forceful corrective action. The penetration of the electric field into the body depends on the frequency of the signal. The penetration of the high frequencies is shallow, while the low frequencies penetrate deep.

On the other hand, the low frequency does not radiate, so the energy-coupling needs excellent contact in safe voltage application; otherwise, no effect exists. This condition complicates the non-invasive applications. Due to the signal having intensive low-frequency components and the broad spectrum of higher frequencies, the penetration will be heterogeneous; the proper frequency distribution cannot be overcome. The solution could be choosing the higher frequency carrier, which delivers its $1/f$ modulation with approximately proper amplitudes [145]. This modulation solution has a further advantage by its energy delivery, which makes additional mild heating [146], supporting the healthy enzymatic reactions in the body.

A further advantage is that the properly chosen carrier frequency delivers the information to selected regions of the heterogeneous target [147]. Furthermore, the current of the amplitude modulated signal flows through the fractal structures of the living organism, and the necessary frequencies could be selected by the structural dynamism as well. The broad modulation spectrum offers various

frequency subgroups, which allows complying with the local demands.

However, it has a disadvantage: demodulation is necessary for the system, which dominantly performs by the cellular membrane nonlinearity [14]. The modulation keeps the system in the regulatory interval, helps the complex living processes correct the faulty regions, and re-establish the healthy control [148] [149].

4.2. Immune Effect of Forcing Homeostasis

One of the effective systemic regulators of homeostatic controls is the immune system. Immune-system terminates many diseases and helps balance the symbiotic life with biotas and broader meaning, as the fundamental cellular reaction, control some inter and extracellular events by molecular chaperone functions [150] [151].

Research on the neural control of the immune response has traditionally focused on the role of the sympathetic nervous system and sensory nerves. However, recent studies have highlighted the role of the efferent parasympathetic system, particularly the vagus nerve, in immunomodulatory actions [58] [152]. The nervous and immune systems communicate in two-way pathways to limit inflammation and maintain homeostasis [58]. The vagus nerve stimulation activates neuroimmune reactions [153].

The vagus nerve is one of the modulating components of innate (like NK-cells) and adaptive (like T-cells) immunity [58]:

- inhibits the TGF-β1, which increases NK-cell expression;
- supports the expression and activity of cytotoxic T-lymphocytes;
- down-regulates the helper T-cells ($CD4^+$ function).

Efferent hepatic vagus activity has anti-inflammatory effects through local IL-1β and IL-6 secretion. This may be an important part of the theory of the beneficial outcome of the relationship between vagus and tumors [154].

The vagal activity reduces the inflammatory response by reducing cytokine release [103]. The B, and C fiber subtypes of the vagal nerve are involved in regulating the heartbeat [103]. This neuroanatomy suggests that the regulation of heart and inflammation by the efferent vagus can be separated. Electrical stimulation (1 V, 5 Hz, 2 ms) was found to be sufficient to elicit an anti-inflammatory effect but did not affect heart rate. Higher striding results decrease in heart rate; consequently, the vagal A fibers are connected to the anti-inflammatory signals. This separation limits the correlation between HRV and vagus-mediated anti-inflammatory effects [103].

The vagal immunomodulatory effect (cholinergic anti-inflammatory pathway) is intertwined with acetylcholine activity. Various immune cells (lymphocytes, macrophages, mast cells, dendritic cells, and bone marrow lymphoid and myeloid cells) express the significant components of cholinergic systems (acetylcholinesterase, choline transporters, AchE, nAChR) and produce acetylcholine. Consequently, the cholinergic system may play a role in regulating the immune

response through immune cells [58].

Other systemic effects of vagus nerve stimulation were observed in better outcomes in conditions such as irritable bowel syndrome, metabolic syndrome, diabetes, sepsis, pancreatitis, depression, pain, and epilepsy [102]. Low vagus nerve activity correlates with worse outcomes [102].

An important observation of the modulated treatment is the immunogenic hyperthermic action [155], which can be improved by the independent stimuli of the immune system by dendritic cell therapy [156] [157], or viral therapy [158].

4.3. Cancer and Homeostasis

Tumor cells and the connective tissue surrounding them contain immune cells. However, these cells are double-edged weapons; they can inhibit but also promote tumor growth. The inhibition processes are:

1) activated lymphoid cells can control the tumor growth and malignancy;

2) dense infiltration of T lymphocytes correlates with better prognosis.

While there are promoters:

- tumors often break down the tumor-infiltrating lymphocyte activity;
- supports the differentiation of tumor-associated macrophages (TAMs) and myeloid-derived suppressor cells (MDSCs), promote tumor growth by secretion of growth factors, and inhibition of T lymphocytes.

Mediators and cellular implementers of inflammation are essential components of the local environment of tumors. In some tumor types, inflammatory conditions are already present before malignant transformation occurs. Inflammation promotes proliferation, survival of malignant cells, angiogenesis, metastasis, weakens the adaptive immune response, alters the response to hormones and chemotherapeutic agents. The molecular mechanism of this tumor-associated inflammation may be an important therapeutic and diagnostic target [1]. In some types of tumors, oncogenic transformation induces an inflammatory microenvironment that promotes tumor development [159]. The stimulated vagal activity suppresses the inflammatory developments [58]. Most articles examining the relationship between HRV and tumor prognosis consider vagus activity to be systemic as a positive effect. Analysis of the 12 studies yielded consistent results: HRV has prognostic value in tumors, predictive: for both survival and tumor markers [102]. The analysis also showed that the predictive value of HRV may be strong primarily in the advanced stages, the higher initial vagus activity predicted a better prognosis [102]. However, although the vagus effect systemically slows tumorigenesis, its major neurotransmitter the acetylcholine (Ach), promotes local tumor formation [102]. In other study, anti-inflammatory effects of vagus nerve via ACh - *α7*nAChR. The *α7*nAChR is expressed on a number of immune cells, suggesting that the vagus may have an effect on the tumor microenvironment and antitumor immunity [58].

Vagus activity may slow tumor progression in pancreatic tumors because it reduces inflammation. A new vagus index was introduced for pancreatic tumors, the

neuroimmunomodulation index: $\mathrm{NIM} = \frac{\mathrm{RMSSD}}{\mathrm{CRP}}$, where CRP is the C-reactive protein. Following more than 200 patients with pancreatic cancer, the NIM index was found to have a protective value (relative risk: (0.688)) [62]. Initial higher vagus activity (characterized by HRV) was significantly correlated with a lower risk of death in pancreatic tumors regardless of age and treatment received [160]. The possible mediating role of C-reactive protein (CRP) was tested in non-small cell lung cancer (NSCLC) [8], where the CRP was not found to mediate the relationship between HRV and survival time in patients younger than 65 years, but did not predict overall survival. The NIM index was characteristic also in the study NSCLC; where the NIM index indicated also the protective relative risk. Furthermore, a high NIM index correlates with longer survival [62]. However, for advanced NSCLC, HRV should be used to monitor overall patient well-being rather than to judge survival [161].

Another study with meta-analysis (6 studies analyzed, with 1286 patients) also found that HRV has predictive value in cancer patient survival. Also, higher vagus activity may predict longer survival [162]. Similarly, in a study of hospice patients, it was found that HRV (SDNN value) is a prognostic factor in terminal cancer patients [163].

A meta-analysis of 19 high-quality observational studies [164] shows that higher HRV positively correlates with patients' progression of disease and outcome. The individuals with higher HRV and advanced adapting mechanisms seem to have a better prognosis in cancer progression. HRV appears to be a useful aspect to access the general health status of cancer patients.

A study investigating the role of HRV in gastric cancer patients found that HRV decreased in advanced clinical stages (progression) and correlated with tumor size, tumor infiltration, lymph node metastasis, and distant metastasis. Thus, gastric cancer patients had a lower HRV that correlated with the tumor stage. In this research, they also claim that; HRV may serve as a factor in assessing stage and progression in gastric cancer patients [165]. Based on this, HRV can be a promising biomarker, a prognostic factor in gastric cancer patients.

It was also shown that SDNN value significantly predicted the development of CEA levels in colon tumors 1 year after onset. However, when the patient sample was divided into curative and palliative care, it was found that the HRV-CEA relationship could only be demonstrated in palliative care [166].

In the study of liver tumors, it was found that the indices of HRV, including the previously detailed HF, show a significant correlation with the survival time of patients in patients with end-stage hepatocellular tumors [167]. The HRV significantly positively correlated with survival time in HCC patients [154].

Patients with prostate carcinoma (PC) were examined for vagus tone (with HRV measuring the SDNN and RMSSD). HRV shows a significant inverse correlation with PSA levels at follow-up at 6 and 24 months. This correlation was particularly true in metastatic PC patients [168].

Research on breast tumors (metastatic or recurrent) has hypothesized that high-frequency HRV (HF-HRV), a characteristic of parasympathetic nervous system function, may correlate with survival. Vagus activity was found to be strongly associated with survival (well-predicted survival) [169].

One study examined the association between HRV and brain metastases. Low HRV and a low score on the Karnofsky status rating scale were adverse prognostic factors for survival in patients with cerebral metastases. Based on these, it is thought that HRV may also be a prognostic factor in brain metastases [170].

5. Conclusions

The living cellular structures are energetically open. They need transport of the energy sources in and transport of the waste out. The homeostasis drives the complex system to be balanced, structurally, and dynamically tailored to stochastic (probability-based) equilibrium. Without direct cellular communication (no "social signal"), this organized transport would be missing. The malignant transformation breaks this organized transport and seeks to build up new for the new demands. However, there is a fundamental difference that exists: the healthy construction is driven by the collective signal and seeks to optimize the energy use for the highest efficacy. The malignant structure is driven by the topology and biophysical interactions of the competing cells, irrespective of the efficacy of the energy conversion. This collectivism makes a difference in the geometric arrangement, not only in the cell-cell correlations but the autonomic behavior that forms cells individually.

Different pathophysiological mechanisms and risk factors lead to altered signaling of a common homeostatic pathway indicating various diseases. Consequently, its indication has significant biomedical potential. The homeostatic actions are based on self-similarity, leading to structural changes and information flows, which drive the system's dynamics. Many interacting signals in the complex system produce a noise-like summary, which can be measured in variations of the signal in time-domain, and have a definite frequency distribution in noise power, following inverse dependence, called $1/f$ noise. This noise is meaningful and feasible, regardless of whether the system's signal is deterministic or stochastic. Forcing the $1/f$ signal is a possibility to stimulate the homeostatic control of the system. The heart rate variability (HRV) presents a feasible measuring of the individual status of the patient. The activity and effect of the vagus nerve drive numerous pathways of homeostatic control and are well connected to the HRV too.

Some common mechanisms inhibit the vagus activity in the tumorous situation [171], like the local oxidative stress and DNA damage, the inflammatory reactions, and excessive sympathetic activity. Stimuli may correct the inhibitions, either the vagus-nerve directly or by the compulsory spectrum on the local place of the disease.

The active vagus nerve can reduce the risk of cancer and cardiovascular dis-

ease, Alzheimer's disease, and metabolic syndrome by influencing their possible common underlying mechanism. The stimulation of the vagus nerve (VNS) could be a helpful tool fighting to re-establish healthy homeostasis. There is growing evidence that vagus activity slows tumorigenesis, primarily by inhibiting inflammation. Recent studies have shown that neuroimmune modulation increases cytotoxic immunity in the tumor microenvironment. Thus, we appear to modulate the tumor microenvironment and antitumor immunity by influencing vagus nerve activity [58]. It is thought that vagus stimulation, in addition to conventional therapeutic methods, may improve tumor prognosis by aiding in antitumor immunity [58]. The vagus activity and the changes by VNS are well measurable by HRV, and vica versa, the changes of HRV could modify the vagal processes.

Based on the interconnection, measuring vagus activity (primarily by HRV determination) can be a huge help to choose therapies in many diseases. The method has multiple benefits from this safe, complex therapeutic option that improves prognosis in various diseases. It is easy to apply and can be used in conjunction with other routine treatments. It can also be suitable for screening and prevention; it is inexpensive, non-invasive [171]. The HRV controlled VNS is a new direction of the physiologic and psychologic applications [172].

The healthy HRV spectrum shows $1/f$ on average. The averaging is a standard method for investigating diseases, like the evidence-based medicine averages by its various parameters determining the general probability of the studied phenomena. The $1/f$ spectrum is satisfactory for the VNS and HRV, but for personalization, we need differentiation, which means obtaining personal information about the systemic control. However, the frequency distribution shows only which frequencies produce the noise, but no idea about its sequences in time. We had shown the method to analyze the real-time sequences as a basis of personal treatment and follow-up.

The average $1/f$ frequency spectrum is a valuable tool to force the homeostatic arrangement. In therapy, this forcing can be safely and non-invasively administered by modulating a well-chosen radiofrequency carrier and using it to improve the patient's status. The improvement may be measured with conventional checks, but also, the HRV analysis gives information about the achievements of the modulated therapy.

Acknowledgements

This work was supported by the Hungarian National Research Development and Innovation Office PIACI KFI grant: 2019-1.1.1-PIACI-KFI-2019-00011.

Conflicts of Interest

The author declares no conflicts of interest regarding the publication of this paper.

References

[1] Dvorak, H.F. (2015) Tumors: Wounds That Do Not Heal—Redux. *Cancer Immu-*

nology Research, **3**, 1-11. https://doi.org/10.1158/2326-6066.CIR-14-0209

[2] Trigos, A.S., Pearson, R.B., Papenfuss, A.T., *et al.* (2016) Altered Interactions between Unicellular and Multicellular Genes Drive Hallmarks of Transformation in a Diverse Range of Solid Tumors. *PNAS*, **114**, 6406-6411. https://doi.org/10.1073/pnas.1617743114

[3] Davidson, C.D., Wang, W.Y., Zaimi, I., *et al.* (2019) Cell Force-Mediated Matrix Reorganization Underlies Multicellular Network Assembly. *Scientific Reports*, **9**, Article No. 12. https://doi.org/10.1038/s41598-018-37044-1

[4] Balmain, A., Gray, J. and Ponder, B. (2014) The Genetics and Genomics of Cancer. *Nature Genetics*, **33**, 238-244. https://doi.org/10.1038/ng1107

[5] Szigeti, G.P., Szasz, O. and Hegyi, G. (2017) Connections between Warburg's and Szentgyorgyi's Approach about the Causes of Cancer. *Journal of Neoplasm*, **1**, 1-13.

[6] Hanahan, D. and Weinberg, R.A. (2000) The Hallmarks of Cancer. *Cell*, **100**, 57-70. https://doi.org/10.1016/S0092-8674(00)81683-9

[7] Hanahan, D. and Weinberg, R.A. (2011) Hallmarks of Cancer: The Next Generation. *Cell*, **144**, 646-674. https://doi.org/10.1016/j.cell.2011.02.013

[8] Dyas, F.G. (1928) Chronic Irritation as a Cause of Cancer. *JAMA*, **90**, 457. https://doi.org/10.1001/jama.1928.92690330003008c

[9] Dvorak, H.F. (1986) Tumors: Wounds That Do Not Heal, Similarities between Tumor Stroma Generation and Wound Healing. *The New England Journal of Medicine*, **315**, 1650-1659. https://doi.org/10.1056/NEJM198612253152606

[10] Platz, E.A. and De, Marzo, A.M. (2004) Epidemiology of Inflammation and Prostate Cancer. *The Journal of Urology*, **171**, S36-S40. https://doi.org/10.1097/01.ju.0000108131.43160.77

[11] Punyiczki, M. and Fesus, L. (1998) Heat Shock and Apoptosis: The Two Defense Systems of the Organisms May Have Overlapping Molecular Elements. *Annals of the New York Academy of Sciences*, **951**, 67-74. https://doi.org/10.1111/j.1749-6632.1998.tb08978.x

[12] Aktipis, C.A., Bobby, A.M., Jansen, G., *et al.* (2015) Cancer across the Tree of Life: Cooperation and Cheating in Multicellularity. *Philosophical Transactions of the Royal Society B*, **370**, Article ID: 20140219. https://doi.org/10.1098/rstb.2014.0219

[13] Szasz, A. (2020) Preface. In: Szasz, A., Ed., *Challenges and Solutions of Oncological Hyperthermia*, Cambridge Scholars Publishing, Newcastle upon Tyne, 8-13. https://www.cambridgescholars.com/challenges-and-solutions-of-oncological-hyperthermia

[14] Szasz, A. (2021) Time-Fractal Modulation—Possible Modulation Effects in Human Therapy. *Open Journal of Biophysics*, **12**, 38-87. https://doi.org/10.4236/ojbiphy.2022.121003

[15] Conley, B. (2019) Microbial Extracellular Electron Transfer Is a Far-Out Metabolism. The American Society for Microbiology, Washington DC. https://asm.org/Articles/2019/November/Microbial-Extracellular-Electron-Transfer-is-a-Far

[16] Szasz, A., van Noort, D., Scheller, A., *et al.* (1994) Water States in Living Systems. I. Structural Aspects. *Physiological Chemistry and Physics*, **26**, 299-322.

[17] Agmon, N. (1995) The Grotthuss Mechanism. *Chemical Physics Letters*, **244**, 456-462. https://doi.org/10.1016/0009-2614(95)00905-J

[18] Markovitch, O. and Agmon, N. (2007) Structure and Energetics of the Hydronium Hydration Shells. *The Journal of Physical Chemistry A*, **111**, 2253-2256.

https://doi.org/10.1021/jp068960g

[19] Tuckerman, M.E., Laasonen, K., Sprik, M., *et al.* (1995) *Ab Initio* Molecular Dynamics Simulation of the Solvation and Transport of Hydronium and Hydroxyl Ions in Water. *The Journal of Chemical Physics*, **103**, 150-161. https://doi.org/10.1063/1.469654

[20] Tuckerman, M.E., Laasonen, K., Sprik, M. and Parrinello, M. (1995) *Ab Initio* Molecular Dynamics Simulation of the Solvation and Transport of H_3O^+ and OH^- Ions in Water. *The Journal of Physical Chemistry*, **99**, 5749-5752. https://doi.org/10.1021/j100016a003

[21] Marx, D., Tuckerman, M.E., Hutter, J., *et al.* (1999) The Nature of the Hydrated Excess Proton in Water. *Nature*, **397**, 601-604. https://doi.org/10.1038/17579

[22] Csermely, P. (2009) Weak Links: A Universal Key of Network Diversity and Stability. Springer, Berlin. https://doi.org/10.1007/978-3-540-31157-7_3

[23] Szendro, P., Vincze, G. and Szasz, A. (2001) Pink-Noise Behaviour of Biosystems. *European Biophysics Journal*, **30**, 227-231. https://doi.org/10.1007/s002490100143

[24] Lakhtakia, A. (1995) Physical Fractals: Self-Similarity and Square-Integrability. *Speculation in Science and Technology*, **18**, 153-156.

[25] Zbilut, J.P. and Marwan, N. (2008) The Wiener-Khinchin Theorem and Recurrence Quantification. *Physics Letters A*, **372**, 6622-6626. https://doi.org/10.1016/j.physleta.2008.09.027

[26] Lin, Y.K. (1967) Probabilistic Theory of Structural Dynamics. McGraw-Hill, New York.

[27] Aselli, G.B., Porta, A., Montano, N., Gnecchi-Ruscone, T., Lombardi, F. and Cerutti, S. (1992) Linear and Non-Linear Effects in the Beat-by-Beat Variability of Sympathetic Discharge in Decerebrate Cats. 14*th Annual International Conference of the IEEE Engineering in Medicine and Biology Society*, Vol. 7, 482-483. https://doi.org/10.1109/IEMBS.1992.5761070

[28] Strimbu, K. and Tavel, J.A. (2010) What Are Biomarkers? *Current Opinion in HIV and AIDS*, **5**, 463-466. https://doi.org/10.1097/COH.0b013e32833ed177

[29] Dash, P.K., Zhao, J., Hergenroeder, G. and Noore, A.N. (2010) Biomarkers for the Diagnosis, Prognosis, and Evaluation of Treatment Efficacy for Traumatic Brain Injury. *Neurotherapeutics*, **7**, 100-114. https://doi.org/10.1016/j.nurt.2009.10.019

[30] Henry, N.L. and Hayes, D.F. (2012) Cancer Biomarkers. *Molecular Oncology*, **6**, 140-146. https://doi.org/10.1016/j.molonc.2012.01.010

[31] Byrnes, S.A. and Weigl, B.H. (2018) Selecting Analytical Biomarkers for Diagnostic Applications: A First Principles Approach. *Expert Review of Molecular Diagnostics*, **18**, 19-26. https://doi.org/10.1080/14737159.2018.1412258

[32] Boessen, R., Heerspink, H.J.L., De Zeeuw, D.D., Grobbee, D.E., Groenwold, R.H.H. and Roes, K. (2014) Improving Clinical Trial Efficiency by Biomarker-Guided Patient Selection. *Trials*, **15**, 103. http://www.trialsjournal.com/content/15/1/103 https://doi.org/10.1186/1745-6215-15-103

[33] Ru, Y., Dancik, G.M. and Theodorescu, D. (2011) Biomarkers for Prognosis and Treatment Selection in Advanced Bladder Cancer Patients. *Current Opinion in Urology*, **21**, 420-427. https://doi.org/10.1097/MOU.0b013e32834956d6

[34] Sindo, Y., Hazama, S., Suzuki, N., Iguchi, H., Uesugi, K., *et al.* (2017) Predictive Biomarkers for the Efficacy of Peptide Vaccine Treatment: Based on the Results of a Phase II Study on Advanced Pancreatic Cancer. *Journal of Experimental and Clinical Cancer Research*, **36**, 36. https://doi.org/10.1186/s13046-017-0509-1

[35] Luckett, T., King, M.T., Butow, P.N., Oguchi, M., *et al.* (2011) Choosing between the EORTC QLQ-C30 and FACT-G for Measuring Health-Related Quality of Life in Cancer Clinical Research: Issues, Evidence and Recommendations. *Annals of Oncology*, **22**, 2179-2190. https://doi.org/10.1093/annonc/mdq721

[36] Evelyne (2018) Heart Rate Variability as a Prognostic Factor for Cancer Survival—A Systematic Review. *Frontiers in Physiology*, **9**, Article No. 623. https://doi.org/10.3389/fphys.2018.00623

[37] Lee, S.Y., Fiorentini, G., Szasz, A.M., Szigeti, Gy., Szasz, A. and Minnaar, C.A. (2020) Quo Vadis Oncological Hyperthermia (2020)? *Frontiers in Oncology*, **10**, Article No. 1690. https://doi.org/10.3389/fonc.2020.01690

[38] Lu, Y.M., *et al.* (2013) Deep Regional Hyperthermia Combined with Traditional Chinese Medicine in Treating Benign Diseases in Clifford Hospital. *Oncothermia Journal*, **7**, 157-165.

[39] Casadei, V., Sarti, D., Milandri, C., Dentico, P., Guadagni, S. and Fiorentini, C. (2020) Comparing the Effectiveness of Pain Therapy (PT) and Modulated Electro-Hyperthermia (mEHT) versus Pain Therapy Alone in Treating Patients with Painful Bony Metastases: An Observational Trial. In: Szasz, A., Ed., *Challenges and Solutions of Oncological Hyperthermia*, Cambridge Scholars, Washington DC, Ch. 15, 337-345.

[40] Hegyi, G., Molnar, I., Mate, A. and Petrovics, G. (2017) Targeted Radiofrequency Treatment—Oncothermia Application in Non-Oncological Diseases as Special Physiotherapy to Delay the Progressive Development. *Clinics and Practice*, **14**, 73-77. https://doi.org/10.4172/clinical-practice.100098

[41] Zais, O. (2013) Lyme Disease and Oncothermia. *Conference Papers in Medicine*, **2013**, Article ID: 275013. https://doi.org/10.1155/2013/275013

[42] Theodor, W.H. (2003) Transcranial Magnetic Stimulation in Epilepsy. *Epylepsy Currents*, **3**, 191-197. https://doi.org/10.1046/j.1535-7597.2003.03607.x

[43] Nussbaum, E.L., Houghton, P., Anthony, J., Rennie, S., *et al.* (2017) Neuromuscular Electrical Stimulation for Treatment of Muscle Impairment: Critical Review and Recommendations for Clinical Practice. *Physiotherapy Canada*, **69**, 1-76. https://doi.org/10.3138/ptc.2015-88

[44] Liu, A., Voroslakos, M., Kronberg, G., Henin, S., *et al.* (2018) Immediate Neurophysiological Effects of Transcranial Electrical Stimulation. *Nature Communications*, **9**, Article No. 2092. https://doi.org/10.1038/s41467-018-07233-7

[45] Gershon, A.A., Dannon, P.N. and Grunhaus, L. (2003) Transcranial Magnetic Stimulation in the Treatment of Depression. *American Journal of Psychiatry*, **160**, 835-845. http://ajp.psychiatryonline.org https://doi.org/10.1176/appi.ajp.160.5.835

[46] Zygmunt, A. and Stanczyk, J. (2010) Methods of Evaluation of Autonomic Nervous System. *Archives of Medical Science*, **6**, 11-18. https://doi.org/10.5114/aoms.2010.13500

[47] Andersson, U. and Tracy, K.J. (2012) Neural Reflexes in Inflammation and Immunity. *Journal of Experimental Medicine*, **209**, 1057-1068. https://doi.org/10.1084/jem.20120571

[48] Berthoud, H.R. and Neuhuber, W.L. (2000) Functional and Chemical Anatomy of the Afferent Vagal System. *Autonomic Neuroscience*, **85**, 1-17. https://doi.org/10.1016/S1566-0702(00)00215-0

[49] Howland, R.H. (2014) Vagus Nerve Stimulation. *Current Behavioral Neuroscience*

Reports, **1**, 64-73. https://doi.org/10.1007/s40473-014-0010-5

[50] Yap, J.Y.Y., Keatch, C., Lambert, E., Woods, W., *et al.* (2020) Critical Review of Transcutaneous Vagus Nerve Stimulation: Challenges for Translation to Clinical Practice. *Frontiers in Neuroscience*, **14**, Article No. 284. https://doi.org/10.3389/fnins.2020.00284

[51] Koopman, F.A., Chavan, S.S., Miljko, S., Grazio, S., *et al.* (2016) Vagus Nerve Stimulation Inhibits Cytokine Production and Attenuates Disease Severity in Rheumatoid Arthritis. *PNAS*, **113**, 8284-8289. https://doi.org/10.1073/pnas.1605635113

[52] Guo, Y., Koshy, S., Hui, D., Palmer, J.L., Shin, K., Bozkurt, M. and Yusuf, S.W. (2015) Prognostic Value of Heart Rate Variability in Patients with Cancer. *Journal of Clinical Neurophysiology*, **32**, 516-520. https://doi.org/10.1097/WNP.0000000000000210

[53] Teff, K.L. (2008) Visceral Nerves: Vagal and Sympathetic Innervation. *Journal of Parenteral and Enteral Nutrition*, **32**, 569-571. https://doi.org/10.1177/0148607108321705

[54] Mancino, M., Ametler, E., Gascon, P. and Almendro, V. (2011) The Neuronal Influence on Tumor Progression. *Biochimica et Biophysica Acta* (*BBA*)—*Reviews on Cancer*, **1816**, 105-118. https://doi.org/10.1016/j.bbcan.2011.04.005

[55] Wang, L., Xu, J., Xiai, Y., Yin, K., Li, Z., Li, B., Wand, W., Xu, H., Yang, L. and Xu, Z. (2018) Muscarinic Acetylcholine Receptor 3 Mediates Vagus Nerve-Induced Gastric Cancer. *Oncogenesis*, **7**, 88. https://doi.org/10.1038/s41389-018-0099-6

[56] Faulkner, S., Jobling, P., March, B. and Jiang, C.C. (2019) Tumor Neurobiology and the War of Nerves in Cancer. *Cancer Discovery*, **9**, 702-710. https://doi.org/10.1158/2159-8290.CD-18-1398

[57] Gidron, Y., Perry, H. and Glennie, M. (2005) Does the Vagus Nerve Inform the Brain about Pre-Clinical Tumours and Modulate Them? *The Lancet Oncology*, **6**, 245-248. https://doi.org/10.1016/S1470-2045(05)70096-6

[58] Reijmen, E., Vannucci, L., De, Couck, M., De, Greve, J. and Gidron, Y. (2018) Therapeutic Potential of the Vagus Nerve in Cancer. *Immunology Letters*, **202**, 38-43. https://doi.org/10.1016/j.imlet.2018.07.006

[59] De, Visser, K.E. and Coussens, L.M. (2006) The Inflammatory Tumor Microenvironment and Its Impact on Cancer Development. *Contributions to Microbiology*, **13**, 118-137. https://doi.org/10.1159/000092969

[60] Pages, F., Galon, J., Dieu, Nosjean, M.C., Tartour, E., Sautes, Fridman, C. and Fridman, W.H. (2010) Immune Infiltration in Human Tumors: A Prognostic Factor That Should Not Be Ignored. *Oncogene*, **29**, 1093-1102. https://doi.org/10.1038/onc.2009.416

[61] Qian, B.Z. and Pollard, J.W. (2010) Macrophage Diversity Enhances Tumor Progression and Metastasis. *Cell*, **141**, 39-51. https://doi.org/10.1016/j.cell.2010.03.014

[62] Gidron, Y., De Couck, M., Schallier, D., De Greve, J., Van Laethem, J.L. and Marechal, R. (2018) The Relationship between a New Biomarker of Vagal Neuroimmunomodulation and Survival in Two Fatal Cancers. *Journal of Immunology Research*, **2018**, Article ID: 4874193. https://doi.org/10.1155/2018/4874193

[63] De Couck, M. and Caers, R. (2018) Why We Should Stimulate the Vagus Nerve in Cancer. *Clinical Oncology*, **3**, 1515. https://doi.org/10.1155/2018/1236787

[64] Balasubramanian, K., Harikumar, K., Nagaraj, N. and Pati, S. (2017) Vagus Nerve Stimulation Modulated Complexity of Heart Rate Variability Differently during Sleep and Wakefulness. *Annals of Indian Academy of Neurology*, **20**, 403-407.

https://doi.org/10.4103/aian.AIAN_148_17

[65] Goldberger, A.L. and West, B.J. (1987) Chaos in Physiology: Hearth or Disease? In: Degn, H., *et al.*, Eds., *Chaos in Biological Systems*, Springer Science + Business Media, New York, 1-4. https://doi.org/10.1007/978-1-4757-9631-5_1

[66] Mandell, A.J., Knapp, S., Ehlers, C.L. and Russo, P.V. (1983) The Stability of Constrained Randomness: Lithium Prophylaxis at Several Neurobiological Levels. In: Post, R.M. and Ballenger, J.C., Eds., *Neurobiology of the Mood Disorders*, Williams & Wilkins, Baltimore, 744-776.

[67] Kobayashi, M. and Musha, T. (1982) 1/f Fluctuation of Heartbeat Period. *IEEE Transactions on Biomedical Engineering*, **29**, 456-457. https://doi.org/10.1109/TBME.1982.324972

[68] Trimmel, K., Sacha, J. and Huikuri, H.V. (2015) Heart Rate Variability: Clinical Applications and Interaction between HRV and Heart Rate. Frontiers Media, Lausanne. https://doi.org/10.3389/978-2-88919-652-4

[69] Kleiger, R.E., Stein, D.S. and Bigger, M.D. (2005) Heart Rate Variability: Measurement and Clinical Utility. *Annals of Noninvasive Electrocardiology*, **10**, 88-101. https://doi.org/10.1111/j.1542-474X.2005.10101.x

[70] Malik, M. (1996) Heart Rate Variability. Standards of Measurement, Physiological Interpretation, and Clinical Use. Task Force of the European Society of Cardiology and the North American Society of Pacing and Electrophysiology. *European Heart Journal*, **17**, 354-381. https://doi.org/10.1093/oxfordjournals.eurheartj.a014868

[71] Benichous, T., Pereira, B., Mermillod, M., Tauveron, I., *et al.* (2018) Heart Rate Variability in Type 2 Diabetes Mellitus: A Systematic Review and Meta-Analysis. *PLoS ONE*, **13**, e0195166. https://doi.org/10.1371/journal.pone.0195166

[72] Chou, Y.H., Huang, W.L., Chang, C.H., Yang, C.C.H., Kuo, T.B.J., *et al.* (2019) Heart Rate Variability as a Predictor of Rapid Renal Function Deterioration in Chronic Kidney Disease Patients. *Nephrology* (*Carlton*), **24**, 806-813. https://doi.org/10.1111/nep.13514

[73] Da, Silva, V.P., Oliveira, B.R.R., Mello, R.G.T., Moraes, H., *et al.* (2018) Heart Rate Variability Indexes in Dementia: A Systematic Review with a Quantitative Analysis. *Current Alzheimer Research*, **15**, 80-88. https://doi.org/10.2174/1567205014666170531082352

[74] Jung, W., Jang, K.I. and Lee, S.H. (2018) Heart and Brain Interaction of Psychiatric Illness: A Review Focused on Heart Rate Variability, Cognitive Function, and Quantitative Electrocephalography. *Clinical Psychopharmacology and Neuroscience*, **17**, 459-474. https://doi.org/10.9758/cpn.2019.17.4.459

[75] Sajjadieh, A., Shahsavari, A., Safaei, A., Penzel, T., Schoebel, C., *et al.* (2020) The Association of Sleep Duration and Quality with Heart Rate Variability and Blood Pressure. *Tanaffos*, **19**, 135-143.

[76] Kopp, W.J., Synowski, S.J., Newel, M.E., Schmidt, L.A., *et al.* (2011) Autonomic Nervous System Reactivity to Positive and Negative Mood Induction: The Role of Acute Psychological Responses and Frontal Electrocortical Activity. *Biological Psychology*, **86**, 230-238. https://doi.org/10.1016/j.biopsycho.2010.12.003

[77] Sarlis, N.V., Skordas, E.S. and Varotsos, P.A. (2009) Heart Rate Variability in Natural Time and 1/f "Noise". *EPL*, **87**, 18003. https://doi.org/10.1209/0295-5075/87/18003

[78] De Couck, M. and Gidron, Y. (2013) Norms of Vagal Nerve Activity, Indexed by Heart Rate Variability in Cancer Patients. *Cancer Epidemiology*, **37**, 737-741.

https://doi.org/10.1016/j.canep.2013.04.016

[79] Arab, C., Dias, D.P.M., Barbosa, R.T., de Almeida, de Carvalho, T.D., *et al.* (2016) Heart Rate Variability Measure in Breast Cancer Patients and Survivors: A Systematic Review. *Psychoneuroendocrinology*, **68**, 57-68. https://doi.org/10.1016/j.psyneuen.2016.02.018

[80] Lombardi, F., Montano, N., Finocchiaro, M.L., Gnecchi, Ruscone, T., Baselli, G., Cerutti, S. and Malliani, A. (1990) Spectral Analysis of Sympathetic Discharge in Decerebrate Cats. *Journal of the Autonomic Nervous System*, **30**, S97-S99. https://doi.org/10.1016/0165-1838(90)90109-V

[81] Task Force of the European Society of Cardiology the North American Society of Pacing Electrophysiology (1996) Heart Rate Variability: Standards of Measurement, Physiological Interpretation, and Clinical Use. *Circulation*, **93**, 1043-1065.

[82] Tulppo, M.P., Makikallio, T.H., Takala, T.E.S., Seppanen, T. and Huikuri, H.V. (1996) Quantitative Beat-to-Beat Analysis of Heart Rate Dynamics during Exercise. *American Journal of Physiology*, **271**, H244-H252. https://doi.org/10.1152/ajpheart.1996.271.1.H244

[83] Acharya, R.U., Sing, O.W., Ping, L.Y. and Chua, T.L. (2004) Heart Rate Analysis in Normal Subjects of Various Age Groups. *BioMedical Engineering OnLine*, **3**, 24. https://doi.org/10.1186/1475-925X-3-24

[84] Kamen, P.W., Krum, H. and Tonkin, A.M. (1996) Poincare Plot of Heart Rate Variability Allows Quantitative Display of Parasympathetic Nervous Activity. *Clinical Science*, **91**, 201-208. https://doi.org/10.1042/cs0910201

[85] Roth, Y. (2018) Homeostasis Processes Expressed as Flashes in a Poincaré Sections. *Journal of Modern Physics*, **9**, 2135-2140. https://doi.org/10.4236/jmp.2018.912134

[86] Woo, M.A., Stevenson, W.G., Moser, D.K., Trelease, R.B. and Harper, R.H. (1992) Patterns of Beat-to-Beat Heart Rate Variability in Advanced Heart Failure. *American Heart Journal*, **123**, 704-707. https://doi.org/10.1016/0002-8703(92)90510-3

[87] Brennan, M., Palaniswami, M. and Kamen, P. (2001) Do Existing Measures of Poincare Plot Geometry Reflect Nonlinear Features of Heart Rate Variability? *IEEE Transactions on Biomedical Engineering*, **48**, 1342-1347. https://doi.org/10.1109/10.959330

[88] Thu, T.N.P., Hernandez, A.I., Costet, N., Patural, H., Pichot, V., *et al.* (2019) Improving Methodology in Heart Rate Variability Analysis for the Premature Infants: Impact of the Time Length. *PLoS ONE*, **14**, e0220692. https://doi.org/10.1371/journal.pone.0220692

[89] Peng, C.K., Havlin, S., Stanley, H.E. and Goldberger, A.L. (1995) Quantification of Scaling Exponents and Crossover Phenomena in Nonstationary Heartbeat Time Series. *Chaos*, **5**, 82-87. https://doi.org/10.1063/1.166141

[90] Goldberger, A.L., Amaral, L.A.N., Hausdorff, J.M., Ivanov, P.C., Peng, C.K. and Stanley, H.E. (2002) Fractal Dynamics in Physiology: Alterations with Disease and Aging. *PNAS*, **99**, 2466-2472. https://doi.org/10.1073/pnas.012579499

[91] Ho, K.K.L., Moody, G.B., Peng, C.K., *et al.* (1997) Predicting Survival in Heart Failure Case and Control Subjects by Use of Fully Automated Methods for Deriving Nonlinear and Conventional Indices of Heart Rate Dynamis. *Circulation*, **96**, 842-848. https://doi.org/10.1161/01.CIR.96.3.842

[92] Goldberger, A.L., Bhargava, V., West, B. and Mandell, A.J. (1985) Some Observations on the Question: Is Ventricular Fibrillation "Chaos"? *Physica D*, **19**, 282-289. https://doi.org/10.1016/0167-2789(86)90024-2

[93] Goldberger, A.L., Bhargava, V. and West, B.J. (1985) Nonlinear Dynamics of Heartbeat, II. Subharmonic Bifurcations of the Cardiac Interbeat Interval in Sinus Node Disease. *Physica D*, **17**, 207-214. https://doi.org/10.1016/0167-2789(85)90005-3

[94] Goldberger, A.L. and West, B.J. (1987) Applications of Nonlinear Dynamics to Clinical Cardiology. *Annals of the New York Academy of Sciences*, **504**, 195-213. https://doi.org/10.1111/j.1749-6632.1987.tb48733.x

[95] Goldberger, A.L. (2006) Complex Systems. *Proceedings of the American Thoracic Society*, **3**, 467-472. https://doi.org/10.1513/pats.200603-028MS

[96] Turner, J.D. (1988) Frequency Domain Analysis. In: *Instrumentation for Engineers*, Palgrave, London, Ch. 7, 159-179. https://doi.org/10.1007/978-1-4684-6300-2_7

[97] Li, K., Rudiger, H. and Ziemssen, T. (2019) Spectral Analysis of Heart Rate Variability: Time Window Matters. *Frontiers in Neurology*, **10**, Article No. 545. https://doi.org/10.3389/fneur.2019.00545

[98] Shaffer, F. and Ginsberg, J.P. (2017) An Overview of Heart Rate Variability Metrics and Norms. *Frontiers in Public Health*, **5**, Article No. 258. https://doi.org/10.3389/fpubh.2017.00258

[99] Owens, A.P. (2020) The Role of Heart Rate Variability in the Future of Remote Digital Diomarkers. *Frontiers in Neuroscience*, **14**, Article ID: 582145. https://doi.org/10.3389/fnins.2020.582145

[100] Fossion, R., Rivera, A.L. and Estanol, B. (2018) A Physicist's View of Homeostasis: How Time Series of Continuous Monitoring Reflect the Function of Physiological Variabilities in Regulatory Mechanisms. *Physiological Measurement*, **39**, Article ID: 084007. https://doi.org/10.1088/1361-6579/aad8db

[101] Riganello, F., Garbarino, S. and Sannita, W.G. (2012) Heart Rate Variability, Homeostasis, and Brain Function: A Tutorial and Review of Application. *Journal of Psychophysiology*, **26**, 178-203. https://doi.org/10.1027/0269-8803/a000080

[102] De Couck, M., Caers, R., Spiegel, D. and Gidron, Y. (2018) The Role of the Vagus Nerve in Cancer Prognosis: A Systematic and a Comprehensive Review. *Journal of Oncology*, **2018**, Article ID: 1236787. https://doi.org/10.1155/2018/1236787

[103] Cooper, T.M., McKinley, P.S., Seeman, T.E., Choo, T.H., Lee, S. and Sloan, R.P. (2015) Heart Rate Variability Predicts Levels of Inflammatory Markers: Evidence for the Vagal Anti-Inflammatory Pathway. *Brain, Behavior, and Immunity*, **49**, 94-100. https://doi.org/10.1016/j.bbi.2014.12.017

[104] Ohira, H., Matsunaga, M., Osumi, T., Fukuyama, S., Shinoda, J., Yamada, J. and Gidron, Y. (2013) Vagal Nerve Activity as a Moderator of Brain-Immune Relationships. *Journal of Neuroimmunology*, **260**, 28-36. https://doi.org/10.1016/j.jneuroim.2013.04.011

[105] Young, H.A. and Benton, D. (2018) Heart-Rate Variabiity: A Biomarker to Study the Influence of Nutrition on Physiological and Psychological Health? *Behavioural Pharmacology*, **29**, 140-151. https://doi.org/10.1097/FBP.0000000000000383

[106] Hayano, J. and Yuda, E. (2019) Pitfalls of Assessment of Autonomic Function by Heart Rate Variability. *Journal of Physiological Anthropology*, **38**, Article No. 3. https://doi.org/10.1186/s40101-019-0193-2

[107] Quintana, D.S. and Heathers, A.J. (2014) Considerations in the Assessment of Heart Rate Variability in Biobehavioral Research. *Frontiers in Psychology*, **5**, Article No. 805. https://doi.org/10.3389/fpsyg.2014.00805

[108] Szasz, A. and Szasz, O. (2020) Time-Fractal Modulation of Modulated Electro-Hyperthermia (mEHT). In: Szasz, A., Ed., *Challenges and Solutions of Onco-*

logical Hyperthermia, Cambridge Scholars, Washington DC, Ch. 17, 377-415.

[109] Szasz, A.M., Minnaar, C.A., Szentmartoni, Gy., *et al.* (2019) Review of the Clinical Evidences of Modulated Electro-Hyperthermia (mEHT) Method: An Update for the Practicing Oncologist. *Frontiers in Oncology*, **9**, Article No. 1012. https://doi.org/10.3389/fonc.2019.01012

[110] Szasz, O. (2020) Local Treatment with Systemic Effect: Abscopal Outcome. In: Szasz, A., Ed., *Challenges and Solutions of Oncological Hyperthermia*, Cambridge Scholars, Washington DC, Ch. 11, 192-205.

[111] Minnaar, C.A., Kotzen, J.A., Ayeni, O.A., *et al.* (2020) Potentiation of the Abscopal Effect by Modulated Electro-Hyperthermia in Locally Advanced Cervical Cancer Patients. *Frontiers in Oncology*, **10**, Article No. 376. https://doi.org/10.3389/fonc.2020.00376

[112] Andocs, G., Szasz, O. and Szasz, A. (2009) Oncothermia Treatment of Cancer: From the Laboratory to Clinic. *Electromagnetic Biology and Medicine*, **28**, 148-165. https://doi.org/10.1080/15368370902724633

[113] Yang, K.L., Huang, C.C., Chi, M.S., Chiang, H.C., Wang, Y.S. andocs, G., *et al.* (2016) *In Vitro* Comparison of Conventional Hyperthermia and Modulated Electro-Hyperthermia. *Oncotarget*, **7**, 84082-84092. https://doi.org/10.18632/oncotarget.11444

[114] Wust, P., Ghadjar, P., Nadobny, J., *et al.* (2019) Physical Analysis of Temperature-Dependent Effects of Amplitude-Modulated Electromagnetic Hyperthermia. *International Journal of Hypertension*, **36**, 1246-1254. https://doi.org/10.1080/02656736.2019.1692376

[115] Wust, P., Kortum, B., Strauss, U., Nadobny, J., Zschaeck, S., Beck, M., *et al.* (2020) Non-Thermal Effects of Radiofrequency Electromagnetic Fields. *Scientific Reports*, **10**, Article No. 13488. https://doi.org/10.1038/s41598-020-69561-3

[116] Wust, P., Nadobny, J., Zschaeck, S. and Ghadjar, P. (2020) Physics of Hyperthermia—Is Physics Really against Us? In: Szasz, A., Ed., *Challenges and Solutions of Oncological Hyperthermia*, Cambridge Scholars, Washington DC, Ch. 16, 346-376.

[117] Chang, R.B. (2019) Body Thermal Responses and the Vagus Nerve. *Neuroscience Letters*, **698**, 209-216. https://doi.org/10.1016/j.neulet.2019.01.013

[118] Andocs, G., Rehman, M.U., Zhao, Q.L., Tabuchi, Y., Kanamori, M. and Kondo, T. (2016) Comparison of Biological Effects of Modulated Electro-Hyperthermia and Conventional Heat Treatment in Human Lymphoma U937 Cell. *Cell Death Discovery*, **2**, 16039. https://doi.org/10.1038/cddiscovery.2016.39

[119] Andocs, G., Rehman, M.U., Zhao, Q.L., Papp, E., Kondo, T. and Szasz, A. (2015) Nanoheating without Artificial Nanoparticles Part II. Experimental Support of the Nanoheating Concept of the Modulated Electro-Hyperthermia Method, Using U937 Cell Suspension Model. *Biology and Medicine*, **7**, 1-9. https://doi.org/10.4172/0974-8369.1000247

[120] Szasz, A. (2019) Thermal and Nonthermal Effects of Radiofrequency on Living State and Applications as an Adjuvant with Radiation Therapy. *Journal of Radiation and Cancer Research*, **10**, 1-17. https://doi.org/10.4103/jrcr.jrcr_25_18

[121] Danics, L., Schvarcz, Cs., Viana, P., *et al.* (2020) Exhaustion of Protective Heat Shock Response Induces Significant Tumor Damage by Apoptosis after Modulated Electro-Hyperthermia Treatment of Triple Negative Breast Cancer Isografts in Mice. *Cancers*, **12**, 2581. https://doi.org/10.3390/cancers12092581

[122] Forika, G., Balogh, A., Vancsik, T., Zalatnai, A., *et al.* (2020) Modulated Electro-Hyperthermia Resolves Radioresistance of Panc1 Pancreas Adenocarcinoma

and Promotes DNA Damage and Apoptosis *in Vitro*. *International Journal of Molecular Sciences*, **21**, 5100. https://doi.org/10.3390/ijms21145100

[123] Krenacs, T., Meggyeshazi, N., Forika, G., *et al.* (2020) Modulated Electro-Hyperthermia-Induced Tumor Damage Mechanisms Revealed in Cancer Models. *International Journal of Molecular Sciences*, **21**, 6270. https://doi.org/10.3390/ijms21176270

[124] Scheff, J.D., Griffel, B., Corbett, S.A., Calvano, S.E., *et al.* (2014) On Heart Rate Variability and Autonomic Activity in Homeostasis and in Systemic Inflammation. *Mathematical Biosciences*, **252**, 36-44. https://doi.org/10.1016/j.mbs.2014.03.010

[125] Goldberger, A.L., Bhargava, V., West, B.J. and Mandell, A.J. (1985) On a Mechanism of Cardiac Electrical Stability, the Fractal Hypothesis. *Biophysics Journal*, **48**, 525-528. https://doi.org/10.1016/S0006-3495(85)83808-X

[126] Kauffman, S.A. and Johnsen, S. (1991) Coevolution to the Edge of Chaos: Coupled Fitness Landscapes, Poised States, and Coevolutionary Avalanches. *Journal of Theoretical Biology*, **149**, 467-505. https://doi.org/10.1016/S0022-5193(05)80094-3

[127] Bak, P., Tang, C. and Wiesenfeld, K. (1988) Self-Organized Criticality. *Physical Review A*, **38**, 364-374. https://doi.org/10.1103/PhysRevA.38.364

[128] Lewin, R. (1992) Complexity, Life at the Edge of Chaos. University of Chicago Press, Chicago.

[129] Ito, K. and Gunji, Y.P. (1994) Self-Organisation of Living Systems towards Criticality at the Edge of Chaos. *Biosystems*, **33**, 17-24. https://doi.org/10.1016/0303-2647(94)90057-4

[130] Prigogine, I. and Stengers, I. (1985) Order out of Chaos. Flamingo, London. https://doi.org/10.1063/1.2813716

[131] Calaprice A. (2000) The Expanded Quotable Einstein. Princeton University Press, Princeton, 456.

[132] Bernardes, A.T. and dos Santos, R.M. (1997) Immune Network at the Edge of Chaos. *Journal of Theoretical Biology*, **186**, 173-187. https://doi.org/10.1006/jtbi.1996.0316

[133] Bertschinger, N. and Natschlager, T. (2004) Real-Time Computation at the Edge of Chaos in Recurrent Neural Networks. *Neural Computation*, **16**, 1413-1436. https://doi.org/10.1162/089976604323057443

[134] Stokic, D., Hanel, R. and Thurner, S. (2008) Inflation of the Edge of Chaos in a Simple Model of Gene Interaction Networks. *Physical Review E*, **77**, Article ID: 061917. https://doi.org/10.1103/PhysRevE.77.061917

[135] Kauffman, S., Hill, C., Hood, L. and Huang, S. (2014) Transforming Medicine: A Manifesto, Scientific American-World View. https://web.archive.org/web/20140713110927/http://www.saworldview.com/special-report-cancer/transforming-medicine-a-manifesto

[136] Eke, A., Hermán, P., Bassingthwaighte, J.B., Raymond, G.M., Percival, D.B., Cannon, M., Balla, I. and Ikrényi, C. (2000) Physiological Time Series: Distinguishing Fractal Noises from Motions. *Pflügers Archiv—European Journal of Physiology*, **439**, 403-415. https://doi.org/10.1007/s004249900135

[137] Barunik, J. and Kristoufek, L. (2010) On Hurst Exponent Estimation under Heavy-Tailed Distributions. *Physica A*: *Statistical Mechanics and Its Applications*, **389**, 3844-3855. https://doi.org/10.1016/j.physa.2010.05.025

[138] Beran, J. (1994) Statistics for Long-Memory Processes. Taylor & Francis, London.

[139] Arneodo, A., Audit, B., Kestener, P. and Roux, S. (2008) Wavelet-Based Multifractal Analysis. *Scholarpedia*, **3**, 4103. https://doi.org/10.4249/scholarpedia.4103

[140] Ivanov, P.Ch., Amaral, L.A.N., Goldberger, A.L., Havlin, S., Rosenblum, M.G., *et al.* (2001) From 1/f Noise to Multifractal Cascades in Heartbeat Dynamics. *Chaos*, **11**, 641-652. https://doi.org/10.1063/1.1395631

[141] Ivanov, P.Ch., Amaral, L.A.N., Goldberger, A.L., Havlin, S., Rosenblum, M.G., Struzik, Z.R. and Stanley, H.E. (1999) Multifractality in Human Heartbeat Dynamics. *Nature*, **399**, 461-465. https://doi.org/10.1038/20924

[142] Kravitz, R.L., Duan, N. and Braslow, J. (2004) Evidence-Based Medicine, Heterogeneity, and the Trouble with Averages. *The Milbank Quarterly*, **82**, 661-687. https://doi.org/10.1111/j.0887-378X.2004.00327.x

[143] Imai, J. (2021) Regulation of Adaptive Cell Proliferation by Vagal Nerve Signals for Maintenance of Whole-Body Homeostasis: Potential Therapeutic Target for Insulin-Deficient Diabetes. *Tohoku Journal of Experimental Medicine*, **254**, 245-252. https://doi.org/10.1620/tjem.254.245

[144] Matteoli, G. and Boeckxstaens, G.E. (2013) The Vagal Innervation of the Gut and Immune Homeostasis. *Gut*, **62**, 1214-1222. https://doi.org/10.1136/gutjnl-2012-302550

[145] Szigeti, Gy.P., Szasz, O. and Hegyi, G. (2020) Experiment with Personalised Dosing of Hyperthermia. In: Ito, S., Ed., *Current Topics in Medicine and Medical Research*, Chapter 15, Vol. 3, Book Publisher International, New York, 140-157.

[146] Szasz, A. (2013) Challenges and Solutions in Oncological Hyperthermia. *Thermal Medicine*, **29**, 1-23. https://doi.org/10.3191/thermalmed.29.1

[147] Ferenczy, G.L. and Szasz, A. (2020) Technical Challenges and Proposals in Oncological Hyperthermia. In: Szasz, A., Ed., *Challenges and Solutions of Oncological Hyperthermia*, Ch. 3, Cambridge Scholars, Cambridge, 72-90.

[148] Szasz, A. (2014) Oncothermia: Complex Therapy by EM and Fractal Physiology. 31*th URSI General Assembly and Scientific Symposium* (*URSI GASS*), Beijing, 20 October 2014, 1-4. https://doi.org/10.1109/URSIGASS.2014.6930100

[149] Szasz, A. (2015) Bioelectromagnetic Paradigm of Cancer Treatment Oncothermia. In: Rosch, P.J., Ed., *Bioelectromagnetic and Subtle Energy Medicine*, CRC Press, Boca Raton, 323-336.

[150] Zhao, H., Raines, L.N. and Huang, S. (2020) Molecular Chaperones: Molecular Assembly Line Brings Metabolism and Immunity in Shape. *Metabolites*, **10**, 394. https://doi.org/10.3390/metabo10100394

[151] Prohaszka, Z. (2007) Chaperones as Part of Immune Networks. In: Csermely, P. and Vigh, L., Eds., *Molecular Aspects of the Stress Response*: *Chaperones*, *Membranes and Networks*, Landes Bioscience and Springer Science + Business Media, Ch. 14, Berlin, 159-166. https://doi.org/10.1007/978-0-387-39975-1_14

[152] Chavan, S.S., Pavlov, V.A. and Tracey, K.J. (2017) Mechanisms and Therapeutic Relevance of Neuro-Immune Communication. *Immunity*, **46**, 927-942. https://doi.org/10.1016/j.immuni.2017.06.008

[153] Kuwabara, S., Goggins, E. and Tanaka, S. (2021) Neuroimmune Circuits Activated by Vagus Nerve Stimulation. *Nephron*, 1-5. https://doi.org/10.1159/000518176

[154] Parent, R. (2019) The Potential Implication of the Autonomic Nervous System in Hepatocellular Carcinoma. *Cellular and Molecular Gastroenterology and Hepatology*, **8**, 145-148. https://doi.org/10.1016/j.jcmgh.2019.03.002

[155] Szasz, A. (2020) Towards the Immunogenic Hyperthermic Action: Modulated Electro-Hyperthermia, Clinical Oncology and Research. *Science Repository*, **3**, 5-6. https://doi.org/10.31487/j.COR.2020.09.07

[156] Tsang, Y.W., Huang, C.C., Yang, K.L., Chi, M.S., Chiang, H.C., Wang, Y.S., Andocs, G., Szasz, A., Li, W.T. and Chi, K.H. (2015) Improving Immunological Tumor Microenvironment Using Electro-Hyperthermia Followed by Dendritic Cell Immunotherapy. *Oncothermia Journal*, **15**, 55-66. https://doi.org/10.1186/s12885-015-1690-2

[157] Qin, W., Akutsu, Y., Andocs, G., *et al*. (2014) Modulated Electro-Hyperthermia Enhances Dendritic Cell Therapy through an Abscopal Effect in Mice. *Oncology Reports*, **32**, 2373-2379. https://doi.org/10.3892/or.2014.3500

[158] Van, Gool, S.W., Makalowski, J., Feyen, O., Prix, L., Schirrmacher, V. and Stuecker, W. (2018) The Induction of Immunogenic Cell Death (ICD) during Maintenance Chemotherapy and Subsequent Multimodal Immunotherapy for Glioblastoma (GBM*). Austin Oncology Case Reports*, **3**, 1-8.

[159] Mantovani, A., Allavena, P., Sica, A. and Balkwill, F. (2008) Cancer-Related Inflammation. *Nature*, **454**, 436-444. https://doi.org/10.1038/nature07205

[160] De Couck, M., Marechal, R., Moorthamers, S., Van, Laethem, J.L. and Gidron, Y. (2016) Vagal Nerve Activity Predicts Overall Survival in Metastatic Pancreatic Cancer, Mediated by Inflammation. *Cancer Epidemiology*, **40**, 47-51. https://doi.org/10.1016/j.canep.2015.11.007

[161] Kim, K., Chae, J. and Lee, S. (2015) The Role of Heart Rate Variability in Advanced Non-Small-Cell Lung Cancer Patients. *Journal of Palliative Care*, **31**, 103-108. https://doi.org/10.1177/082585971503100206

[162] Zhou, X., Ma, Z., Zhan, L., Zhu, S., Wang, J., Wang, B. and Fu, W. (2016) Heart Rate Variability in the Prediction of Survival in Patients with Cancer: A Systematic Review and Meta-Analysis. *Journal of Psychosomatic Research*, **89**, 20-25. https://doi.org/10.1016/j.jpsychores.2016.08.004

[163] Kim, D.H., Kim, J.A., Choi, Y.S., Kim, S.H., Lee, J.Y. and Kim, Y.E. (2010) Heart Rate Variability and Length of Survival in Hospice Cancer Patients. *Journal of Korean Medical Science*, **25**, 1140-1145. https://doi.org/10.3346/jkms.2010.25.8.1140

[164] Kloter, E., Barrueto, K., Klein, S.D., Scholkmann, F. and Wolf, U. (2018) Heart Rate Variability as a Prognostic Factor for Cancer Survival—A Systematic Review. *Frontiers in Physiology*, **9**, Article No. 623. https://doi.org/10.3389/fphys.2018.00623

[165] Hu, S., Lou, J., Zhang, Y. and Chen, P. (2018) Low Heart Rate Variability Relates to the Progression of Gastric Cancer. *World Journal of Surgical Oncology*, **16**, 49. https://doi.org/10.1186/s12957-018-1348-z

[166] Mouton, C., Ronson, A., Racavi, D., Delhaye, F., Kupper, N., Paesmans, M., Moreau, M., Nogaret, J.M., Hendisz, A. and Gidron, Y. (2012) The Relationship between Heart Rate Variability and Time-Course of Carcinoembryonic Antigen in Colorectal Cancer. *Autonomic Neuroscience*: *Basic and Clinical*, **166**, 96-99. https://doi.org/10.1016/j.autneu.2011.10.002

[167] Chiang, J.K., Moo, M., Kuo, T.B.J. and Fu, C.H. (2010) Association between Cardiovascular Autonomic Functions and Time to Death in Patients with Terminal Hepatocellular Carcinoma. *Journal of Pain and Symptom Management*, **39**, 673-679. https://doi.org/10.1016/j.jpainsymman.2009.09.014

[168] De Couck, M., Van Brummelen, D., Schallier, D., De Greve, J. and Gidron, Y. (2013) The Relationship between Vagal Nerve Activity and Clinical Outcomes in

Prostate and Non-Small Cell Lung Cancer Patients. *Oncology Reports*, **30**, 2435-2441. https://doi.org/10.3892/or.2013.2725

[169] Giese-Davis, J., Wilhelm, F.H., Tamagawa, R., Palesh, O., Neri, E., Taylor, C.B., Kraemer, H.C. and Spiegel, D. (2015) Higher Vagal Activity as Related to Survival in Patients with Advanced Breast Cancer: An Analysis of Autonomic Dysregulation. *Psychosomatic Medicine*, **77**, 346-355. https://doi.org/10.1097/PSY.0000000000000167

[170] Wang, Y.M., Wu, H.T., Huang, E.Y., Kou, Y.R. and H, S.S. (2013) Heart Rate Variability Is Associated with Survival in Patients with Brain Metastasis: A Preliminary Report. *BioMedResearch International*, **2013**, Article ID: 503421. https://doi.org/10.1155/2013/503421

[171] De Couck, M., Mravec, B. and Gidron, Y. (2012) You May Need the Vagus Nerve to Understand Pathophysiology and to Treat Diseases. *Clinical Science*, **122**, 323-328. https://doi.org/10.1042/CS20110299

[172] Kaniuysas, E., Kampusch, S., Tittgemeyer, M., Panetsos, F., Gines, R.F., *et al.* (2019) Currentdirections in the Auricular Vagus Nerve Stimulation I—A Physiological Perspective. *Frontiers in Neuroscinece*, **13**, Article No. 854. https://doi.org/10.3389/fnins.2019.00854

Scientific Research Publishing

Open Journal of Biophysics, 2022, 12, 132-152
https://www.scirp.org/journal/ojbiphy
ISSN Online: 2164-5396
ISSN Print: 2164-5388

Evaluation of Peppermint Leaf Flavonoids as SARS-CoV-2 Spike Receptor-Binding Domain Attachment Inhibitors to the Human ACE2 Receptor: A Molecular Docking Study

Marcelo Lopes Pereira Júnior[1]*, Rafael Timóteo de Sousa Junior[1], Georges Daniel Amvame Nze[1], William Ferreira Giozza[1], Luiz Antônio Ribeiro Júnior[2]

[1]Department of Electrical Engineering, University of Brasília, Brasília, Brazil
[2]Institute of Physics, University of Brasília, Brasília, Brazil
Email: *marcelo.lopes@unb.br

How to cite this paper: Júnior, M.L.P., de Sousa Junior, R.T., Nze, G.D.A., Giozza, W.F. and Júnior, L.A.R. (2022) Evaluation of Peppermint Leaf Flavonoids as SARS-CoV-2 Spike Receptor-Binding Domain Attachment Inhibitors to the Human ACE2 Receptor: A Molecular Docking Study. *Open Journal of Biophysics*, **12**, 132-152.
https://doi.org/10.4236/ojbiphy.2022.122005

Received: January 22, 2022
Accepted: April 5, 2022
Published: April 8, 2022

Abstract

Virtual screening is a computational technique widely used for identifying small molecules which are most likely to bind to a protein target. In the present work, a molecular docking study is carried out to propose potential candidates for preventing the RBD/ACE2 attachment. These candidates are sixteen different flavonoids present in the peppermint leaf. Results showed that Luteolin 7-O-neohesperidoside is the peppermint flavonoid with a higher binding affinity regarding the RBD/ACE2 complex (about −9.18 Kcal/mol). On the other hand, Sakuranetin presented the lowest affinity (about −6.38 Kcal/mol). Binding affinities of the other peppermint flavonoids ranged from −6.44 Kcal/mol up to −9.05 Kcal/mol. The binding site surface analysis showed pocket-like regions on the RBD/ACE2 complex that yield several interactions (mostly hydrogen bonds) between the flavonoid and the amino acid residues of the proteins. This study can open channels for the understanding of the roles of flavonoids against COVID-19 infection.

Keywords

Coronavirus, Sars-CoV-2, Peppermint Flavonoids, RBD/ACE2 Inhibitors

1. Introduction

The COVID-19 is an infectious disease caused by the coronavirus SARS-CoV-2 [1] [2] [3] [4] [5]. It has reached the status of a pandemic in March of 2020. Up to January of 2022, it has already infected more than 300 million people, leading

to the death of more than 5 million ones [6]. Since the earlier stages of this pandemic, a worldwide effort has been devoted to producing vaccines and antiviral drugs to combat this virus. Some successful investigations yielded vaccines that have started to be applied very recently [7]-[14]. Despite the beginning of vaccination, no consensus about an efficient treatment for already infected patients has been reached so far.

Sars-CoV-2 has a crown-like (spherical) form, and its surface protein (Spike) is directly involved in the infectious process [15] [16] [17]. The receptor of this virus in human cells is the angiotensin-converting enzyme 2 (ACE2) [18] [19] [20]. Sars-CoV-2 surface protein has two subdivisions, named S1 and S2, being S1 the receptor-binding domain (RBD) [21] [22] [23] [24]. The RBD plays a major role in the attachment mechanism of Spike protein to ACE2 [25]. After the attachment between them, the virus enters the cell and starts the replication process [21]. In this sense, the strategy of virtual screening for possible inhibitors for the RBD/ACE2 attachment [26] may pave the way for novel therapeutic approaches for the treatment of COVID-19.

Drug repurposing is a feasible way to combat diseases with some similarities [27] [28] [29]. In this scenario, the use of phytochemicals is always an important option to be considered [30]. Among their sub-classes, the flavonoids—a class of small molecules found in fruits, vegetables, flowers, honey, teas, and wines, stand out [31] [32] [33]. Their pharmacological properties include antimicrobial, antioxidant, anti-inflammatory, and antiviral functions [34] [35] [36].

Flavonoids have been employed as inhibitors for the infection mechanism of several diseases [37]. Among them, one can mention malaria, leishmaniasis, Chagas, and dengue [38]-[43]. They have also been considered in studies aimed at developing therapeutic approaches for cancer treatment [44] [45] [46]. Very recently, it was reported that Luteolin (a flavonoid found in leaves and shells) is efficient as an anti-inflammatory that can interact with the Sars-CoV-2 surface [47] and its main protease [48]. More specifically, it is adsorbed in the Spike protein, inhibiting the Sars-CoV-2 attachment to the ACE2, thus preventing infection. Ngwa and colleagues used computer simulations to address the feasibility of Caflanone, Hesperetin, and Myricetin flavonoids in acting as inhibitors for the ACE2 active site attachment [49]. Their results pointed to the ability of Caflanone in inhibiting the transmission of the Sars-CoV-2 virus from mother to fetus in pregnancy. Pandey *et al.* conducted molecular docking and dynamics simulations considering ten flavonoid and non-flavonoid compounds (by using phytochemicals and hydroxychloroquine, respectively) to verify their performance in inhibiting the RBD/ACE2 interaction [50]. Their findings indicate that Fisetin, Quercetin, and Kamferol molecules couple to RBD/ACE2 complex with good binding affinities. In this sense, they can be explored as possible anti-Sars-CoV-2 agents. Despite the success of these molecules inhibiting the RBD/ACE2, other flavonoids should be tested to broaden the list of possible inhibitors and to confirm their potential in developing new therapeutic approaches for the treat-

ment of COVID-19.

Herein, in silico molecular docking analysis was carried out to propose potential flavonoid candidates in preventing the RBD/ACE2 attachment. These candidates are sixteen different flavonoids present in the Peppermint (Mentha piperita) leaf [51]-[57]. Peppermint is a perennial herb and medicinal plant native to Europe widely used for treating stomach pains, headaches, and inflammation of muscles [52] [56] [57]. Well-known for their flavoring and fragrance traits, peppermint leaves and the essential oil extracted from them are used in food, cosmetic and pharmaceutical products [51] [52] [53] [54]. Our results revealed that Luteolin 7-O-neohesperidoside is the peppermint flavonoid with a higher binding affinity regarding the RBD/ACE2 complex (about −9.18 Kcal/mol). On the other hand, Sakuranetin was the one with the lowest affinity (about −6.38 Kcal/mol). Binding affinities of the other peppermint flavonoids ranged from −6.44 Kcal/mol up to −9.05 Kcal/mol. These binding affinities are equivalent to other ones reported in the literature for the interaction between flavonoids and the RBD/ACE2 complex [47] [48] [58]-[64]. Moreover, the binding site surface analysis showed pocket-like regions on the RBD/ACE2 complex that yield several interactions (mostly hydrogen bonds) between the flavonoid and the amino acid residues of the proteins. Definitively, experimental studies and clinical trials should be further performed to evaluate the efficacy of these compounds in the inhibition of the RBD/ACE2 attachment.

2. Materials and Methods

Since Sars-CoV-2 infects human cells through the RBD/ACE2 coupling, the idea of checking for small molecules that may inhibit this interaction is recurring and can be useful to propose a combatant drug [65]. Here, we used molecular docking to study the interaction between the peppermint flavonoids with the RBD/ACE2 complex. Below, we present the proteins, inhibitors (flavonoids), and the computational protocol involved in our study.

2.1. Protein Preparation

Figure 1 presents the main proteins involved RBD/ACE2 interaction that were obtained from Protein Data Bank, ID 6M0J [66]. In the left panel of this figure, the ACE2 protein is in blue, while the RBD Sars-CoV-2 one is in red. Three essential regions of inhibition between these proteins were highlighted with the black squares R1, R2, and R3. In the right side of **Figure 1** we show the binding site surface colored as gray, red, blue, and white for carbon, oxygen, nitrogen, and hydrogen atoms, respectively. The yellow rectangle highlights the total surface for inhibition with a clear cavity within region R2. The protein resolution is 2.45 Å, and no pKa prediction was carried out. The modeled structure has 41 residues less than the deposited one, but all the important residues in the RDB/ACE2 interface were considered in our study. Just metal ions were considered in the docking study, water molecules were not included.

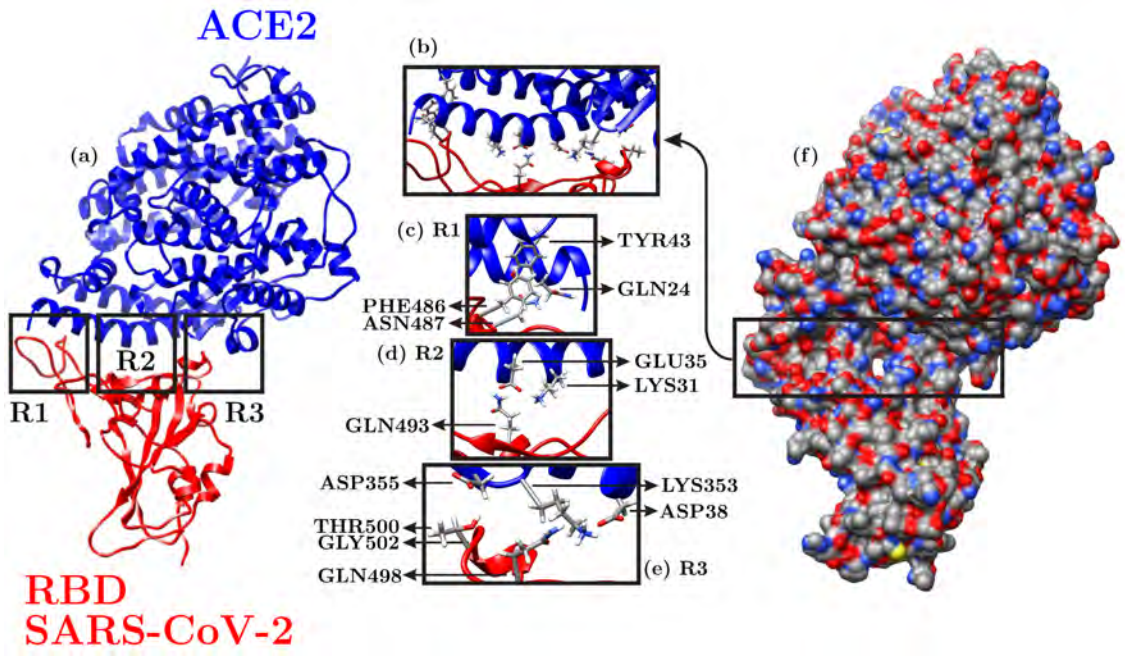

Figure 1. Schematic representation of the (a) main proteins involved RBD/ACE2 interaction. These proteins were obtained from Protein Data Bank, ID 6M0J [66]. (b) The binding site surface has the following color scheme: gray, red, blue, and white for carbon, oxygen, nitrogen, and hydrogen atoms, respectively. Only the three regions (R1, R2, and R3) were considered in the docking processes since they define the whole RBD/ACE2 interface. The TYR4, GLN24, PHE486, and ASN487 are the residues present in the region R1; GLU35, LYS31, and GLN493 are the residues present in the region R2; ASP355, THR500, GLY502, GLN498, LYS353, and ASP38 are the residues present in the region R3.

2.2. Ligand Preparation

The peppermint leaf contains sixteen flavonoids [51] [54], classified into three subcategories: Flavones (Flavonols), Flavorings, and Flavanones [51] [54]. The flavonoids studied here are Acacetin, Apigenin, Apigenin 7-O-neohesperidoside (Apigenin*), Chryseoriol, Hesperidin, Hesperitin, Ladanein, Luteolin, Luteolin 7-O-glucoside (Luteolin*), Luteolin 7-O-glucuronide (Luteolin**), Luteolin 7-O-neohesperidoside (Luteolin***), Narigenin, Pebrellin, Sakuranetin, Thymusin, and Xanthomicrol. Their 3D structures were extracted from PubChem [67]. The chemical structures of these flavonoids can be seen in **Figure 2**, while relevant information such as PubChem ID, molecular weight, molecular formula, and subcategory of the flavonoid is presented in **Table 1**.

2.3. Molecular Docking Simulation

Molecular docking consists of computationally analyzing the non-covalent binding between macromolecules (receptor) and small molecules (ligand). Here, the macromolecule is the RBD/ACE2 protein complex (**Figure 1**), while the ligands are the sixteen flavonoids present in the peppermint leaf (**Figure 2**). SWISSDOCK server was used for the docking simulations [68] [69]. In SWISSDOCK, the docking energies are obtained through the CHARMM (Chemistry at HARvard Macromolecular Mechanics) force field [68] [69] using a blind docking strategy

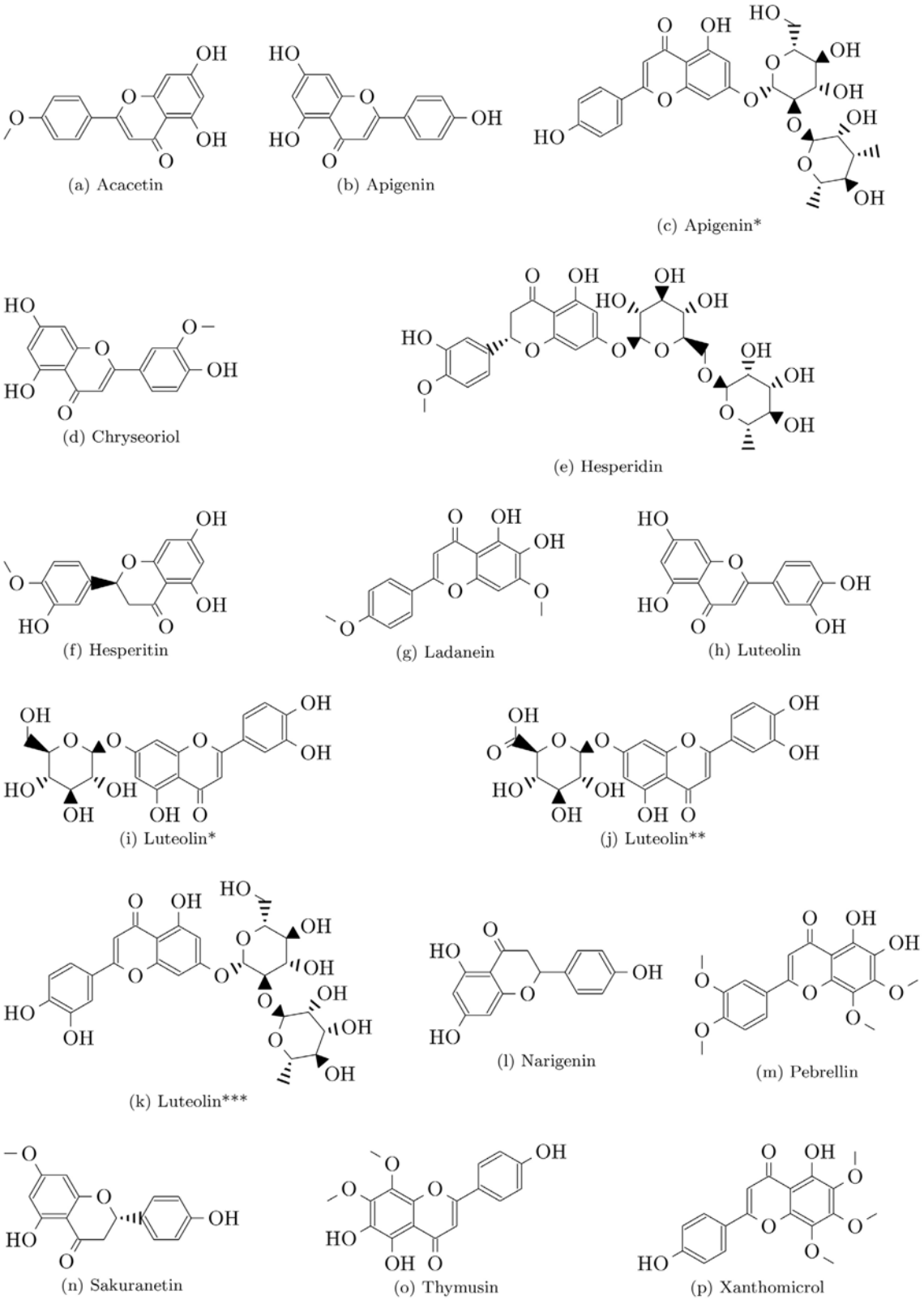

Figure 2. Chemical structure of peppermint leaf flavonoids: (a)Acacetin, (b) Apigenin, (c) Apigenin 7-O-neohesperidoside (Apigenin*), (d) Chryseoriol, (e) Hesperidin, (f) Hesperitin, (g) Ladanein, (h) Luteolin, (i) Luteolin 7-O-glucoside (Luteolin*), (j) Luteolin 7-O-glucuronide (Luteolin**), (k) Luteolin 7-O-neohesperidoside (Luteolin***), (l) Narigenin, (m) Pebrellin, (n) Sakuranetin, (o) Thymusin, and (p) Xanthomicrol.

Table 1. Potential inhibitors (peppermint leaf flavonoids) of RBD/ACE2 complex and their compound information.

Compound	PubChem CID	Mol. Weight (g/mol)	Mol. Formula	Type
Acacetin	5280442	284.26	$C_{16}H_{12}O_5$	Flavones and Flavonols
Apigenin	5280443	270.24	$C_{15}H_{10}O_5$	Flavones and Flavonols
Apigenin*	5282150	578.5	$C_{27}H_{30}O_{14}$	Flavones and Flavonols
Chryseoriol	5280666	300.26	$C_{16}H_{12}O_6$	Flavones and Flavonols
Hesperidin	10621	610.6	$C_{28}H_{34}O_{15}$	Flavorings
Hesperitin	72281	302.28	$C_{16}H_{14}O_6$	Flavanones
Ladanein	3084066	314.29	$C_{17}H_{14}O_6$	Flavones and Flavonols
Luteolin	5280445	286.24	$C_{15}H_{10}O_6$	Flavones and Flavonols
Luteolin*	5280637	448.4	$C_{21}H_{20}O_{11}$	Flavones and Flavonols
Luteolin**	5280601	462.4	$C_{21}H_{18}O_{12}$	Flavones and Flavonols
Luteolin***	5282152	594.5	$C_{27}H_{30}O_{15}$	Flavones and Flavonols
Naringenin	932	272.25	$C_{15}H_{12}O_5$	Flavorings
Pebrellin	632255	374.3	$C_{19}H_{18}O_8$	Flavones and Flavonols
Sakuranetin	73571	286.28	$C_{16}H_{14}O_5$	Flavanones
Thymusin	628895	330.29	$C_{17}H_{14}O_7$	Flavones and Flavonols
Xanthomicrol	73207	344.3	$C_{18}H_{16}O_7$	Flavones and Flavonols

that spans over 100 trial configurations for each target/ligand input [70]. The target/ligand configuration with higher binding affinity is selected using the UCFS CHIMERA software [71], a visualization tool capable of directly importing data from the SWISSDOCK server. Finally, the Protein-Ligand Interaction Profiler (PLIP) server [72] is used to characterize the target/ligand interaction for the configuration with a higher binding affinity for each flavonoid regarding the RBD/ACE2 complex. It is worth mentioning that the screening for the ligand position was limited just to the ACE2/RDB interface (regions R1, R2, and R3 in the left panel of **Figure 1**). This interface is the crucial region to be considered for blocking the coronavirus entry and replication cycle. The simulation (docking) box used in the screening for the ligand position was limited just to the ACE2/RDB interface (regions R1, R2, and R3 in the left panel of **Figure 1**). The docking box has 27.5 Å × 9.0 Å × 8.5 Å of dimension and it was centered at (31.5, −36.0, 1.5) Å. These parameters cover the three regions depicted in **Figure 1**. The accuracy in estimating the ligand positions and related binding affinities are ±2 Å and ±0.01 Kcal/mol, respectively.

3. Results

After successful docking of the peppermint flavonoids to the RBD/ACE2 complex, several modes of ligand/target interactions were generated with a particular

docking score (binding affinity). The binding mode with the lowest binding affinity is regarded as the best one, once it tends to be the most stable. The binding affinity results (ΔG) obtained here are summarized in Table 2. SWISSDOCK simulations for all the ligands in Figure 2 revealed significant binding affinities with the target RBD/ACE2 proteins. Luteolin 7-O-neohesperidoside is the peppermint flavonoid with a higher binding affinity regarding the RBD/ACE2 complex (about −9.18 Kcal/mol). On the other hand, Sakuranetin was the one with the lowest affinity (approximately −6.38 Kcal/mol). Binding affinities of the other peppermint flavonoids ranged from −6.44 Kcal/mol up to −9.05 Kcal/mol. Sakuranetin has presented hydrogen and π-stacking bond distances higher than 3.05 Å, leading to weak bond strengths and a lower binding affinity. The other flavonoids showed bond distances varying from 1.86 Å to 2.96 Å. The hydrogen bond between Sakuranetin and the amino acid LYS335 has 3.73 Å (the largest bond obtained in our study). Consequently, Sakuranetin has the lower van der Waals interaction, about −35.3 Kcal/mol, as shown in Figure 7.

As one can note in Table 1 and Table 2, the best docked flavonoids have greater molecular weight. All the binding affinities are close to the ones reported for the RBD/ACE2 interaction with other species of flavonoids [47] [48] [58]-[64]. Moreover, they can outperform the binding affinities reported by docking studies using other types of compounds targeting RBD/ACE2 [26] [73]-[79], such as Chloroquine and Hydroxychloroquine, which are lower than −8.0 Kcal/mol

Table 2. Peppermint leaf-based flavonoid candidates undergoing docking experiment with their most favorable conformation (lowest binding affinity ΔG in Kcal/mol).

Compound	ΔG [Kcal/mol]
Acacetin	−6.70
Apigenin	−6.87
Apigenin 7-O-neohesperidoside	−8.08
Chryseoriol	−6.78
Hesperidin	−8.67
Hesperitin	−6.80
Ladanein	−6.56
Luteolin	−7.24
Luteolin 7-O-glucoside	−8.01
Luteolin 7-O-glucuronide	−7.74
Luteolin 7-O-neohesperidoside	−9.18
Naringenin	−6.44
Pebrellin	−7.07
Sakuranetin	−6.38
Thymusin	−6.94
Xanthomicrol	−6.83

[26]. This fact can be attributed to the abundant phenolic hydroxyl group in flavonoids. The hydroxyl group in the sugar group of flavonoids tends to bind more easily with the heteroatoms of amino acids from RBD/ACE2, as discussed later. In this sense, peppermint flavonoids can compose the list of potential phytochemical inhibitors for the RBD/ACE2 interaction.

Figure 3 and Figure 4 illustrate the binding site surface (BSS) for the putative

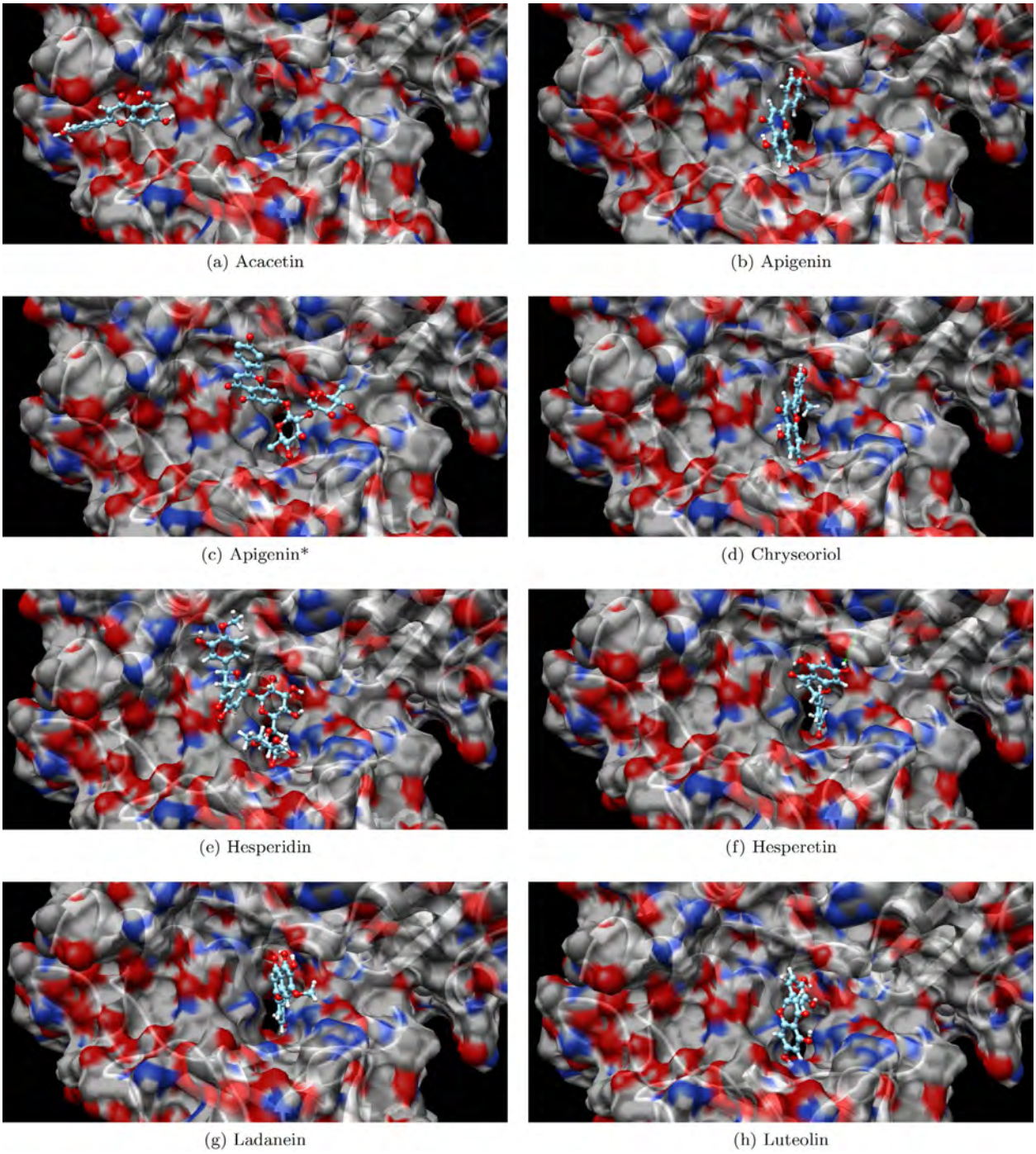

Figure 3. Binding site surface (BSS) for the putative best docking target/ligand configurations of (a) Acacetin, (b) Apigenin, (c) Apigenin*, (d) Chryseoriol, (e) Hesperidin, (f) Hesperetin, (d) Ladanein, and (d) Luteolin.

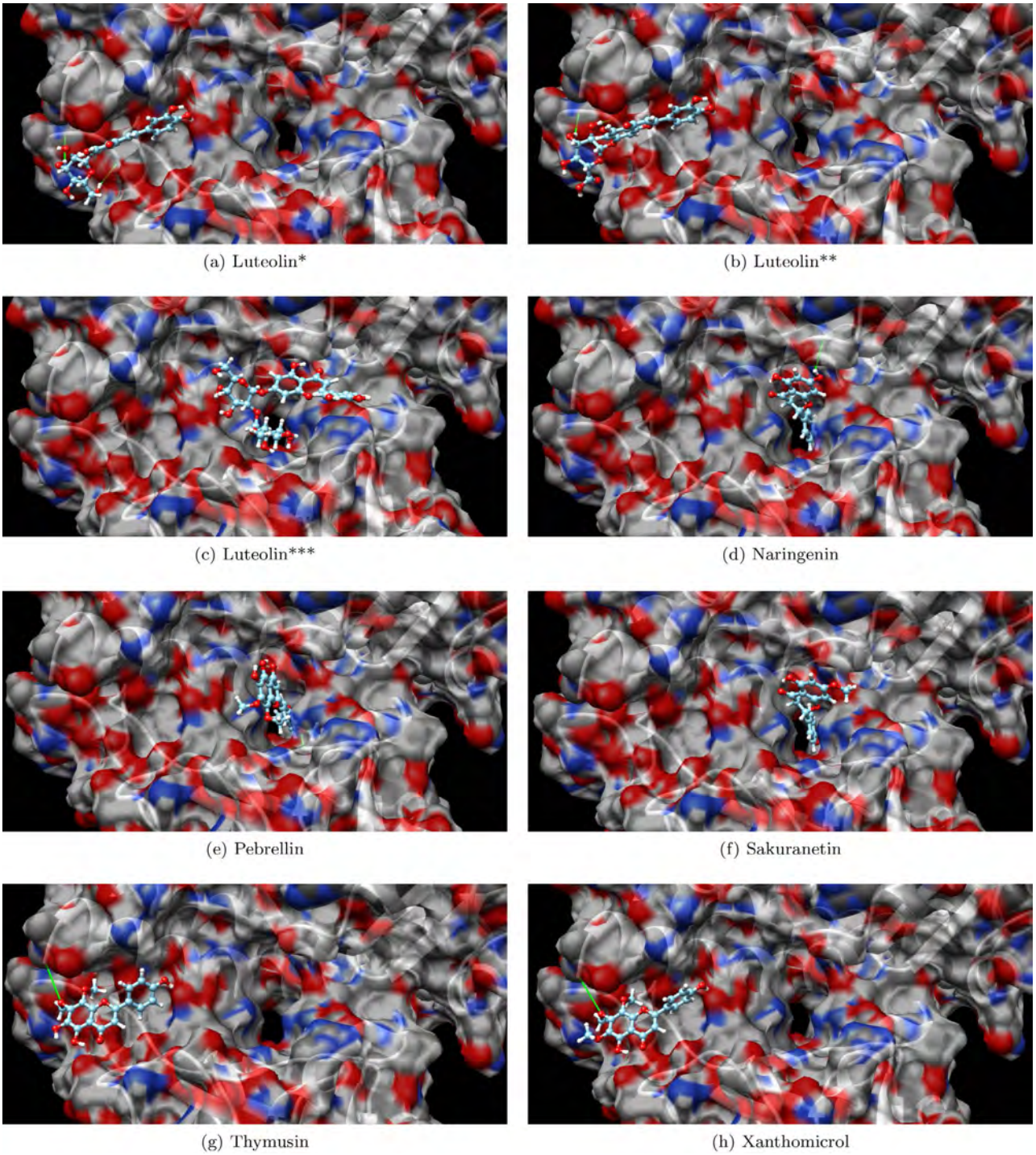

Figure 4. Binding site surface (BSS) for the putative best docking target/ligand configurations of (a) Luteloin*, (b) Luteloin**, (c) Luteloin***, (d) Naringenin, (e) Pebrellin, (f) Sakuranetin, (d) Thymusin, and (d) Xanthomicrol.

best docking target/ligand configurations. For the sake of clarity, these figures show the BSS only for the RBD/ACE2 region highlighted by the yellow rectangle in **Figure 1(b)**. The following color scheme is adopted for the BSSs: gray, red, blue, and white for carbon, oxygen, nitrogen, and hydrogen atoms, respectively. In the ball-stick representation for the flavonoids, the carbon, oxygen, and hy-

drogen atoms are shown in the colors cyan, red, and white, respectively. As a general trend, one can note that the flavonoids fit inside the core pocket region (cavity) of the RBD/ACE2 complex. This cavity is displayed as region 2 in **Figure 1(a)**. Acacetin, Luteolin*, Luteolin**, Thymusin, and Xanthomicrol were adsorbed on region 1 (see **Figure 1(a)**) of the RBD/ACE2 complex. The ligands tend to interact with the oxygen atoms (red spots in the BSS) in regions 1 and 2. These regions establish pocket-like media that yield interactions (mostly hydrogen bonds) between flavonoids and amino acid residues of proteins.

Figure 5 and **Figure 6** provide a clear picture of the interaction between the amino acid residues of the proteins and peppermint flavonoids. The docked poses (obtained using PLIP [72] show the residues names and the bond types. In the stick representation of flavonoids, the carbon and oxygen atoms are in orange and red colors, respectively. The hydrogen, hydrophobic, and π-staking bonds are denoted by the blue, dashed gray, and dashed yellow lines, respectively. The yellow sphere represents the charge center. In **Figure 5**, one can note that Acacetin, Apigenin, Apigenin*, Chryseoriol, Hesperidin, Hesperetin, Ladenein, and Luteolin interact with RBD/ACE2 mainly through 4, 5, 5, 6, 12, 5, 4, and 8 hydrogen bonds with distinct amino acid residues in both RBD and ACE2 proteins. Similarly, **Figure 6** shows the interaction mechanism between Luteloin*, Luteloin**, Luteloin***, Naringenin, Pebrellin, Sakuranetin, Thymusin, and Xanthomicrol with RBD/ACE2 is mediated by 7, 5, 9, 8, 5, 5, 4, and 4 hydrogen bonds with distinct amino acid residues in both RBD and ACE2 proteins, respectively. In total, 12 hydrophobic bonds were found. The flavonoids and amino acid residues of the proteins involved in this kind of interaction are highlighted below. Some π-stacking bonds are also present in the RBD/ACE2 interactions with flavonoids expecting for the Hesperidin (**Figure 5(e)**), Luteolin* (**Figure 6(a)**), and Xanthomicrol (**Figure 6(h)**) cases.

Generally speaking, we identified 31 distinct amino acid residues of the RBD/ACE2 interacting with the peppermint flavonoids. The RBD amino acid residues (and their occurrence) are TYR738 (4), LYS682 (5), GLU761 (6), GLN674 (6), TYR770 (6), ARG688 (8), ASP670 (2), GLY761 (4), GLY741 (2), GLN39 (1), ALA740 (1), LYS723 (3), ARG673 (1), and SER759 (1). The ACE2 amino acid residues (and their occurrence) are GLU5 (3), SER1 (5), ASP12 (7), PHE372 (4), ARG375 (9), ASN15 (8), GLU19 (9), PRO371 (1), ANS15 (1), THR71 (1), ALA369 (4), ARG37 (1), ALA368 (1), LYS335 (2), ASP20 (1), TYR760 (1), and LYS8 (1). This result suggests that the target RBD/ACE2 amino acid residues for this class of phytochemicals are ARG375, ASN15, and GLU19 from ACE2, and ARG668 from RBD, based on their higher occurrence. The flavonoids that present hydrophobic bonds with the RBD/ACE2 amino acids, highlighted in the following as (flavonoid/residue), are Ladanein/GLU19, Luteolin/LYS682, Hesperetin/ASN15, Hesperetin/GLU19, Pebrellin/TYR760, Sakuranetin/GLU19, Thymusin/LY58, Acacetin/GLU5, Apigenin/ASN15, Apigenin/PRO371, Apigenin/TYR770, and Chryseoriol/LYS682. Finally, we estimate the number of times a particular

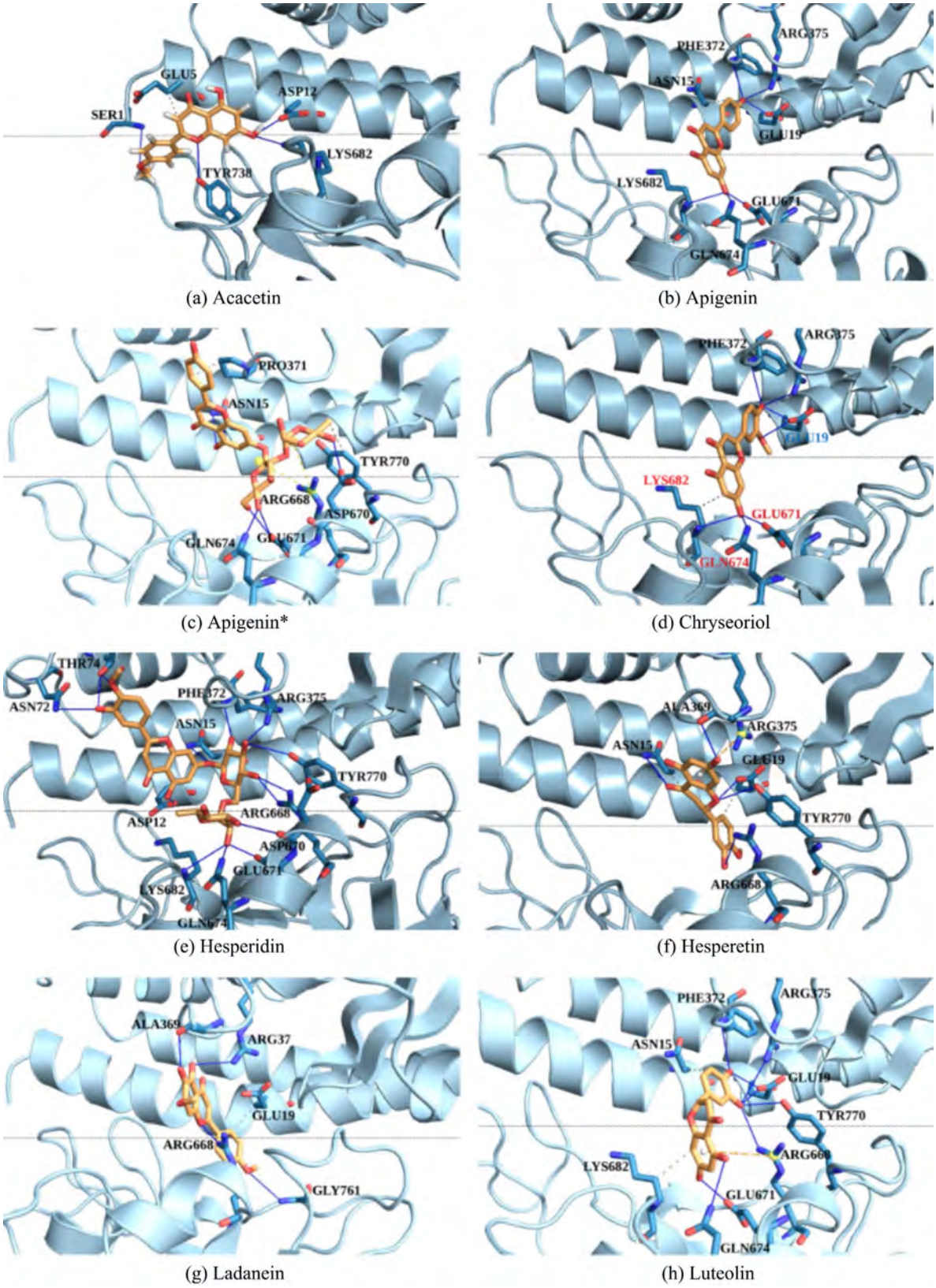

Figure 5. PLIP docked poses for the RBD/ACE2 interaction with (a) Acacetin, (b) Apigenin, (c) Apigenin*, (d) Chryseoriol, (e) Hesperidin, (f) Hesperetin, (d) Ladanein, and (d) Luteolin. The hydrogen, hydrophobic, and π-staking bonds are denoted by the blue, dashed gray, and dashed yellow lines, respectively. The yellow sphere represents the charge center.

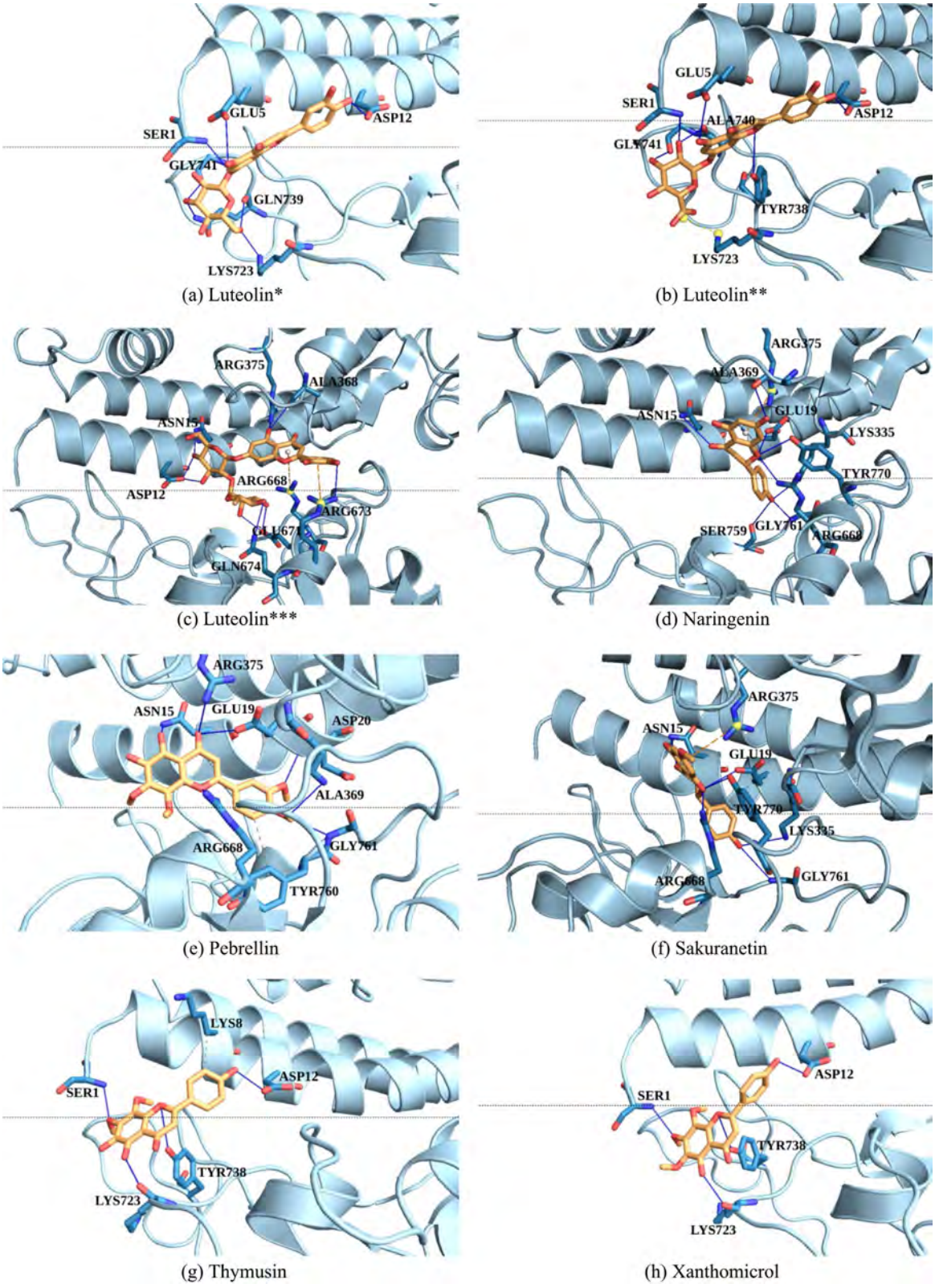

Figure 6. PLIP docked poses for the RBD/ACE2 interaction with (a) Luteloin*, (b) Luteloin**, (c) Luteloin***, (d) Naringenin, (e) Pebrellin, (f) Sakuranetin, (d) Thymusin, and (d) Xanthomicrol. The hydrogen, hydrophobic, and π-staking bonds are denoted by the blue, dashed gray, and dashed yellow lines, respectively. The yellow sphere represents the charge center. ACE2 and RBD moieties are shown above and below the horizontal line, respectively.

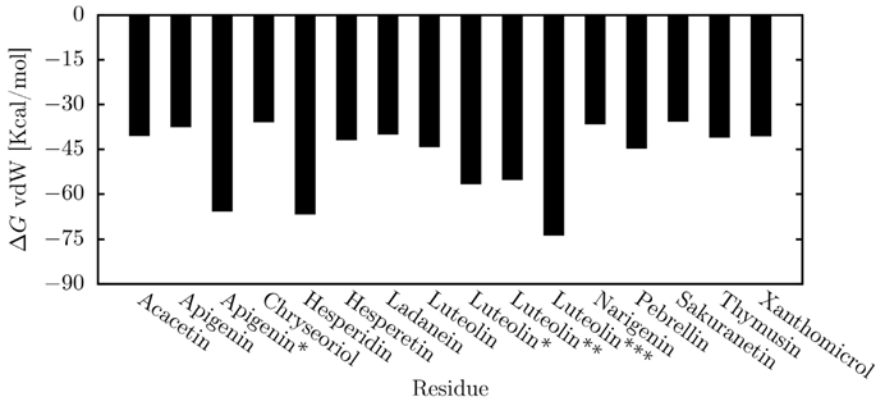

Figure 7. van der Waals interactions (ΔG vdW) between the protein and ligands.

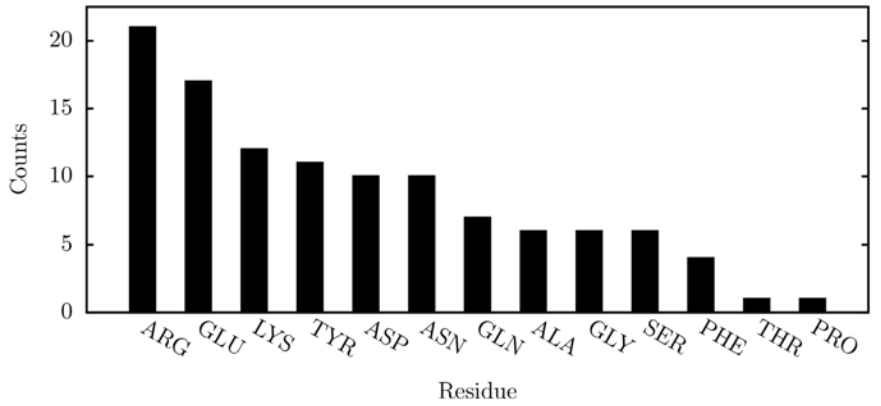

Figure 8. Counts of bonds between ligands and amino acids of a specific kind. This figure suggests that ARG are the crucial amino acids in promoting the flavonoids attachment to RDB.

amino acid interacts with the ligands. We count 21 bonds (14 hydrogen bonds and the van der Waals bonds) between the ligands and amino acids of kind ARG. This trend suggests that ARG are the crucial amino acids in promoting the flavonoids attachment to RDB (**Figure 7** & **Figure 8**).

4. Conclusions

In summary, a set of phytochemicals (peppermint flavonoids) were screened against the SARS-CoV-2 Spike receptor-binding domain interacting with the human ACE2 receptor. The approach is based on computationally fitting small molecules for the target RBD/ACE2 complex proteins using the 3D structure of the active site with SWISSDOCK [68] [69], subsequently the ranking of the docked compounds with Quimera [71] and interaction analysis with PLIP [72]. Results revealed that Luteolin 7-O-neohesperidoside has a binding affinity of about −9.18 Kcal/mol, the higher one among the flavonoids studied here. On the other hand, Sakuranetin was the one with the lowest affinity (about −6.38 Kcal/mol). Binding affinities of the other peppermint flavonoids ranged from −6.44 Kcal/mol up to −9.05 Kcal/mol. These values outperform the binding affinities

reported by docking studies using other types of compounds in which the RBD/ACE2 complex was also the target [80] [81].

The binding site surface analysis showed pocket-like regions on the RBD/ACE2 complex that yield several interactions (mostly hydrogen bonds) between the flavonoid and the amino acid residues of the proteins. The interaction mechanism between the flavonoids and amino acid residues of the proteins is mediated by hydrogen bonds, essentially. The presence of some hydrophobic and π-stacking bonds was also observed. In total, we identified 31 distinct amino acid residues of the RBD/ACE2 interacting with the peppermint flavonoids. The target RBD/ACE2 amino acid residues for this class of phytochemicals are ARG375, ASN15, and GLU19 from ACE2, and ARG668 from RBD, based on their higher occurrence.

Some *in vitro* studies investigated the antiviral activity of flavonoids in combating SARS-CoV [64] [82] and SARS-CoV2 [83] [84] [85] [86] infection. Hesperetin, Luteolin, and Apigenin have been demonstrated as potent inhibitors of SARS-CoV-2 3CLpro *in vitro* and can be considered proper candidates for further optimization and development of therapeutic interventions, particularly those related to inflammation processes and immunity [86]. A Luteolin derivative and Apigenin showed the best docking scores in our study.

Acknowledgements

The authors gratefully acknowledge the financial support from Brazilian Research Councils CNPq, CAPES, and FAPDF and CENAPAD-SP for providing the computational facilities. M.L.P.J. gratefully acknowledges the financial support from CAPES grant 88882.383674/2019-01. L.A.R.J. gratefully acknowledges respectively, the financial support from FAP-DF grants 00193-00000853/2021-28 and 00193-00000857/2021-14, CNPq grant 302236/2018-0, and UnB/DPI/DEX Edital 01/2020 grant 23106.057604/2020-05. The molecular graphics and analyses were performed with UCSF Chimera, developed by the Resource for Biocomputing, Visualization, and Informatics at the University of California, San Francisco, with support from NIH P41-GM103311. R.T.S.J. gratefully acknowledges, respectively, the support from EC Horizon 2020 HEROES project grant 101021801, CNPq grants 465741/2014-2 and 312180/2019-5, CAPES grant 88887.144009/2017-00, and FAP-DF grants 0193.001366/2016 and 0193.001365/2016. R.T.S.J. and L.A.R.J gratefully acknowledge the support from ABIN grant 08/2019. W.F.G gratefully acknowledges the financial support FAP-DF grant 00193-00000853/2021-28.

Conflicts of Interest

The authors declare no conflicts of interest regarding the publication of this paper.

References

[1] Chen, H., Guo, J., Wang, C., Luo, F., Yu, X., Zhang, W., Li, J., Zhao, D., Xu, D.,

Gong, Q., *et al.* (2020) Clinical Characteristics and Intrauterine Vertical Transmission Potential of Covid-19 Infection in Nine Pregnant Women: A Retrospective Review of Medical Records. *The Lancet*, **395**, 809-815. https://doi.org/10.1016/S0140-6736(20)30360-3

[2] Rothan, H.A. and Byrareddy, S.N. (2020) The Epidemiology and Pathogenesis of Coronavirus Disease (COVID-19) Outbreak. *Journal of Autoimmunity*, **109**, Article ID: 102433. https://doi.org/10.1016/j.jaut.2020.102433

[3] Guo, Y.-R., Cao, Q.-D., Hong, Z.-S., Tan, Y.-Y., Chen, S.-D., Jin, H.-J., Tan, K.-S., Wang, D.-Y. and Yan, Y. (2020) The Origin, Transmission and Clinical Therapies on Coronavirus Disease 2019 (COVID-19) Outbreak—An Update on the Status. *Military Medical Research*, **7**, Article No. 11. https://doi.org/10.1186/s40779-020-00240-0

[4] Tu, Y.-F., Chien, C.-S., Yarmishyn, A.A., Lin, Y.-Y., Luo, Y.-H., Lin, Y.-T., Lai, W.-Y., Yang, D.-M., Chou, S., Yang, Y.-P., *et al.* (2020) A Review of Sars-cov-2 and the Ongoing Clinical Trials. *International Journal of Molecular Sciences*, **21**, Article No. 2657. https://doi.org/10.3390/ijms21072657

[5] Wang, L., Wang, Y., Ye, D. and Liu, Q. (2020) Review of the 2019 Novel Coronavirus (SARS-CoV-2) Based on Current Evidence. *International Journal of Antimicrobial Agents*, **55**, Article ID: 105948. https://doi.org/10.1016/j.ijantimicag.2020.105948

[6] World Health Organization (n.d.) Coronavirus Disease (COVID-19) Pandemic. https://www.who.int/emergencies/diseases/novel-coronavirus-2019

[7] Sharma, O., Sultan, A.A., Ding, H. and Triggle, C.R. (2020) A Review of the Progress and Challenges of Developing a Vaccine for Covid19. *Frontiers in Immunology*, **11**, Article No. 585354. https://doi.org/10.3389/fimmu.2020.585354

[8] Voysey, M., Clemens, S.A.C., Madhi, S.A., Weckx, L.Y., Folegatti, P.M., Aley, P.K., Angus, B., Baillie, V.L., Barnabas, S.L., Bhorat, Q.E., *et al.* (2021) Safety and Efficacy of the Chadox1 Ncov-19 Vaccine (azd1222) Against Sars-cov-2: An Interim Analysis of Four Randomised Controlled Trials in Brazil, South Africa, and the UK. *The Lancet*, **397**, 99-111. https://doi.org/10.1016/S0140-6736(20)32661-1

[9] Corbett, K.S., Flynn, B., Foulds, K.E., Francica, J.R., Boyoglu-Barnum, S., Werner, A.P., Flach, B., O'Connell, S., Bock, K.W., Minai, M., *et al.* (2020) Evaluation of the Mrna-1273 Vaccine against SARS-CoV-2 in Nonhuman Primates. *New England Journal of Medicine*, **383**, 1544-1555. https://doi.org/10.1056/NEJMoa2024671

[10] Baden, L.R., El Sahly, H.M., Essink, B., Kotloff, K., Frey, S., Novak, R., Diemert, D., Spector, S.A., Rouphael, N., Buddy Creech, C., *et al.* (2021) Efficacy and Safety of the Mrna-1273 SARS-CoV-2 Vaccine. *New England Journal of Medicine*, **384**, 403-416. https://doi.org/10.1056/NEJMoa2035389

[11] Anderson, E.J., Rouphael, N.G., Widge, A.T., Jackson, L.A., Roberts, P.C., Makhene, M., Chappell, J.D., Denison, M.R., Stevens, L.J., Pruijssers, A.J., *et al.* (2020) Safety and Immunogenicity of Sars-cov-2 Mrna-1273 Vaccine in Older Adults. *New England Journal of Medicine*, **383**, 2427-2438. https://doi.org/10.1056/NEJMoa2028436

[12] Zhang, Y.-J., Zeng, G., Pan, H.-X., Li, C.-G., Kan, B., Hu, Y.-L., Mao, H.-Y., Xin, Q.-Q., Chu, K., Han, W.-X., *et al.* (2020) Immunogenicity and Safety of a Sars-cov-2 Inactivated Vaccine in Healthy Adults Aged 18-59 Years: Report of the Randomized, Double-Blind, and Placebo-Controlled Phase 2 Clinical Trial. *Medrxiv*. https://doi.org/10.1101/2020.07.31.20161216

[13] Jones, I. and Roy, P. (2021) Sputnik V COVID-19 Vaccine Candidate Appears Safe and Effective. *The Lancet*, **397**, 642-643.

https://doi.org/10.1016/S0140-6736(21)00191-4

[14] Burki, T.K. (2020) The Russian Vaccine for COVID-19. *The Lancet Respiratory Medicine*, **8**, e85-e86. https://doi.org/10.1016/S2213-2600(20)30402-1

[15] Wu, Y., Xu, X., Chen, Z., Duan, J., Hashimoto, K., Yang, L., Liu, C. and Yang, C. (2020) Nervous System Involvement after Infection With Covid-19 and other Coronaviruses. *Brain, Behavior, and Immunity*, **87**, 18-22. https://doi.org/10.1016/j.bbi.2020.03.031

[16] Chhikara, B.S., Rathi, B., Singh, J. and Poonam, F.N.U. (2020) Corona Virus Sars-CoV-2 Disease COVID-19: Infection, Prevention and Clinical Advances of the Prospective Chemical Drug Therapeutics. *Chemical Biology Letters*, **7**, 63-72. https://doi.org/10.1007/s00058-020-1496-8

[17] Liang, Y., Wang, M.-L., Chien, C.-S., Yarmishyn, A.A., Yang, Y.-P., Lai, W.-Y., Luo, Y.-H., Lin, Y.-T., Chen, Y.-J., Chang, P.-C., *et al.* (2020) Highlight of Immune Pathogenic Response and Hematopathologic Effect in SARS-CoV, MERS-CoV, and SARS-Cov-2 Infection. *Frontiers in Immunology*, **11**, Article No. 1022. https://doi.org/10.3389/fimmu.2020.01022

[18] Zhang, H., Penninger, J.M., Li, Y., Zhong, N. and Slutsky, A.S. (2020) Angiotensin-Converting Enzyme 2 (ACE2) as a SARS-CoV-2 Receptor: Molecular Mechanisms and Potential Therapeutic Target. *Intensive Care Medicine*, **46**, 586-590. https://doi.org/10.1007/s00134-020-05985-9

[19] Li, W., Moore, M.J., Vasilieva, N., Sui, J., Wong, S.K., Berne, M.A., Somasundaran, M., Sullivan, J.L., Luzuriaga, K., Greenough, T.C., *et al.* (2003) Angiotensin-Converting Enzyme 2 Is a Functional Receptor for the SARS Coronavirus. *Nature*, **426**, 450-454. https://doi.org/10.1038/nature02145

[20] Kuba, K., Imai, Y., Rao, S., Gao, H., Guo, F., Guan, B., Huan, Y., Yang, P., Zhang, Y., Deng, W., *et al.* (2005) A Crucial Role of Angiotensin Converting Enzyme 2 (ACE2) in SARS Coronavirus-Induced Lung Injury. *Nature Medicine*, **11**, 875-879. https://doi.org/10.1038/nm1267

[21] Xiu, S., Dick, A., Ju, H., Mirzaie, S., Abdi, F., Cocklin, S., Zhan, P. and Liu, X. (2020) Inhibitors of SARS-CoV-2 Entry: Current and Future Opportunities. *Journal of Medicinal Chemistry*, **63**, 12256-12274. https://doi.org/10.1021/acs.jmedchem.0c00502

[22] Tai, W., He, L., Zhang, X., Pu, J., Voronin, D., Jiang, S., Zhou, Y. and Du, L. (2020) Characterization of the Receptor-Binding Domain (RBD) of 2019 Novel Coronavirus: Implication for Development of RBD Protein as a Viral Attachment Inhibitor and Vaccine. *Cellular & Molecular Immunology*, **17**, 613-620. https://doi.org/10.1038/s41423-020-0400-4

[23] Spinello, A., Saltalamacchia, A. and Alessandra, M. (2020) Is the Rigidity of SARS-CoV-2 Spike Receptor-Binding Motif the Hallmark for Its Enhanced Infectivity? Insights from All-Atom Simulations. *The Journal of Physical Chemistry Letters*, **11**, 4785-4790. https://doi.org/10.1021/acs.jpclett.0c01148

[24] Han, Y. and Král, P. (2020) Computational Design of Ace2-Based Pep-Tide Inhibitors of SARS-CoV-2. *ACS Nano*, **14**, 5143-5147. https://doi.org/10.1021/acsnano.0c02857

[25] Singh, A., Steinkellner, G., Köchl, K., Gruber, K. and Gruber, C.C. (2021) Serine 477 Plays a Crucial Role in the Interaction of the SARS-CoV-2 Spike Protein with the Human Receptor ACE2. *Scientific Reports*, **11**, Article No. 4320. https://doi.org/10.1038/s41598-021-83761-5

[26] Basu, A., Sarkar, A. and Maulik, U. (2020) Molecular Docking Study of Potential

Phytochemicals and Their Effects on the Complex of SARS-CoV2 Spike Protein and Human ACE2. *Scientific Reports*, **10**, Article No. 17699. https://doi.org/10.1038/s41598-020-74715-4

[27] Zhou, Y., Hou, Y., Shen, J., Huang, Y., Martin, W. and Cheng, F. (2020) Network-Based Drug Repurposing for Novel Coronavirus 2019-nCoV/SARS-CoV-2. *Cell Discovery*, **6**, Article No. 4. https://doi.org/10.1038/s41421-020-0153-3

[28] Gordon, D.E., Jang, G.M., Bouhaddou, M., Xu, J., Obernier, K., White, K.M., OMeara, M.J., Rezelj, V.V., Guo, J.Z., Swaney, D.L., *et al.* (2020) A SARS-CoV-2 Protein Interaction Map Reveals Targets for Drug Repurposing. *Nature*, **583**, 459-468. https://doi.org/10.1038/s41586-020-2286-9

[29] Pandey, A., Nikam, A.N., Shreya, A.B., Mutalik, S.P., Gopalan, D., Kulkarni, S., Padya, B.S., Fernandes, G., Mutalik, S. and Prassl, R. (2020) Potential Therapeutic Targets for Combating SARS-CoV-2: Drug Repurposing, Clinical Trials and Recent Advancements. *Life Sciences*, **256**, Article ID: 117883. https://doi.org/10.1016/j.lfs.2020.117883

[30] Swain, S.S., Panda, S.K. and Luyten, W. (2020) Phytochemicals against SARS-CoV as Potential Drug Leads. *Biomedical Journal*, **44**, 74-85.

[31] Panche, A.N., Diwan, A.D. and Chandra, S.R. (2016) Flavonoids: An Overview. *Journal of Nutritional Science*, **5**, Article No. e47. https://doi.org/10.1017/jns.2016.41

[32] Harborne, J.B., Marby, H. and Marby, T.J. (2013) The Flavonoids. Springer, Boston.

[33] Hertog, M.G.L., Hollman, P.C.H. and Katan, M.B. (1992) Content of Potentially Anticarcinogenic Flavonoids of 28 Vegetables and 9 Fruits Commonly Consumed in the Netherlands. *Journal of Agricultural and Food Chemistry*, **40**, 2379-2383. https://doi.org/10.1021/jf00024a011

[34] Kumar, S. and Pandey, A.K. (2013) Chemistry and Biological Activities of Flavonoids: An Overview. *The Scientific World Journal*, **2013**, Article ID: 162750. https://doi.org/10.1155/2013/162750

[35] Sharma, D.K. (2006) Pharmacological Properties of Flavonoids Including Flavonolignans-Integration of Petrocrops with Drug Development from Plants. *Journal of Scientific and Industrial Research*, **65**, 477-484.

[36] Kim, H.P., Son, K.H., Chang, H.W. and Kang, S.S. (2004) Anti-Inflammatory Plant Flavonoids and Cellular Action Mechanisms. *Journal of Pharmacological Sciences*, **96**, 229-245. https://doi.org/10.1254/jphs.CRJ04003X

[37] Cushnie, T.P. and Lamb, A.J. (2005) Antimicrobial Activity of Flavonoids. *International Journal of Antimicrobial Agents*, **26**, 343-356. https://doi.org/10.1016/j.ijantimicag.2005.09.002

[38] Lehane, A.M. and Saliba, K.J. (2008) Common Dietary Flavonoids Inhibit the Growth of the Intraerythrocytic Malaria Parasite. *BMC Research Notes*, **1**, Article No. 26. https://doi.org/10.1186/1756-0500-1-26

[39] Muzitano, M.F., Falcão, C.A.B., Cruz, E.A., Bergonzi, M.C., Bilia, A.R., Vincieri, F.F., Rossi-Bergmann, B. and Costa, S.S. (2009) Oral Metabolism and Efficacy of Kalanchoe Pinnata Flavonoids in a Murine Model of Cutaneous Leishmaniasis. *Planta Medica*, **75**, 307-311. https://doi.org/10.1055/s-0028-1088382

[40] Marín, C., Ramírez-Macías, I., López-Céspedes, A., Olmo, F., Villegas, N., Díaz, J.G., Rosales, M.J., Gutiérrez-Sánchez, R. and Sánchez-Moreno, M. (2011) *In Vitro* and *in Vivo* Trypanocidal Activity of Flavonoids from Delphinium Staphisagria against Chagas Disease. *Journal of Natural Products*, **74**, 744-750. https://doi.org/10.1021/np1008043

[41] Sanchez, I., Gómez-Garibay, F., Taboada, J. and Ruiz, B.H. (2000) Antiviral Effect of Flavonoids on the Dengue *Virus. Phytotherapy Research*, **14**, 89-92. https://doi.org/10.1002/(SICI)1099-1573(200003)14:2%3C89::AID-PTR569%3E3.0.CO;2-C

[42] Kiat, T.S., Pippen, R., Yusof, R., Ibrahim, H., Khalid, N., and Abd Rahman, N. (2006) Inhibitory Activity of Cyclohexenyl Chalcone Derivatives and Flavonoids of Fingerroot, *Boesenbergia Rotunda* (L.), towards Dengue-2 Virus NS3 Protease. *Bioorganic & Medicinal Chemistry Letters*, **16**, 3337-3340. https://doi.org/10.1016/j.bmcl.2005.12.075

[43] de Sousa, L.R.F., Wu, H., Nebo, L., Fernandes, J.B., Kiefer, W., Kanitz, M., Bodem, J., Diederich, W.E., Schirmeister, T., Vieira, P.C., *et al.* (2015) Flavonoids as Noncompetitive Inhibitors of Dengue Virus NS2B-NS3 Pro-Tease: Inhibition Kinetics and Docking Studies. *Bioorganic & Medicinal Chemistry*, **23**, 466-470. https://doi.org/10.1016/j.bmc.2014.12.015

[44] Abotaleb, M., Samuel, S.M., Varghese, E., Varghese, S., Kubatka, P., Liskova, A. and Büsselberg, D. (2019) Flavonoids in Cancer and Apoptosis. *Cancers*, **11**, Article No. 28. https://doi.org/10.3390/cancers11010028

[45] Wang, H.-K. (2000) The Therapeutic Potential of Flavonoids. *Expert Opinion on Investigational Drugs*, **9**, 2103-2119. https://doi.org/10.1517/13543784.9.9.2103

[46] Park, E.-J. and Pezzuto, J.M. (2012) Flavonoids in Cancer Prevention. *Anti-Cancer Agents in Medicinal Chemistry*, **12**, 836-851. https://doi.org/10.2174/187152012802650075

[47] Yu, R., Chen, L., Lan, R., Shen, R. and Li, P. (2020) Computational Screening of Antagonists against the SARS-CoV-2 (COVID-19) Coronavirus by Molecular Docking. *International Journal of Antimicrobial Agents*, **56**, Article ID: 106012. https://doi.org/10.1016/j.ijantimicag.2020.106012

[48] Muchtaridi, M., Fauzi, M., Ikram, N.K.K., Gazzali, A.M. and Wahab, H.A. (2020) Natural Flavonoids as Potential Angiotensin-Converting Enzyme 2 Inhibitors for Anti-SARS-CoV-2. *Molecules*, **25**, Article No. 3980. https://doi.org/10.3390/molecules25173980

[49] Ngwa, W., Kumar, R., Thompson, D., Lyerly, W., Moore, R., Reid, T.-E., Lowe, H. and Toyang, N. (2020) Potential of Flavonoid-Inspired Phytomedicines against Covid-19. *Molecules*, **25**, Article No. 2707. https://doi.org/10.3390/molecules25112707

[50] Pandey, P., Rane, J.S., Chatterjee, A., Kumar, A., Khan, R., Prakash, A. and Ray, S. (2020) Targeting SARS-cov-2 Spike Protein of Covid-19 with Naturally Occurring Phytochemicals: An *in Silico* Study for Drug Development. *Journal of Biomolecular Structure and Dynamics*. https://doi.org/10.1080/07391102.2020.1862705

[51] Dolzhenko, Y., Bertea, C.M., Occhipinti, A., Bossi, S. and Maffei, M.E. (2010) UV-B Modulates the Interplay between Terpenoids and Flavonoids in Peppermint (*Menthe* × *Piperita* L.). *Journal of Photochemistry and Photobiology B: Biology*, **100**, 67-75. https://doi.org/10.1016/j.jphotobiol.2010.05.003

[52] McKay, D.L. and Blumberg, J.B. (2006) A Review of the Bioactivity and Potential Health Benefits of Chamomile Tea (*Matricaria recutita* L.). Phytotherapy Research, **20**, 519-530. https://doi.org/10.1002/ptr.1900

[53] Bodalska, A., Kowalczyk, A., Wlodarczyk, M. and Fecka, I. (2020) Analysis of Polyphenolic Composition of a Herbal Medicinal Product Peppermint Tincture. *Molecules*, **25**, Article No. 69. https://doi.org/10.3390/molecules25010069

[54] Areias, F.M., Valentao, P., Andrade, P.B., Ferreres, F. and Seabra, R.M. (2001) Phenolic Fingerprint of Peppermint Leaves. *Food Chemistry*, **73**, 307-311.

https://doi.org/10.1016/S0308-8146(00)00302-2

[55] Riachi, L.G. and De Maria, C.A.B. (2015) Peppermint Antioxidants Revisited. *Food Chemistry*, **176**, 72-81. https://doi.org/10.1016/j.foodchem.2014.12.028

[56] Mahendran, G. and Rahman, L.-U. (2020) Ethnomedicinal, Phytochemical and Pharmacological Updates on Peppermint (*mentha× Piperita* L.): A Review. *Phytotherapy Research*, **34**, 2088-2139. https://doi.org/10.1002/ptr.6664

[57] Peterson, J. and Dwyer, J. (1998) Flavonoids: Dietary Occurrence and Biochemical Activity. *Nutrition Research*, **18**, 1995-2018. https://doi.org/10.1016/S0271-5317(98)00169-9

[58] de Oliveira, O.V., Rocha, G.B., Paluch, A.S. and Costa, L.T. (2020) Repurposing Approved Drugs As Inhibitors of SARS-CoV-2 S-Protein From Molecular Modeling and Virtual Screening. *Journal of Biomolecular Structure and Dynamics*, **39**, 2924-2933. https://doi.org/10.1080/07391102.2020.1772885

[59] Muhseen, Z.T., Hameed, A.R., Al-Hasani, H.M.H., Ul Qamar, M.T. and Li, G. (2020) Promising Terpenes as SARS-CoV-2 Spike Receptor-Binding Domain (RBD) Attachment Inhibitors to the Human ACE2 Receptor: Integrated Computational Approach. *Journal of Molecular Liquids*, **320**, Article ID: 114493. https://doi.org/10.1016/j.molliq.2020.114493

[60] Hu, X., Cai, X., Song, X., Li, C., Zhao, J., Luo, W., Zhang, Q., Otte Ekumi, I. and He, Z. (2020) Possible Sarscoronavirus 2 Inhibitor Revealed by Simulated Molecular Docking to Viral Main Protease and Host Toll-Like Receptor. *Future Virology*, **15**, 359-368. https://doi.org/10.2217/fvl-2020-0099

[61] Istifli, E.S., Netz, P.A., Tepe, A.S., Husunet, M.T., Sarikurkcu, C. and Tepe, B. (2020) *In Silico* Analysis of the Interactions of Certain Flavonoids with the Receptor-Binding Domain of 2019 Novel Coronavirus and Cellular Proteases and Their Pharmacokinetic Properties. *Journal of Biomolecular Structure and Dynamics*, **40**, 2460-2474. https://doi.org/10.1080/07391102.2020.1840444

[62] Peterson, L. (2020) Covid-19 and Flavonoids: *In Silico* Molecular Dynamics Docking to the Active Catalytic Site of SARS-CoV and SARS-CoV-2 Main Protease. *Social Science Research Network*, Article ID: 3599426. https://doi.org/10.2139/ssrn.3599426

[63] Das, S., Sarmah, S., Lyndem, S. and Roy, A.S. (2020) An Investigation into the Identification of Potential Inhibitors of Sars-cov-2 Main Protease Using Molecular Docking Study. *Journal of Biomolecular Structure and Dynamics*, **39**, 3347-3357. https://doi.org/10.1080/07391102.2020.1763201

[64] Russo, M., Moccia, S., Spagnuolo, C., Tedesco, I. and Russo, G.L. (2020) Roles of Flavonoids against Coronavirus Infection. *Chemico-Biological Interactions*, **328**, Article ID: 109211. https://doi.org/10.1016/j.cbi.2020.109211

[65] Bojadzic, D., Alcazar, O., Chen, J. and Buchwald, P. (2020) Small-Molecule *in Vitro* Inhibitors of the Coronavirus Spike-ACE2 Protein-Protein Interaction as Blockers of Viral Attachment and Entry for SARS-CoV-2. *ACS Infectious Diseases*, **7**, 1519-1534. https://doi.org/10.1021/acsinfecdis.1c00070

[66] Lan, J., Ge, J., Yu, J., Shan, S., Zhou, H., Fan, S., Zhang, Q., Shi, X., Wang, Q., Zhang, L., *et al.* (2020) Structure of the Sars-cov-2 Spike Receptor-Binding Domain Bound to the Ace2 Receptor. *Nature*, **581**, 215-220. https://doi.org/10.1038/s41586-020-2180-5

[67] National Library of Medicine—Pubchem. https://pubchem.ncbi.nlm.nih.gov/

[68] Grosdidier, A., Zoete, V. and Michielin, O. (2011) Fast Docking Using the Charmm Force Field with EADock DSS. *Journal of Computational Chemistry*, **32**, 2149-2159.

https://doi.org/10.1002/jcc.21797

[69] Grosdidier, A., Zoete, V. and Michielin, O. (2011) Swissdock, A Protein-Small Molecule Docking Web Service Based on EADock DSS. *Nucleic Acids Research*, **39**, W270-W277. https://doi.org/10.1093/nar/gkr366

[70] Cheng, B. and Li, T. (2020) Discovery of Alliin as a Putative Inhibitor of the Main Protease of SARS-CoV-2 by Molecular Docking. *BioTechniques*, **69**, 108-112. https://doi.org/10.2144/btn-2020-0038

[71] Pettersen, E.F., Goddard, T.D., Huang, C.C., Couch, G.S., Greenblatt, D.M., Meng, E.C. and Ferrin, T.E. (2004) UCSF Chimera—A Visualization System for Exploratory Research and Analysis. *Journal of Computational Chemistry*, **25**, 1605-1612. https://doi.org/10.1002/jcc.20084

[72] Salentin, S., Schreiber, S., Joachim Haupt, V., Adasme, M.F. and Schroeder, M. (2015) PLIP: Fully Automated Protein-Ligand Interaction Profiler. *Nucleic Acids Research*, **43**, W443-W447. https://doi.org/10.1093/nar/gkv315

[73] Luan, B., Huynh, T., Cheng, X., Lan, G. and Wang, H.-R. (2020) Targeting Proteases for Treating Covid-19. *Journal of Proteome Research*, **19**, 4316-4326. https://doi.org/10.1021/acs.jproteome.0c00430

[74] Alexpandi, R., De Mesquita, J.F., Pandian, S.K. and Ravi, A.V. (2020) Quinolines-based Sars-cov2 3clpro and Rdrp Inhibitors and Spike-rbd-ace2 Inhibitor for Drugrepurposing Against Covid-19: An *in Silico* Analysis. *Frontiers in Microbiology,* **11**, Article No. 1796. https://doi.org/10.3389/fmicb.2020.01796

[75] Choudhary, S., Malik, Y.S. and Tomar, S. (2020) Identification of Sars-cov-2 Cell Entry Inhibitors by Drug Repurposing Using *in Silico* Structure-Based Virtual Screening Approach. *Frontiers in Immunology*, **11**, Article No. 1664. https://doi.org/10.3389/fimmu.2020.01664

[76] Trezza, A., Iovinelli, D., Santucci, A., Prischi, F. and Spiga, O. (2020) An Integrated Drug Repurposing Strategy for the Rapid Identification of Potential SARS-CoV-2 Viral Inhibitors. *Scientific Reports*, **10**, Article No. 13866. https://doi.org/10.1038/s41598-020-70863-9

[77] Wei, T.-Z., Wang, H., Wu, X.-Q., Lu, Y., Guan, S.-H., Dong, F.-Q., Zhu, G., Bao, Y.-Z., Zhang, J., Wang, G.-Y., *et al.* (2020) *In Silico* Screening of Potential Spike Glycoprotein Inhibitors of SARS-CoV-2 with Drug Repurposing Strategy. *Chinese Journal of Integrative Medicine*, **26**, 663-669. https://doi.org/10.1007/s11655-020-3427-6

[78] Panda, P.K., Arul, M.N., Patel, P., Verma, S.K., Luo, W., Rubahn, H.-G., Mishra, Y.K., Suar, M. and Ahuja, R. (2020) Structure-Based Drug Designing and Immunoinformatics Approach for SARS-CoV-2. *Science Advances*, **6**, Article ID: eabb8097. https://doi.org/10.1126/sciadv.abb8097

[79] Utomo, R.Y., Meiyanto, E. and Meiyanto, E. (2020) Revealing the Potency of Citrus and Galangal Constituents to Halt SARS-CoV-2 Infection. *Preprints*, **2020**, Article ID: 2020030214. https://doi.org/10.1126/sciadv.abb8097

[80] Cherrak, S.A., Merzouk, H. and Mokhtari-Soulimane, N. (2020) Potential Bioactive Glycosylated Flavonoids as SARS-CoV-2 Main Protease Inhibitors: A Molecular Docking and Simulation Studies. *PLoS ONE*, **15**, Article ID: e0240653. https://doi.org/10.1371/journal.pone.0240653

[81] Bhowmik, D., Nandi, R., Prakash, A. and Kumar, D. (2021) Evaluation of Flavonoids as 2019-nCoV Cell Entry Inhibitor through Molecular Docking and Pharmacological Analysis. *Heliyon*, **7**, Article ID: e06515. https://doi.org/10.1016/j.heliyon.2021.e06515

[82] Lal Badshah, S., Faisal, S., Akhtar, M., Benjamin Gabriel, P., Abdul Hamid, E. and Mariusz, J. (2021) Antiviral Activities of Flavonoids. *Biomedicine & Pharmacotherapy*, **140**, Article ID: 111596. https://doi.org/10.1016/j.biopha.2021.111596

[83] Abian, O., Ortega-Alarcon, D., Jimenez-Alesanco, A., Ceballos-Laita, L., Vega, S., Reyburn, H.T., Rizzuti, B. and Velazquez-Campoy, A. (2020) Structural Stability of Sars-CoV-2 3CLpro and Identification of Quercetin as an Inhibitor by Experimental Screening. *International Journal of Biological Macromolecules*, **164**, 1693-1703. https://doi.org/10.1016/j.ijbiomac.2020.07.235

[84] Liskova, A., Samec, M., Koklesova, L., Samuel, S.M., Zhai, K., Al-Ishaq, R.K., Abotaleb, M., Nosal, V., Kajo, K., Ashrafizadeh, M., *et al.* (2021) Flavonoids against the Sars-cov-2 Induced Inflammatory Storm. *Biomedicine & Pharmacotherapy*, **138**, Article ID: 111430. https://doi.org/10.1016/j.biopha.2021.111430

[85] Seadawy, M.G., Gad, A.F., Shamel, M., Elharty, B., Mohamed, M.F., Elfiky, A.A., Ahmed, A. and Zekri, A.R.N. (2021) *In Vitro*-Natural Compounds (Thymol, Carvacrol, Hesperidine, and Thymoquinone) against SARS-CoV-2 Strain Isolated from Egypt. *Biomedical Journal of Scientific & Technical Research*, **34**, 26750-26757. https://doi.org/10.26717/BJSTR.2021.34.005552

[86] Solnier, J. and Fladerer, J.-P. (2020) Flavonoids: A Complementary Approach to Conventional Therapy of COVID-19? *Phytochemistry Reviews*, **20**, 773-795. https://doi.org/10.1007/s11101-020-09720-6

Scientific Research Publishing

Open Journal of Biophysics, 2022, 12, 153-163
https://www.scirp.org/journal/ojbiphy
ISSN Online: 2164-5396
ISSN Print: 2164-5388

A Bio-Physical Analysis of Extracellular Ion Mobility and Electric Field Stress

Xiaodi Zhang, Hui Zhang*

College of Physics & Electronic Engineering, Xianyang Normal University, Xianyang, China
Email: *973624841@qq.com

How to cite this paper: Zhang, X.D. and Zhang, H. (2022) A Bio-Physical Analysis of Extracellular Ion Mobility and Electric Field Stress. *Open Journal of Biophysics*, **12**, 153-163.
https://doi.org/10.4236/ojbiphy.2022.122006

Received: February 11, 2022
Accepted: April 16, 2022
Published: April 19, 2022

Abstract

The electric field stress applied to the cell in the electric field will cause the biological effects of the cell on electromagnetic field. In this paper, the single-shell spherical cell is equated to dielectric spheres, and a biophysical method is used to solve the boundary value problem, and then Maxwell tensor analysis is used to discuss the electric field stresses affecting the applied electric field applied to the cells. The results of numerical analysis show that the ion mobility decreases nonlinearly with increasing frequency in the lower region of the applied electric field frequency, and increases with increasing equivalent dielectric constant at a certain frequency, and the magnitude of the electric field stress is almost independent of the frequency; as the frequency increases, the ion mobility tends to a minimum value and is almost independent of the equivalent dielectric constant, while the applied electric field frequency and the cell dielectric constant both affect the cell normal and the tangential stresses. Therefore, the frequency applied electric field and cell dielectric constant affect the extracellular ion mobility, electric field stress applied to the cell membrane by the electric field; the extracellular ion mobility caused by the electric field in the low frequency range is more pronounced than that in the high frequency, and electric field stress is the basic cause of cell deformation.

Keywords

Mobility, Electric Stress, Biological Effects of Electromagnetic Field

1. Introduction

Electric fields can regulate cell growth [1], cytoskeleton reorganization [2], activation of intracellular channels [3], protein secretion and gene expression [4] *et al.* Also experimental studies have revealed that changing electric fields can

cause cell deformation, cell fusion, rotation, and cell damage [5]. These phenomena had triggered mechanistic studies on the biological effects of electric fields.

In the late 1950s, Schwan *et al.* [6] began a series of studies on the action of electric fields on biological cells, which viewed as simple geometric shells with electromagnetic properties. In the early 1970s [7], Helfrich added the theory of elasticity to the lipid layer to study the action of applied electric fields on phospholipid vesicles, and Peterlin *et al.*, in 2007, viewed the phospholipid layer as an anisotropic medium to discuss the mechanism of cellular deformation under the action of electric fields [8]. So far, the interaction of static fields, time-varying electric fields, and pulsed waves with biological cells has also been studied [9]-[16]. It is generally accepted that the additional electric fields generated by electric fields inside and outside the cell, the electric field forces exerted on the cell, and the changes induced in ion concentrations on both sides of the cell membrane are responsible for the biological effects of cellular electromagnetic fields.

Under the action of applied electric field, the analysis of the field in cell membrane, inside and outside the membrane is often assumed there is no free charge in the solution region, and the electric field is solved by the method of separation of variables. For the analysis of the forces exerted on the cell by external electric fields, the Maxwell stress tensor method is commonly used [11] [17]. These methods are based on the bio-electromagnetic theory and the model of the interaction between the electric field and the target body, by solving boundary value problem to obtain the electric field distribution in the study area, and then to analyze the stresses exerted on the cell by the stress tensor. This method can give the threshold value of the field intensity that causes the effects, but the limitation is that the influence of the thermal motion and the fact that there is a free charge in the study area are not considered.

Based on this, this paper uses the theory of bio-electromagnetism to discuss the factors that affect the ion mobility outside the cell membrane and the stress of the electric field applied to the cell membrane when an electric charge is present outside the spherical cell.

2. Model

The spherical cell is usually represented by the single-shell spherical model shown in **Figure 1(a)**, where R_0 is the outer radius of the cell membrane, d is the thickness of the cell membrane, ε_{m1}, ε_i, ε_e, σ_{m1}, σ_i and σ_e are the dielectric constant and conductivity of the cell membrane, the inner and outer medium of the cell membrane, respectively. Based on the bio-electromagnetic theory, the single-shelled spherical cell can be equated with a homogeneous media sphere with dielectric constant ε_p and conductivity σ_p as shown in **Figure 1(b)**, and there is a relationship as Equation (1) and (2) show [18] [19].

$$\varepsilon_p = \varepsilon_m \frac{R_0^3\left(\varepsilon_i + 2\varepsilon_{m1}\right) + 2a^3\left(\varepsilon_i - \varepsilon_{m1}\right)}{R_0^3\left(\varepsilon_i + 2\varepsilon_{m1}\right) - a^3\left(\varepsilon_i - \varepsilon_{m1}\right)}, \quad a = R_0 - d \tag{1}$$

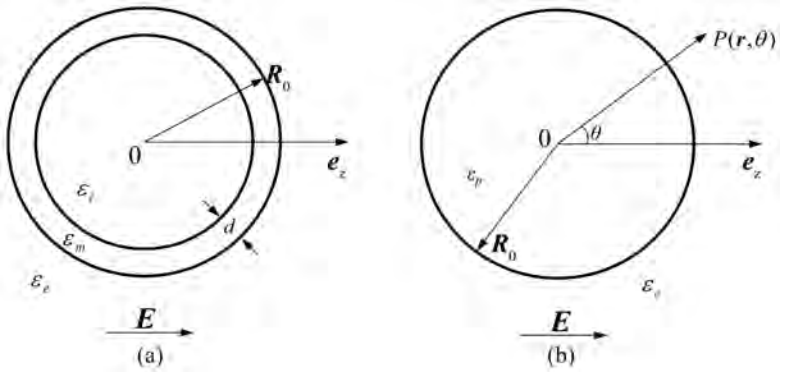

Figure 1. A physical model of the biological cell.

$$\sigma_p = \sigma_m \frac{2(1-v')\sigma_m + (1+2v')\sigma_i}{(2+v')\sigma_m + (1-v')\sigma_i}, \quad v' = \left(\frac{1-d}{R_0}\right)^3 \tag{2}$$

In this paper, the equivalent dielectric sphere is used as the study model, as shown in Figure 1(b). The spherical coordinate system is established with the center of the dielectric sphere as the coordinate origin and the direction of the external electric field as the z-direction, and the applied electric field is $\boldsymbol{E} = \boldsymbol{e}_z E_0 \exp(-i\omega t)$, where E_0, ω are the amplitude and frequency of the applied electric field, respectively. Assume that the ions in the extracellular medium is charged with $\pm e$, and their mobility is $\pm u$, and the average values of ion concentrations at zero field is $n^+ = n^- = n_0$.

3. Theoretical Analysis

3.1. Ion Mobility

If the external electric field acting on the cell is weak, according to the Poisson equation which the potential of the extracellular region satisfies and the continuity equation the ion density satisfies, the extracellular ion mobility u satisfies Equation (3):

$$\nabla^2 u(\boldsymbol{r}) = \gamma^2 u(\boldsymbol{r}) \tag{3}$$

where $u(\boldsymbol{r}) = u^+(\boldsymbol{r}) + u^-(\boldsymbol{r})$, $\gamma^2 = \frac{i\omega}{D} + \chi^2$, $\chi = \left(\frac{2n_0 e^2}{\varepsilon_0 \varepsilon_e KT}\right)^{1/2} = \left(\frac{\sigma_e}{\varepsilon_0 \varepsilon_e D}\right)^{1/2}$ is the reciprocal of the Debye shielding length, D is the ion diffusion coefficient, and the relationship D with the mobility u is: $Dq = uKT$.

The general solution of Equation (3) is dressed as Equation (4):

$$u(\boldsymbol{r},\theta) = B\exp(-\gamma r)\left(\frac{1}{\gamma r} + \frac{1}{(\gamma r)^2}\right)\cos\theta \tag{4}$$

where B is the coefficient to be determined.

3.2. The Field Distribution

Based on the electromagnetic field theory, suppose that the internal and external

electrical potential values of the equivalent dielectric sphere are $\varphi_p(\boldsymbol{r},t)$ and $\varphi_e(\boldsymbol{r},t)$, respectively, then $\varphi_p(\boldsymbol{r},t)$ and $\varphi_e(\boldsymbol{r},t)$ satisfy Equation (5) and (6) [20]:

$$\nabla^2\varphi_e(\boldsymbol{r},t) = -\frac{e}{\varepsilon_0\varepsilon_e}\left[n^+(\boldsymbol{r},t) - n^-(\boldsymbol{r},t)\right], \quad r > R \tag{5}$$

$$\nabla^2\varphi_p(\boldsymbol{r},t) = 0, \quad r < R_0 \tag{6}$$

The $\varphi_p(\boldsymbol{r},t)$ and $\varphi_e(\boldsymbol{r},t)$ satisfies the boundary conditions as Equation (7):

$$\begin{cases} r = a: & \varphi_p = \varphi_e \\ & \varepsilon_p\dfrac{\partial\varphi_p}{\partial r} = \varepsilon_e\dfrac{\partial\varphi_e}{\partial r} \\ & \sigma_e\dfrac{\partial\varphi_e}{\partial r} + qD\dfrac{\partial u}{\partial r} = 0 \\ r\to\infty: & \boldsymbol{E}_e = \boldsymbol{E} \\ r\to 0: & \varphi_p \text{ is limited value} \end{cases} \tag{7}$$

Solving the above boundary value problem, then we get Equation (8):

$$\begin{cases} \varphi_e(\boldsymbol{r},\theta) = \left\{-E_0 r + \dfrac{A}{r^2} - \dfrac{qB}{\varepsilon_0\varepsilon_e\gamma^2}\exp(-\gamma r)\left(\dfrac{1}{\gamma r} + \dfrac{1}{(\gamma r)^2}\right)\right\}\cos\theta \\ \varphi_p(\boldsymbol{r},\theta) = -Cr\cos\theta \end{cases} \tag{8}$$

where

$$\begin{cases} A = \dfrac{\varepsilon_p - (\varepsilon_{ge} + \varepsilon_p R)}{\varepsilon_p + 2(\varepsilon_{ge} + \varepsilon_p R)} R_0^3 E_0 \\ B = \dfrac{-3\varepsilon_p R}{\varepsilon_p + 2(\varepsilon_{ge} + \varepsilon_p R)} \cdot \dfrac{\gamma^2 R_0\varepsilon_0\varepsilon_e}{e} E_0 R_0^3 \exp(\gamma R_0)\left(\dfrac{1}{\gamma R_0} + \dfrac{1}{(\gamma R_0)^2}\right)^{-1} \\ C = -\dfrac{3\varepsilon_{ge}}{\varepsilon_p + 2(\varepsilon_{ge} + \varepsilon_p R)} E_0 \end{cases} \tag{9}$$

$$\varepsilon_{ge} = \varepsilon_e + \frac{\sigma_e}{i\omega\varepsilon_0}, \quad R = \frac{\sigma_e}{i\omega\varepsilon_0\varepsilon_e}\frac{\gamma R_0 + 1}{(\gamma R_0)^2 + 2(\gamma R_0 + 1)}.$$

3.3. The Electric Field and the Electrical Stress on the Cell Membrane

From the relationship $\boldsymbol{E} = -\nabla\varphi$, the electric field strength $\boldsymbol{E}_e$ outside the equivalent medium sphere (cell) is $\boldsymbol{E}_e = E_r\boldsymbol{e}_r + E_t\boldsymbol{e}_t$, where $\boldsymbol{e}_r$, $\boldsymbol{e}_t$ denote the unit vector in the normal and tangential directions of the cell membrane surface, respectively, and we have Equation (10):

$$\begin{cases} E_r = \left[E_0 + \dfrac{2A}{r^3} - \dfrac{e}{\varepsilon_0\varepsilon_e}\dfrac{B}{\gamma^2 r}\exp(-\gamma r)\left(1 + \dfrac{2}{\gamma r} + \dfrac{2}{\gamma^2 r^2}\right)\right]\cos\theta \\ E_t = \left[-E_0 + \dfrac{A}{r^3} - \dfrac{e}{\varepsilon_0\varepsilon_e}\dfrac{B}{\gamma^2 r}\exp(-\gamma r)\left(\dfrac{1}{\gamma r} + \dfrac{1}{\gamma^2 r^2}\right)\right]\sin\theta \end{cases} \tag{10}$$

Since the electromagnetic wave has momentum, it is incident on the equivalent medium sphere (cell surface) and exerts a certain pressure on the cell. From electromagnetic field theory, the momentum flow density tensor is shown as Equation (11):

$$\vec{T} = -\boldsymbol{ED} - \boldsymbol{BH} + \frac{1}{2}\vec{I}\left(\boldsymbol{E}\cdot\boldsymbol{D} + \boldsymbol{B}\cdot\boldsymbol{H}\right) \tag{11}$$

where $\boldsymbol{E}$, $\boldsymbol{H}$ denote the electric field and the magnetic field exposed to cell, respectively. If only the electric field effect is considered, the average value of the electric field stress applied to the unit area outside the cell membrane for a varying electric field is calculated as Equation (12):

$$\begin{aligned}\boldsymbol{P} &= \left\langle -\boldsymbol{e}_r \cdot \vec{T}_e \right\rangle = \frac{1}{4}Re\left(\varepsilon_e \boldsymbol{E}_r \cdot \boldsymbol{E}_r^* - \varepsilon_e \boldsymbol{E}_t \cdot \boldsymbol{E}_t^*\right)\boldsymbol{e}_r + \frac{1}{4}Re\left(\varepsilon_e \boldsymbol{E}_r \cdot \boldsymbol{E}_t^*\right)\boldsymbol{e}_t \\ &= P_r \boldsymbol{e}_r + P_t \boldsymbol{e}_t\end{aligned} \tag{12}$$

In the above equation, $\vec{T}_e = -\varepsilon_e \boldsymbol{EE} + \frac{1}{2}\vec{I}\varepsilon_e\left(\boldsymbol{E}\cdot\boldsymbol{E}\right)$, $\langle\cdots\rangle$ represents the average value in one cycle.

4. Numerical Analysis and Discussion

In the analysis of the mechanism of the bio-effects of electromagnetic fields, the typical values of the cell geometric and the electrical parameters are often used: $R_0 = 10\ \mu\text{m}$, $d = 5\ \text{nm}$, $\varepsilon_m = 4.4\times10^{-11}\ \text{F}\cdot\text{m}^{-1}$, $\varepsilon_i = 6.4\times10^{-10}\ \text{F}\cdot\text{m}^{-1}$, $\varepsilon_e = 6.4\times10^{-10}\ \text{F}\cdot\text{m}^{-1}$, $\sigma_m = 3\times10^{-7}\ \text{S}\cdot\text{m}^{-1}$, $\sigma_i = 0.3\ \text{S}\cdot\text{m}^{-1}$, $\sigma_e = 1.2\ \text{S}\cdot\text{m}^{-1}$. From the equivalent Equations (1), (2), the typical parameter values correspond to $\varepsilon_p = 6.35\times10^{-10}\ \text{F}\cdot\text{m}^{-1}$ and $\sigma_p = 0.0018\ \text{S}\cdot\text{m}^{-1}$, respectively. In the following numerical analysis, the equivalent permittivity of the dielectric sphere is taken around the values of these parameters. Consider that for small ions, the diffusion coefficient D is taken as 2×10^9 m^2/s [21] and the Debye length x is taken as 10^8 m^{-1} [20].

4.1. Effect of the Frequency and the Equivalent Permittivity on Extracellular Ion Mobility

Figure 2 shows the relationship between the ionic mobility of cell membrane surface and the frequency of external electric field, where $\theta = 0.5$, the curves of data1, data2 and data are corresponding to ε_p = 0.5, 6.4 × 10^{-11} Fm^{-1}, 6.35 × 10^{-11} Fm^{-1} and 9.6 × 10^{-11} Fm^{-1}, respectively. Figure 2 shows that the ion mobility decreases nonlinearly with increasing frequency in the region of lower frequency of the applied electric field (e.g., frequency less than 5 × 10^6 Hz) and increases with the increasing of the equivalent permittivity at a certain frequency; With the increasing of the frequency, the ion mobility tends to a minimum value and is almost independent of the equivalent permittivity.

The diffusion coefficient D is a physical quantity that indicates how fast the ions move by diffusion from a high concentration to a low concentration, driven by a concentration gradient. The ion mobility u characterizes how fast the ions

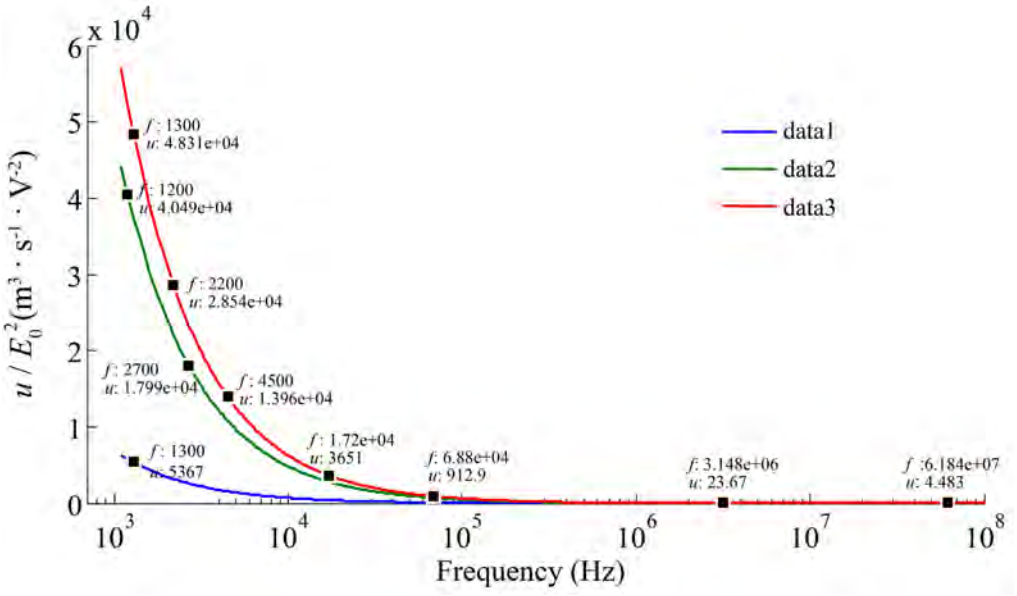

Figure 2. Ion mobility varies with frequency.

move under the action of an electric field and it is equal to the drift velocity per unit electric field. From Einstein's relation, a larger ion mobility u corresponds to a larger diffusion rate of ions from higher to lower concentrations. From Figure 2, it can also be concluded that, under the action of external electric field, in the lower frequency region, the larger the equivalent permittivity, the faster the ion diffusion rate from high to low concentration; The higher the frequency, the less the effect of the equivalent permittivity and the frequency on the ion mobility.

In biological cells, there is a defined concentration relationship inside and outside the cell membrane, and the ion migration across the membrane modulated by the external electric field will affect the physiological and living state of the cell. Figure 2 also illustrates that low frequency electric fields will cause strong biological effects on cells compare to high frequency electric fields.

4.2. Electric Field Stress on the Cell

4.2.1. Effect of the Frequency and the Equivalent Permittivity on the Electric Field Stress

Figure 3(a) and Figure 3(b) give the curves of the normal force P_n, tangential force P_t (tangential force along the cell surface) versus the applied electric field frequency at $\theta = 0.5$, respectively, where $R_0 = 10^{-5}$ m, the curves data1, data2 and data3 are corresponding to $\varepsilon_p = 6.4\times10^{-11}\ \mathrm{F\cdot m^{-1}}$, $\varepsilon_p = 6.35\times10^{-10}\ \mathrm{F\cdot m^{-1}}$ and $\varepsilon_p = 9.6\times10^{-10}\ \mathrm{F\cdot m^{-1}}$, respectively. Figure 3 shows that at a certain position on the cell surface ($\theta = 0.5$) and within a certain frequency range (e.g., frequency less than 5×10^6 Hz), the normal and tangential forces acting on the cell surface hardly change with the increasing frequency; With further increase in frequency, the normal force on the cell decreases slowly, and when the frequency reaches a certain value, e.g., the frequency is 8.41×10^6 Hz, the normal force

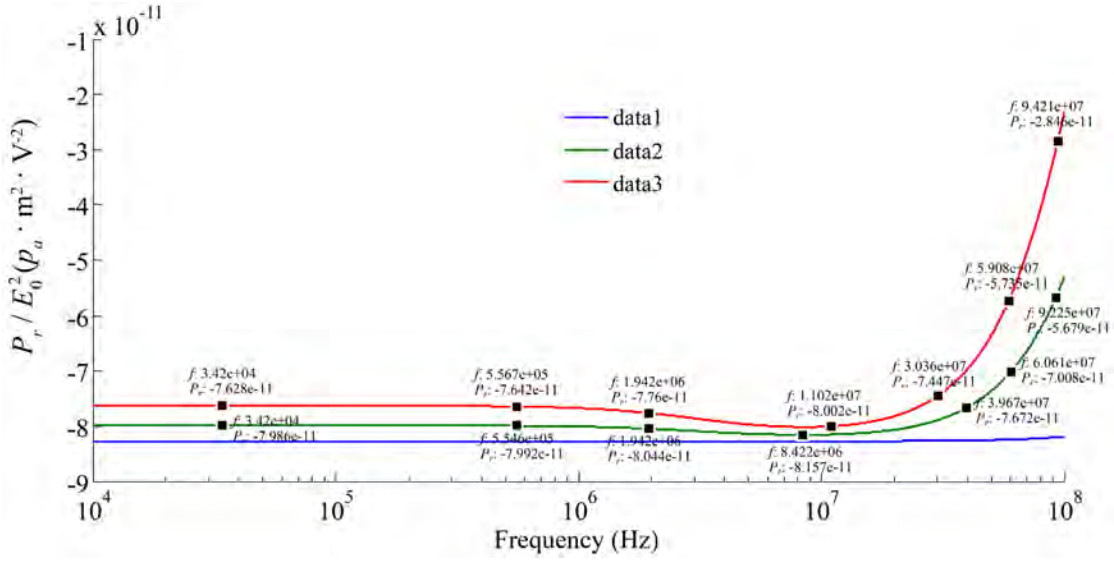

(a)

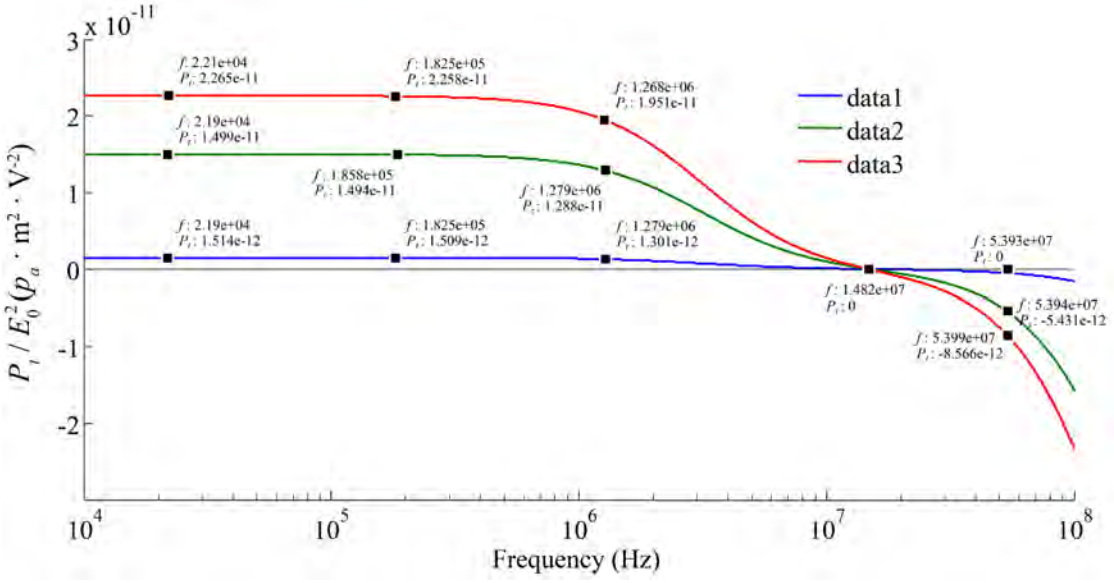

(b)

Figure 3. The electric stress varies with the frequency.

starts to increase, and the normal force is always expressed as pressure on the cell in the whole frequency range; For a certain frequency, the size of the normal force decreases and the size of the tangential force increases with the increase of the equivalent dielectric constant; For the cells with different equivalent permittivity, the threshold value of the change of the direction of the tangential force acting on the cell membrane surface is at same value, such as the frequency is 1.48×10^7 Hz.

4.2.2. Distribution of Electric Field Stress on the Cell Membrane Surface

To analyze the effect of the frequency on the electric field stress distribution acting on the cell surface, **Figure 4(a)** and **Figure 4(b)** give the electric field stress

distribution on the intersection formed the spherical cell surface and the *x-o-z* plane, where $\varepsilon_p = 6.35\times10^{-10}\ \mathrm{F\cdot m^{-1}}$, the curves of data1, data2 and data3 is the P_r, P_t and P, respectively. The frequency of applied electric field in **Figure 4(a)** and **Figure 4(b)** is 1.5×10^6 Hz and 6.7×10^7 Hz, respectively. It is show that the normal and tangential electric field stresses are smaller near the same direction as the external electric field, *i.e.* near $\theta = 0^\circ, 180^\circ$; Near the vertical direction, the maximum normal force and the minimum tangential force are exhibited, and the maximum value of the tangential force is approximately near $\theta = 45^\circ$ and -45°; Within a certain angle range, the electric field stresses are exhibited as the pull force on the cell membrane, *i.e.* for the frequency is 6.7×10^7 Hz, when $-12^\circ < \Delta\theta < 12^\circ$ and $168^\circ < \Delta\theta < 192^\circ$, then $P_r > 0$.

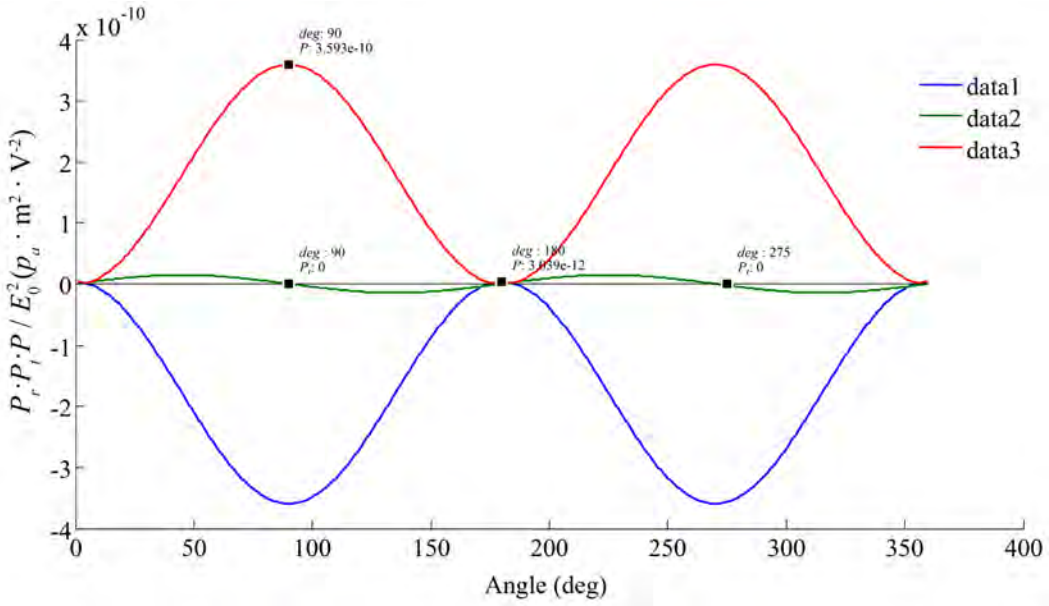

(a)

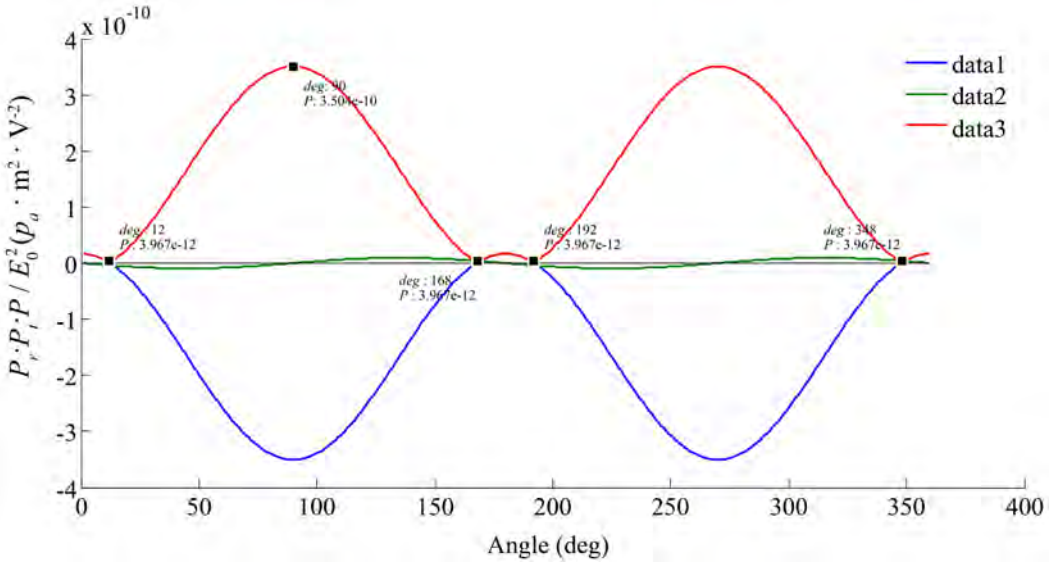

(b)

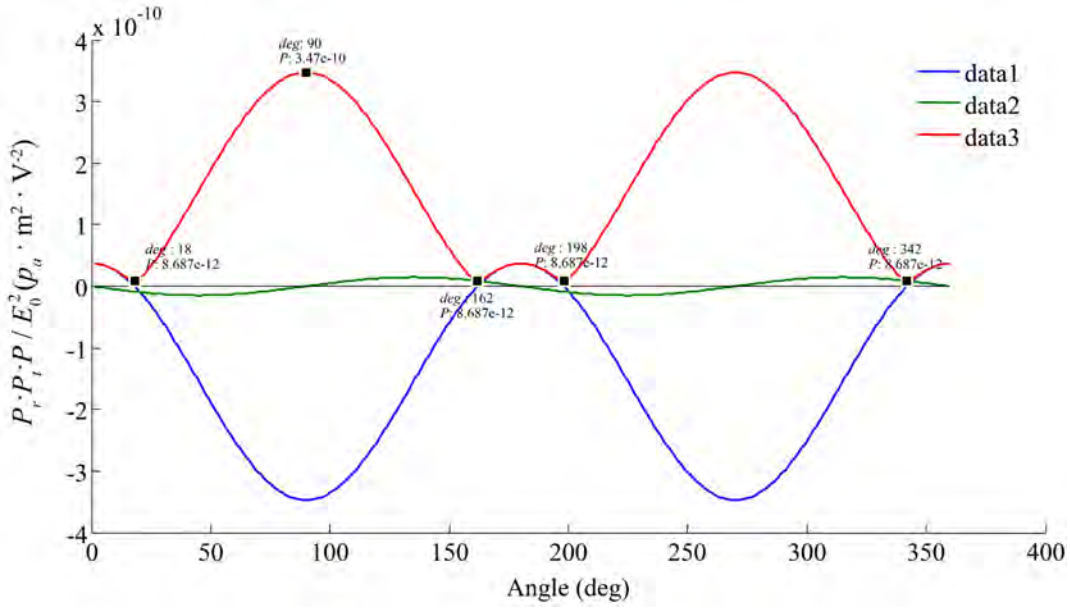

(c)

Figure 4. The electric stress varies with the polar angle.

Figure 4(c) shows the variation of P_r, P_t and P with θ, where the external field frequency is 6.7 × 10^7 Hz and $\varepsilon_p = 9.6\times10^{-10}\ \mathrm{F\cdot m^{-1}}$. Comparing **Figure 4(b)** and **Figure 4(c)**, it can be seen that with the increase of ε_p, the maximum value of P_r, P is in decreases, but the value of $\Delta\theta$ is increases gradually.

The force exerted by the electric field on the cell membrane is decomposed into normal force perpendicular to the membrane surface (pressure or tension) and tangential force along the surface. The action of electric field force can cause the cell deformation. The frequency of the applied electric field and the change of the cell electrical parameters will lead to the cell deformation.

5. Conclusions

1) In a certain frequency range, the changes in frequency and cellular electrical parameters affect the extracellular ion mobility. In the lower frequency range (e.g., less than 5 × 10^6 Hz), the ion mobility decreases rapidly with the increasing frequency; At the same frequency, the mobility increases with increasing equivalent dielectric constant; With further increase of external electric field frequency, the ion mobility tends to the minimum value and is almost independent of the dielectric constant. It can be seen that the ion mobility caused by high equivalent permittivity in the low frequency electric field region is more pronounced compared to the lower equivalent permittivity and the high frequency region.

2) The electric fields exert the electric field forces on the cell surface. In the small frequency range, the frequency hardly affects the magnitude of electric field stress; With the increase of frequency, the frequency and the changes of the cell equivalent dielectric constant will affect the electric field stress applied to the cell. The electric field stress is the fundamental cause of the cell deformation.

The study of the biological effects of electromagnetic fields has always been a hot topic in bio-electromagnetics research. The content of this paper can be used as the basic analysis theory of the biological effects of the electromagnetic field.

Conflicts of Interest

The authors declare no conflicts of interest regarding the publication of this paper.

References

[1] Radisic, M., Park, H., Shing, H., *et al.* (2004) Functional Assembly of Engineered Myocardium by Electrical Stimulation of Cardiac Myocytes Cultured on Scaffolds. *PNAS*, **101**, 18129-18134. https://doi.org/10.1073/pnas.0407817101

[2] Sheikh, A.Q., Taghian, T., Hemingway, B., *et al.* (2013) Regulation of Endothelial MAPK/ERK Signalling and Capillary Morphogenesis by Low-Amplitude Electric Field. *Journal of the Royal Society Interface*, **10**, Article ID: 20120548. https://doi.org/10.1098/rsif.2012.0548

[3] Rackauskas, G., Saygili, E., Rana, O.R., *et al.* (2015) Sub-Threshold High Frequency Electrical Field Stimulation Induces VEGF Expression in Cardiomyocytes. *Cell Transplantation*, **24**, 1653-1659. https://doi.org/10.3727/096368914X682783

[4] Llucia-Valldeperas, A., Sanchez, B., Soler-Botija, G., *et al.* (2014) Physiological Conditioning by Electric Field Stimulation Promotes Cardiomyogenic Gene Expression in Human Cardiomyocyte Progenitor Cells. *Stem Cell Research & Therapy*, **5**, 93. https://doi.org/10.1186/scrt482

[5] Schwan, H.P. (1982) Nonthermal Cellular Effects of Electromagnetic Fields: AC-Field Induced Ponderomotoric Forces. *British Journal of Cancer*, **5**, 220-224.

[6] Schaw, H.P. (1957) Electrical Properties of Tissue and Cell Suspensions. *Advances in Biological and Medical Physics*, **5**, 147-209. https://doi.org/10.1016/B978-1-4832-3111-2.50008-0

[7] Helfrich, W. (1973) Elastic Properties of Lipid Bilayers: Theory and Possible Experiments. *Zeitschrift für Naturforschung*, **28C**, 693-703. https://doi.org/10.1515/znc-1973-11-1209

[8] Peterlin, P., Svetina, S. and Žeks, B. (2007) The Prolate-to-Oblate Shape Transition of Phospholipid of an AC Electric Field Can Be Explained by the Dielectric Anisotropy of a Phospholipid Bilayer. *Journal of Physics*: *Condensed Matter*, **16**, Article ID: 136220. https://doi.org/10.1088/0953-8984/19/13/136220

[9] Vlahovska, P.M., Gracià, R.S., Aranda-Espinoza, S., *et al.* (2009) Electrohydrodynamic Model of Vesicle Deformation in Alternating Electric Fields. *Biophysical Journal*, **96**, 4789-4803. https://doi.org/10.1016/j.bpj.2009.03.054

[10] Yamamoto, T., Espinoza, S., Dimova, R., *et al.* (2010) Stability of Spherical Vesicle in Electric Fields. *Langmuir*, **26**, 12390-12407. https://doi.org/10.1021/la1011132

[11] Peterlin, P. (2010) Frequency Dependent Electrodeformation of Giant Phospholipid Vesicles in AC Electric Field. *Journal of Biological Physics*, **36**, 339-354. https://doi.org/10.1007/s10867-010-9187-3

[12] Salipante, P.F. and Vlahovska, P.M. (2014) Vesicle Deformation in DC Pulses. *Soft Matter*, **10**, 3386-3393. https://doi.org/10.1039/C3SM52870G

[13] Mcconnell, L., Vlahovska, P.M., Miksis, M.J., *et al.* (2015) Vesicle Dynamics in Uniform Electric Fields: Squaring and Breathing. *Soft Matter*, **11**, 4840-4846.

https://doi.org/10.1039/C5SM00585J

[14] Sinhaa, K.P. and Thaokarb, R.M. (2019) Shape Deformation of a Vesicle under Axi-symmetric Non-Uniform Alternating Electric Field. *Journal of Physics Condensed Matter*, **31**, Article ID: 035101. https://doi.org/10.1088/1361-648X/aaef15

[15] Zhang, H., Wang, L.Y., Zhang, P.J., *et al.* (2018) Modulation of Membrane Potential and Ion Concentration of Isolate Ellipsoidal Cell Exposed to Static Electric Field. *Scientia Sinica* (*Technologica*), **48**, 783-790. https://doi.org/10.1360/N092017-00266

[16] Zhang, H., Wang, Y.L., Zhang, X.D., *et al.* (2017) The Effect of Impulse Wave on Ion Migration across Cell Membrane. *Journal of Northwest University* (*Natural Science Edition*), **47**, 481-486.

[17] Zhang, H., Wang, Y., Zhang, P.J., *et al.* (2021) Estimation of Biophysical Properties of Cell Exposed to Electric Field. *Chinese Physics B*, **30**, 038702-038709. https://doi.org/10.1088/1674-1056/abc543

[18] Zhao, C.X. (2018) Analysis of Equivalent Dielectric Constant of Double-Layer Ellipsoid and Design of Related Artificial Electromagnetic Materials. Lanzhou University, Lanzhou.

[19] Qin, Y.R. (2005) Modeling of Cell Membrane Voltage Changes in Suspension under External Electric Field. South China University of Technology, Guangzhou.

[20] Garcia, A., Grosse, C. and Brito, P. (1985) On the Effect of Volume Charge Distribution on the Maxwell-Wagner Relaxation. *Journal of Physics D: Applied Physics*, **18**, 739-745. https://doi.org/10.1088/0022-3727/18/4/018

[21] Grosse, C. and Schwan, H.P. (1992) Cellular Membrane Potentials Induced by Alternating Fields. *Biophysical Journal*, **63**, 1632-1642. https://doi.org/10.1016/S0006-3495(92)81740-X

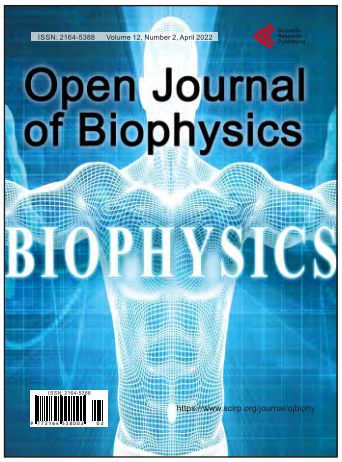

Call for Papers

Open Journal of Biophysics

ISSN Print: 2164-5388 ISSN Online: 2164-5396
https://www.scirp.org/journal/ojbiphy

Open Journal of Biophysics (OJBIPHY) is an international journal dedicated to the latest advancement of biophysics. The goal of this journal is to provide a platform for scientists and academicians all over the world to promote, share, and discuss various new issues and developments in different areas of biophysics.

Subject Coverage

All manuscripts must be prepared in English, and are subject to a rigorous and fair peer-review process. Accepted papers will immediately appear online followed by printed hard copy. The journal publishes original papers including but not limited to the following fields:

- Bioelectromagnetics
- Bioenergetics
- Bioinformatics and Computational Biophysics
- Biological Imaging
- Biomedical Imaging and Bioengineering
- Biophysics of Disease
- Biophysics of Photosynthesis
- Cardiovascular Biophysics
- Cell Biophysics
- Medical Biophysics
- Membrane Biophysics
- Molecular Biophysics and Structural Biology
- Physical Methods
- Physiology and Biophysics of the Inner Ear
- Proteins and Nucleic Acids Biophysics
- Radiobiology
- Receptors and Ionic Channels Biophysics
- Sensory Biophysics and Neurophysiology
- Systems Biophysics
- Theoretical and Mathematical Biophysics

We are also interested in: 1) Short Reports—2-5 page papers where an author can either present an idea with theoretical background but has not yet completed the research needed for a complete paper or preliminary data; 2) Book Reviews—Comments and critiques.

Notes for Intending Authors

Submitted papers should not have been previously published nor be currently under consideration for publication elsewhere. Paper submission will be handled electronically through the website. All papers are refereed through a peer review process. For more details about the submissions, please access the website.

Website and E-Mail

https://www.scirp.org/journal/ojbiphy **E-mail: ojbiphy@scirp.org**

What is SCIRP?

Scientific Research Publishing (SCIRP) is one of the largest Open Access journal publishers. It is currently publishing more than 200 open access, online, peer-reviewed journals covering a wide range of academic disciplines. SCIRP serves the worldwide academic communities and contributes to the progress and application of science with its publication.

What is Open Access?

All original research papers published by SCIRP are made freely and permanently accessible online immediately upon publication. To be able to provide open access journals, SCIRP defrays operation costs from authors and subscription charges only for its printed version. Open access publishing allows an immediate, worldwide, barrier-free, open access to the full text of research papers, which is in the best interests of the scientific community.

- High visibility for maximum global exposure with open access publishing model
- Rigorous peer review of research papers
- Prompt faster publication with less cost
- Guaranteed targeted, multidisciplinary audience

Scientific Research Publishing

Website: https://www.scirp.org

Subscription: sub@scirp.org

Advertisement: service@scirp.org